

# Distributed Gradient-Regularized Newton Method: Scheduled Consensus and $\mathcal{O}(\varepsilon^{-1})$ Global Iteration Complexity\*

Wei Hu<sup>†</sup>   Pengcheng Xie<sup>‡</sup>   Ya-Xiang Yuan<sup>§</sup>   Li Zhang<sup>¶</sup>

May 20, 2026

## Abstract

We propose DISGREM, a fully decentralized second-order method for convex consensus optimization over networks. Each agent solves a local Newton system with vanishing gradient-norm regularization  $\lambda_{i,k} = \sqrt{M}\|\tilde{g}_{i,k}\|$  and an eigenvalue-shift stabilizer, communicating through a two-stage gossip-mixing mechanism. We introduce a reference-step framework that reduces the network-wide update to an inexact centralized regularized Newton step, replacing the static Hessian-heterogeneity assumptions of prior work with an increment-based dispersion analysis that imposes no irreducible accuracy floor. Under a bounded-iterates assumption, after a burn-in phase whose order is controlled by the scheduled consensus accuracy, the post-burn-in phase achieves  $\|\nabla f(\bar{x}_k)\| \leq \varepsilon$  in  $\mathcal{O}(\varepsilon^{-1})$  iterations—matching the centralized regularized Newton rate—without line search or stepsize tuning. For a logarithmic schedule with  $p \geq 3$ , the total iteration complexity remains  $\mathcal{O}(\varepsilon^{-1})$ . For a fixed connected network, this yields  $\mathcal{O}(\varepsilon^{-1} \log(1/\varepsilon))$  neighbor communication rounds; more explicitly, the dependence on the mixing rate is  $\mathcal{O}((1-\rho)^{-1}\varepsilon^{-1} \log(1/\varepsilon))$  as  $\rho \rightarrow 1$ . Under strong convexity and a relative tracking-accuracy condition, we further establish conditional local superlinear convergence of order  $3/2$ . In our nine-problem benchmark suite, the DISGREM family attains  $\text{relF} \leq 10^{-6}$  on every test instance, while the tested baselines stagnate or diverge on at least one problem.

**Keywords.** decentralized optimization, second-order methods, gradient regularization, Newton method, consensus optimization, communication efficiency

**AMS subject classifications.** 90C25, 90C30, 65K05, 68W15

## 1 Introduction

We consider the decentralized consensus optimization problem

$$\min_{x \in \mathbb{R}^d} f(x) := \frac{1}{N} \sum_{i=1}^N f_i(x), \quad (1.1)$$

\*Submitted to the editors March 3, 2026.

<sup>†</sup>LSEC, ICMSEC, Academy of Mathematics and Systems Science, Chinese Academy of Sciences, Beijing 100190, China; and University of Chinese Academy of Sciences, Beijing 100049, China ([huwei@amss.ac.cn](mailto:huwei@amss.ac.cn)). Corresponding author.

<sup>‡</sup>Lawrence Berkeley National Laboratory, Berkeley, CA 94720, USA ([pxie@lbl.gov](mailto:pxie@lbl.gov), [pxie98@gmail.com](mailto:pxie98@gmail.com)).

<sup>§</sup>LSEC, ICMSEC, Academy of Mathematics and Systems Science, Chinese Academy of Sciences, Beijing 100190, China ([yyx@lsec.cc.ac.cn](mailto:yyx@lsec.cc.ac.cn)).

<sup>¶</sup>LSEC, ICMSEC, Academy of Mathematics and Systems Science, Chinese Academy of Sciences, Beijing 100190, China ([zhangli2022@lsec.cc.ac.cn](mailto:zhangli2022@lsec.cc.ac.cn)).

where each local cost  $f_i$  is known only to agent  $i$  of a connected network and agents communicate exclusively with their immediate neighbors. Throughout the paper, unless otherwise stated, unqualified vector and stacked-vector norms are Euclidean norms; for matrices,  $\|\cdot\|_2$  and  $\|\cdot\|_F$  denote the spectral and Frobenius norms. Each outer iteration involves one or more gossip rounds, so communication is a primary bottleneck in decentralized implementations; consequently, reducing the iteration count typically lowers the overall communication budget. First-order decentralized methods may need prohibitively many iterations on ill-conditioned problems. Second-order information can cut this count substantially, yet decentralized second-order methods face additional difficulties: curvature data are expensive to transmit, and global convergence typically requires stepsize tuning or line search. These issues are part of a broader theme in modern optimization: how to exploit curvature, local approximation structure, and model information while limiting expensive oracle calls, communication, or computation. Related perspectives appear in derivative-free trust-region modeling, underdetermined quadratic interpolation, least-norm and least- $H^2$  model updating, transformed-objective optimization, subspace optimization, and approximation-based acceleration; see, for example, Xie and Yuan [37, 38, 39, 40, 41], Xie and Wild [42], He and Xie [43].

In the centralized setting, the regularized Newton method of Mishchenko [5] takes a different approach, updating the iterate via an explicitly regularized system:

$$x_{k+1} = x_k - (\nabla^2 f(x_k) + \lambda_k I)^{-1} \nabla f(x_k).$$

With a vanishing regularization parameter  $\lambda_k \asymp \sqrt{\|\nabla f(x_k)\|}$ , this method achieves the optimal  $\mathcal{O}(1/k^2)$  functional rate under convexity and Lipschitz Hessians—equivalently,  $\|\nabla f(x_k)\| \leq \varepsilon$  in  $\mathcal{O}(\varepsilon^{-1})$  iterations—requiring no line search or stepsize tuning. Doikov and Nesterov [18] show that gradient-norm regularization can replace the more expensive cubic model [1, 10] while preserving the same complexity guarantees; Gratton et al. [17] extend the approach to nonconvex objectives via negative-curvature exploitation. The use of regularization and curvature modification is also connected to other numerical optimization mechanisms, including trust-region methods on non-Euclidean or constrained geometries [44, 45], and practical derivative-free or mixed-integer model-based solvers. A natural question is whether this  $\mathcal{O}(\varepsilon^{-1})$  iteration complexity can be preserved in a fully decentralized setting. The difficulty is that the vanishing regularization  $\lambda_k \asymp \sqrt{\|\nabla f(x_k)\|}$  relies on globally consistent gradient and curvature information. When each agent sees only a local approximation corrupted by consensus error, the balance between regularization and curvature breaks down, and existing methods resort to line search or static heterogeneity assumptions to recover convergence.

Two specific challenges arise. First, each agent inverts a local regularized system whose average generally differs from the global Newton step; this gap depends on inter-agent agreement and must be controlled without static heterogeneity constants. Second, Hessian trackers can become transiently indefinite due to imperfect consensus, threatening the well-posedness of local solves. Our algorithm DISGREM (Distributed Gradient-Regularized Newton Method) addresses the first challenge through an increment-based dispersion recursion that bounds tracker mismatch via Lipschitz differences, and the second through an eigenvalue-shift stabilizer that ensures well-posedness at every iteration. DISGREM requires only a single scaling parameter  $M \geq L_2$  and does not need stepsize tuning or line search. To our knowledge, no prior fully decentralized method achieves the same post-burn-in centralized-order iteration bound to arbitrary accuracy with gradient-norm regularization under these conditions. In this sense, our work complements recent efforts that use carefully constructed local models or surrogate information to reduce expensive optimization costs, including regional minimal updating [42], local approximation strategies in large-scale subspaces [43], and neural-network approximation diagnostics based on objective-value or shape changes [46].

We summarize our main contributions as follows:

- **A fully decentralized gradient-regularized Newton framework.** We propose DISGREM, in which each agent solves a local Newton system with vanishing regularization  $\lambda_{i,k} = \sqrt{M\|\tilde{g}_{i,k}\|}$ . A two-stage gossip mechanism and an eigenvalue-shift stabilizer ensure that all local systems remain well posed without line search or explicit positive-semidefinite (PSD) projection.
- **An analytical reduction to an inexact centralized Newton step.** We introduce a reference-step construction that quantifies the gap between the averaged local step and the ideal global Newton step, thereby reducing the decentralized dynamics to an inexact centralized regularized Newton iteration. This framework also replaces the usual static heterogeneity assumption by an increment-based dispersion recursion, avoiding an irreducible heterogeneity floor in the final accuracy bound.
- **Global guarantees and a conditional local superlinear result.** Under convexity, Lipschitz Hessians, and the bounded-iterates assumption (Assumption 5.1), after a burn-in phase controlled by the scheduled consensus accuracy, the post-burn-in phase requires  $\mathcal{O}(\varepsilon^{-1})$  iterations for achieving  $\|\nabla f(\bar{x}_k)\| \leq \varepsilon$ . The  $\mathcal{O}(\varepsilon^{-1})$  bound is conditional on Assumption 5.1: this trajectory boundedness is not proved from the problem data but is empirically verified on all tested instances (Section 6). For a logarithmic mixing schedule with  $p \geq 3$ , the burn-in estimate is compatible with the  $\mathcal{O}(\varepsilon^{-1})$  post-burn-in term, so the total iteration complexity matches the centralized regularized Newton rate. For a fixed connected network, the communication rounds scale as  $\mathcal{O}(\varepsilon^{-1} \log(1/\varepsilon))$ ; explicitly, the spectral-gap dependence is  $\mathcal{O}((1-\rho)^{-1} \varepsilon^{-1} \log(1/\varepsilon))$  as  $\rho \rightarrow 1$ . Under strong convexity and a relative tracking-accuracy condition, we further establish conditional local  $Q$ -superlinear convergence of order  $3/2$ .
- **Practical variants and empirical robustness.** We develop communication-efficient and adaptive variants, namely CEDISGREM and ADADISGREM. Across nine benchmark problems, the DISGREM family achieves a strong accuracy–robustness balance among the tested methods, while ADADISGREM achieves the highest robustness in the multi-start experiments.

Section 2 reviews related work. Sections 3–5 present the notation, assumptions, algorithmic variants, and convergence theory. Section 6 reports numerical results. Appendices A and B collect the longer proofs, while Appendix C reports supplementary experiments.

## 2 Related work

**First-order decentralized methods.** Decentralized (sub)gradient descent originates with Nedić and Ozdaglar [8]. EXTRA [11] and exact diffusion [14] remove the bias of constant-stepsize methods through correction steps or primal-dual reformulations. Gradient tracking [9, 29, 30] achieves exact convergence with a single doubly stochastic matrix by accumulating gradient increments; Alghunaim et al. [21] unify these two perspectives. These methods converge at  $\mathcal{O}(1/k)$  or linearly for strongly convex objectives, but the iteration complexity scales with  $(1-\rho)^{-1}$  or  $(1-\rho)^{-2}$ , a severe penalty on poorly connected graphs. Acceleration [4, 27] and communication compression [23, 26] are orthogonal improvements; we adopt the latter for Hessian data in Section 4.4.

**Second-order and quasi-Newton decentralized methods.** Network Newton [6] approximates the global Newton direction via a truncated Hessian power series; Newton tracking [7] embeds Newton-type updates into gradient tracking. DQM [3] replaces exact Hessians with BFGS surrogates; Bajović et al. [22] studies distributed Newton-type corrections with diagonal approximations, and Li et al. [31] propose communication-efficient approximate Newton and variance-reduced methods for networked optimization. ESOM [28] combines exact second-order information with an alternating

direction method of multipliers (ADMM) consensus step. SONATA [12] solves a sequence of strongly convex local surrogates and handles nonconvex objectives, while Network-GIANT [13] constructs a global Newton direction through harmonic-mean Hessian consensus. All of these methods require explicit stepsize tuning, penalty parameter selection, or line search. Furthermore, to the best of our knowledge, none attains the optimal centralized Newton iteration complexity of  $\mathcal{O}(1/k^2)$  for general convex problems in a rigorous global sense. While exact methods like ESOM and Newton tracking can reach arbitrary precision for strongly convex objectives, their convergence heavily relies on static Hessian-heterogeneity constants (e.g.,  $\sigma_H$ ) to dictate conservative stepsizes. Other approximate decentralized Newton methods simply ignore this heterogeneity or suffer from an irreducible accuracy floor  $\|\nabla f(\bar{x})\| \leq \mathcal{O}(\sigma_H)$ . Daneshmand et al. [16] pursue a different approach, combining gradient tracking with cubic regularization and local Hessian subsampling to achieve an iteration count comparable to centralized cubic Newton. However, their convergence guarantee holds only up to the statistical precision of the Hessian estimator—an inherent accuracy floor from subsampling—and the method still requires a stepsize parameter. Our increment-based dispersion analysis, combined with exact Hessian tracking and gradient-norm regularization, eliminates both the heterogeneity floor and the statistical precision floor, yielding convergence to arbitrary  $\varepsilon$  without any stepsize.

**Communication-efficient and inversion-free approaches.** The  $\mathcal{O}(d^2)$  per-round cost of transmitting Hessian data and the  $\mathcal{O}(d^3)$  cost of solving Newton systems are the two main bottlenecks of decentralized second-order methods. Zhang et al. [20] combine lazy Hessian updates with compression for distributed cubic Newton but rely on a central parameter server; our CEDISGREM achieves analogous savings in a fully peer-to-peer topology. On the computation side, DINAS [15] avoids Hessian inversion through iterative linear solvers, and INDO [19] proposes an inversion-free method for consensus optimization. Incorporating such inexact solvers into the DISGREM framework is a promising direction, as discussed in Section 7.

**Regularized Newton and cubic regularization.** Our starting point is the centralized regularized Newton method of Mishchenko [5]: setting  $\lambda_k \asymp \sqrt{\|\nabla f(x_k)\|}$  yields the tight  $\mathcal{O}(1/k^2)$  functional rate under convexity and Lipschitz Hessians, with no stepsize to choose. The idea has roots in cubic regularization [1, 10], which achieves the same rate through an adaptive cubic model. Doikov and Nesterov [18] establish that gradient-norm regularization can replace the cubic model across a broad class of problems. Gratton et al. [17] extend it to nonconvex objectives via negative-curvature exploitation. Doikov and Nesterov [24] study local convergence of higher-order tensor methods, and Doikov et al. [25] analyze lazy Hessian updates in the centralized setting, an idea we also explore in Section 6.3. As far as we know, there is no prior work that combines gradient-norm regularization (as opposed to cubic regularization) with full gradient and Hessian tracking in a decentralized setting, achieving a centralized-order post-burn-in iteration bound without stepsize tuning, line search, or static heterogeneity constants.

**Model-based and approximation-driven optimization.** In some (derivative-free) trust-region methods, quadratic models built from interpolation or underdetermined interpolation play a central role; see, for example, the line-search/trust-region hybrid method of Xie and Yuan [37], transformed-objective derivative-free optimization [38], the optimality-aware underdetermined interpolation model of Xie and Yuan [39], and least- $H^2$  norm updating of quadratic interpolation models [40]. Related model-update and model-selection ideas include barycentric weight-region analysis [47], regional minimal updating [42], and the relationship between geometric poisedness and outlier detection [48]. Large-scale settings motivate subspace and local-approximation strategies, including two-dimensional model-based subspace methods [41], model-driven subspaces [43], and numerical methods tailored for unconstrained optimization [49]. Further related applications and extensions include privacy-preserving black-box optimization [53], neural-network approximation and objective-

shape diagnostics [46, 54], inverse problems under uncertainty [55]. These works differ from the decentralized Newton framework studied here, but they share the common goal of designing optimization algorithms whose local models, regularization mechanisms, or surrogate information improve robustness and reduce the dominant computational or communication cost.

### 3 Preliminaries and assumptions

#### 3.1 Network model and notation

Unless otherwise stated,  $\|\cdot\|$  denotes the Euclidean norm for vectors and stacked vectors. For matrices,  $\|\cdot\|_2$  and  $\|\cdot\|_F$  denote the spectral and Frobenius norms, respectively.

We model the communication network as an undirected, connected graph  $\mathcal{G} = (\mathcal{V}, \mathcal{E})$ , where  $\mathcal{V} = \{1, \dots, N\}$  is the set of agents and  $\mathcal{E}$  is the set of communication links. Agents  $i$  and  $j$  can exchange information if and only if  $(i, j) \in \mathcal{E}$ . Information mixing over this network is represented by a symmetric, doubly stochastic matrix  $W \in \mathbb{R}^{N \times N}$  that respects the graph topology, meaning  $W_{ij} > 0$  only if  $(i, j) \in \mathcal{E}$  or  $i = j$ . We assume that  $W$  has positive diagonal entries and satisfies  $W_{ij} \geq 0$ ,  $W\mathbf{1} = \mathbf{1}$ ,  $\mathbf{1}^\top W = \mathbf{1}^\top$ . Let  $\left(\frac{1}{N}\mathbf{1}\mathbf{1}^\top\right) := \frac{1}{N}\mathbf{1}\mathbf{1}^\top$  denote the averaging projector,  $I - \left(\frac{1}{N}\mathbf{1}\mathbf{1}^\top\right) := I - \left(\frac{1}{N}\mathbf{1}\mathbf{1}^\top\right)$  the complementary projector, and

$$\rho := \left\| W - \left( \frac{1}{N} \mathbf{1} \mathbf{1}^\top \right) \right\|_2 \in [0, 1).$$

The positive diagonal condition is satisfied by the Metropolis–Hastings weights used in our experiments and rules out the periodic case in which an eigenvalue  $-1$  would give  $\rho = 1$ . For stacked vectors  $Z = [z_1; \dots; z_N] \in \mathbb{R}^{Nd}$  we use the Euclidean norm  $\|Z\|$  and write  $\bar{z} := \frac{1}{N} \sum_{i=1}^N z_i$  for the average. Stacked primal variables are denoted  $X = [x_1; \dots; x_N] \in \mathbb{R}^{Nd}$ , and we define the separable network objective

$$F(X) := \sum_{i=1}^N f_i(x_i).$$

Then

$$\begin{aligned} \nabla F(X) &= [\nabla f_1(x_1); \dots; \nabla f_N(x_N)] \in \mathbb{R}^{Nd}, \\ \nabla^2 F(X) &= \text{blkdiag}(\nabla^2 f_1(x_1), \dots, \nabla^2 f_N(x_N)), \end{aligned}$$

where  $\text{blkdiag}(\cdot)$  denotes the block-diagonal matrix. We also introduce the stacked Hessian vectorization

$$\mathcal{H}(X) := [\text{vec}(\nabla^2 f_1(x_1)); \dots; \text{vec}(\nabla^2 f_N(x_N))] \in \mathbb{R}^{Nd^2},$$

where  $\text{vec}(\cdot)$  stacks the columns of a matrix into a single vector. When evaluated at a consensus point  $x$ , we write  $\mathcal{H}(\mathbf{1} \otimes x)$ .

Table 1 collects the main symbols used throughout the paper.

To quantify disagreement among agents we define the root-mean-square (RMS) dispersion (also called consensus error or disagreement in the decentralized optimization literature, see e.g. Nedić and Ozdaglar [8], Nedić et al. [9])  $D(Z) := \left(\frac{1}{N} \sum_{i=1}^N \|z_i - \bar{z}\|^2\right)^{1/2}$ . In particular, writing  $X_k := [x_{1,k}; \dots; x_{N,k}]$  for the stacked iterates and  $\tilde{G}_k := [\tilde{g}_{1,k}; \dots; \tilde{g}_{N,k}]$  for the stacked gradient trackers,  $D(X_k)$  and  $D(\tilde{G}_k)$  measure the primal and gradient-tracker disagreements at iteration  $k$ .

Table 1: Notation summary.

Symbol	Meaning
$N, d$	number of agents; problem dimension
$x_{i,k}$	primal iterate of agent $i$ at iteration $k$
$\bar{x}_k$	average iterate $\frac{1}{N} \sum_{i=1}^N x_{i,k}$
$X_k$	stacked vector $[x_{1,k}; \dots; x_{N,k}] \in \mathbb{R}^{Nd}$
$\tilde{x}_{i,k}, \tilde{g}_{i,k}, \tilde{H}_{i,k}$	pre-mixed quantities (after $\tau_k$ gossip rounds)
$g_{i,k}, H_{i,k}$	gradient and Hessian trackers
$\tilde{G}_k$	stacked pre-mixed gradient trackers $[\tilde{g}_{1,k}; \dots; \tilde{g}_{N,k}]$
$W$	doubly stochastic mixing matrix
$\rho := \ W - (\frac{1}{N}\mathbf{1}\mathbf{1}^\top)\ _2$	mixing rate ( $1-\rho$ is the spectral gap)
$\tau_k, t_k$	pre-mixing and post-mixing depths
$D(Z)$	RMS dispersion $(\frac{1}{N} \sum_{i=1}^N \ z_i - \bar{z}\ ^2)^{1/2}$
$M$	regularization scaling ( $M \geq L_2$ )
$\lambda_{i,k}$	$\sqrt{M}\ \tilde{g}_{i,k}\ $ (vanishing regularizer)
$\delta_{i,k}$	eigenvalue-shift stabilizer
$L_1, L_2$	gradient and Hessian Lipschitz constants
$\ \cdot\ , \ \cdot\ _2, \ \cdot\ _F$	Euclidean norm for vectors; spectral and Frobenius norms for matrices

### 3.2 Assumptions

#### Assumption 3.1.

- (i) Each  $f_i$  is convex and twice continuously differentiable with  $L_1$ -Lipschitz gradient and  $L_2$ -Lipschitz Hessian:

$$\|\nabla f_i(x) - \nabla f_i(y)\| \leq L_1 \|x - y\|, \quad \left\| \nabla^2 f_i(x) - \nabla^2 f_i(y) \right\|_2 \leq L_2 \|x - y\|.$$

- (ii)  $W$  is symmetric, doubly stochastic, has positive diagonal entries, and  $\rho = \left\| W - \left(\frac{1}{N}\mathbf{1}\mathbf{1}^\top\right) \right\|_2 < 1$ .

- (iii) The average objective  $f$  is coercive:  $f(x) \rightarrow +\infty$  as  $\|x\| \rightarrow \infty$ . Equivalently, for every  $c \in \mathbb{R}$  the sublevel set  $\{x : f(x) \leq c\}$  is bounded.

*Remark 3.2.* Coercivity guarantees existence of minimizers and bounded sublevel sets. It is satisfied, for instance, whenever the objective contains an  $\ell_2$  regularizer.

## 4 The DisGrem algorithm

### 4.1 Design motivation

Lifting the regularized Newton method to a decentralized setting requires mimicking the global Newton step without a central coordinator. This presents three coupled mathematical and algorithmic difficulties, which motivate the design of DISGREM.

**1. The gap between averaging and inversion.** The ideal centralized step solves the global average system

$$s_k^* = -\left(\frac{1}{N} \sum_{i=1}^N \nabla^2 f_i(\bar{x}_k) + \lambda_k I\right)^{-1} \frac{1}{N} \sum_{i=1}^N \nabla f_i(\bar{x}_k).$$

In a decentralized network, each agent  $i$  solves a local regularized system and produces a local step  $s_{i,k} = -(\tilde{H}_{i,k} + \tilde{\lambda}_{i,k} I)^{-1} \tilde{g}_{i,k}$ . Due to the non-commutativity of averaging and matrix inversion, the

average step  $\bar{s}_k$  generally differs from the step obtained by inverting the averaged system:

$$\bar{s}_k = -\frac{1}{N} \sum_{i=1}^N (\tilde{H}_{i,k} + \tilde{\lambda}_{i,k} I)^{-1} \tilde{g}_{i,k} \neq -\left(\frac{1}{N} \sum_{i=1}^N (\tilde{H}_{i,k} + \tilde{\lambda}_{i,k} I)\right)^{-1} \frac{1}{N} \sum_{i=1}^N \tilde{g}_{i,k},$$

in general. This discrepancy is governed by the inter-agent disagreement in  $(x_{i,k}, g_{i,k}, H_{i,k})$ . DISGREM mitigates it by introducing a multi-round pre-mixing stage that drives the local inputs closer to their network-wide means, tightly controlling the step dispersion.

**2. Transient indefiniteness from imperfect consensus.** Decentralized tracking propagates Hessian increments  $\nabla^2 f_j(x_{j,k+1}) - \nabla^2 f_j(x_{j,k})$  across the network. Although the true local Hessians satisfy  $\nabla^2 f_i(x) \succeq 0$  for convex objectives, the tracked surrogate decomposes as

$$\tilde{H}_{i,k} = \underbrace{\nabla^2 f(\bar{x}_k)}_{\succeq 0} + \underbrace{(\tilde{H}_{i,k} - \nabla^2 f(\bar{x}_k))}_{\text{tracking error}},$$

where the tracking error accumulates gossip-mixed Hessian increments and can have negative eigenvalues. During the transient phase before consensus is reached,  $\lambda_{\min}(\tilde{H}_{i,k})$  may be negative, rendering the local system ill-posed. We introduce an eigenvalue-shift stabilizer  $\delta_{i,k} := \max\{0, -\lambda_{\min}(\tilde{H}_{i,k})\}$ . It makes the local coefficient matrix positive definite whenever  $\tilde{g}_{i,k} \neq 0$ . When  $\tilde{g}_{i,k} = 0$ , the local step is set to zero.

**3. Stepsize-free local regularization.** The vanishing choice  $\lambda_k \asymp \sqrt{\|\nabla f(\bar{x}_k)\|}$  is responsible for the optimal  $\mathcal{O}(1/k^2)$  centralized rate. In the absence of global gradient knowledge, DISGREM sets a local vanishing regularizer  $\lambda_{i,k} = \sqrt{M\|\tilde{g}_{i,k}\|}$ . The scaling parameter  $M \geq L_2$  acts as a damping mechanism: it bounds the local step magnitude ( $\|s_{i,k}\| \leq \sqrt{\|\tilde{g}_{i,k}\|/M}$ ) analogous to a trust-region radius, removing the need for per-iteration stepsize tuning or line search.

## 4.2 DisGrem: full algorithm

Each node  $i$  stores a primal variable  $x_{i,k} \in \mathbb{R}^d$ , a gradient tracker  $g_{i,k} \in \mathbb{R}^d$ , and a Hessian tracker  $H_{i,k} \in \mathbb{R}^{d \times d}$ . For compactness, the result of  $t$  successive neighbor-gossip rounds is written as  $\sum_{j=1}^N [W^t]_{ij} z_j$ . Operationally, with  $\mathcal{N}_i^+ := \mathcal{N}_i \cup \{i\}$ , this quantity is obtained by  $t$  local updates  $z_i^{(\ell+1)} = \sum_{j \in \mathcal{N}_i^+} W_{ij} z_j^{(\ell)}$ ; no direct all-to-all communication is required.

**Algorithm 1** DISGREM

1: **Input:**  $\{x_{i,0}\}$ ,  $W$ ,  $M > 0$ , mixing schedule  $\{\tau_k, t_k\}$ .

2: **Initialize:**  $g_{i,0} \leftarrow \nabla f_i(x_{i,0})$ ,  $H_{i,0} \leftarrow \nabla^2 f_i(x_{i,0})$  for all  $i$ .

3: **for**  $k = 0, 1, 2, \dots$  **do**

4:   **(A) Pre-mixing** ( $\tau_k \geq 1$  neighbor-gossip rounds):

    Initialize  $z_i^{(0)} \leftarrow (x_{i,k}, g_{i,k}, H_{i,k})$ .

    For  $\ell = 0, \dots, \tau_k - 1$ , update

$$z_i^{(\ell+1)} \leftarrow \sum_{j \in \mathcal{N}_i^+} W_{ij} z_j^{(\ell)}.$$

    Set  $(\tilde{x}_{i,k}, \tilde{g}_{i,k}, \tilde{H}_{i,k}) \leftarrow z_i^{(\tau_k)}$ .

5:   **(B) Local Newton step** (each agent  $i$  in parallel):

$\lambda_{i,k} \leftarrow \sqrt{M} \|\tilde{g}_{i,k}\|$ ,  $\delta_{i,k} \leftarrow \max\{0, -\lambda_{\min}(\tilde{H}_{i,k})\}$ .

    If  $\tilde{g}_{i,k} = 0$ , set  $s_{i,k} \leftarrow 0$ ; otherwise solve

$$(\tilde{H}_{i,k} + (\lambda_{i,k} + \delta_{i,k})I)s_{i,k} = -\tilde{g}_{i,k}.$$

$y_{i,k+1} \leftarrow \tilde{x}_{i,k} + s_{i,k}$ .

6:   **(C) Post-mixing** ( $t_k \geq 1$  neighbor-gossip rounds):

    Initialize  $u_i^{(0)} \leftarrow y_{i,k+1}$ .

    For  $\ell = 0, \dots, t_k - 1$ , update

$$u_i^{(\ell+1)} \leftarrow \sum_{j \in \mathcal{N}_i^+} W_{ij} u_j^{(\ell)}.$$

    Set  $x_{i,k+1} \leftarrow u_i^{(t_k)}$ .

7:   **(D) Tracker updates:**

    Initialize  $v_i^{(0)} \leftarrow \tilde{g}_{i,k} + \nabla f_i(x_{i,k+1}) - \nabla f_i(x_{i,k})$ .

    Initialize  $R_i^{(0)} \leftarrow \tilde{H}_{i,k} + \nabla^2 f_i(x_{i,k+1}) - \nabla^2 f_i(x_{i,k})$ .

    For  $\ell = 0, \dots, t_k - 1$ , update

$$v_i^{(\ell+1)} \leftarrow \sum_{j \in \mathcal{N}_i^+} W_{ij} v_j^{(\ell)},$$

$$R_i^{(\ell+1)} \leftarrow \sum_{j \in \mathcal{N}_i^+} W_{ij} R_j^{(\ell)}.$$

    Set  $g_{i,k+1} \leftarrow v_i^{(t_k)}$  and  $H_{i,k+1} \leftarrow R_i^{(t_k)}$ .

8: **end for**

**4.3 Communication cost per iteration**

Each outer iteration of DISGREM involves  $(\tau_k + 2t_k)$  rounds of neighbor communication. In each round every agent  $i$  sends messages to and receives messages from its  $|\mathcal{N}_i|$  neighbors. The payload differs across the three communication stages. Pre-mixing exchanges  $(x, g, H)$ , namely two  $d$ -dimensional vectors and one symmetric Hessian matrix. Post-mixing exchanges only the trial variable  $y$ . The tracker update exchanges one gradient-tracker input and one Hessian-tracker input. The post-mixing step (C) and the tracker-update step (D) must be performed sequentially. Agent  $i$  must first receive the mixed  $y$  variables to compute  $x_{i,k+1}$ ; only then can it evaluate the exact gradients and Hessians at  $x_{i,k+1}$  to form the tracker inputs. Consequently, step (C) requires  $t_k$  rounds and step (D) requires an additional  $t_k$  rounds, giving a total of  $(\tau_k + 2t_k)$  communication rounds per outer iteration.

With double precision (8 bytes per float), the sent message volume per agent per outer iteration

in the uncompressed algorithm is

$$\begin{aligned} C_{\text{iter}}^{\text{send}}(k) &= 8|\mathcal{N}_i| \left[ \tau_k \left( 2d + \frac{d(d+1)}{2} \right) + t_k d + t_k \left( d + \frac{d(d+1)}{2} \right) \right] \\ &= 8|\mathcal{N}_i| (\tau_k + t_k) \left( 2d + \frac{d(d+1)}{2} \right) \text{ bytes.} \end{aligned} \quad (4.1)$$

All communication figures reported in Section 6 use the same stage-wise payload accounting, summed over the directed off-diagonal entries of the mixing matrix and reported in cumulative MB.

#### 4.4 Practical variants

We develop three practical variants of Algorithm 1: two address communication cost and parameter selection individually, while a third combines both mechanisms. All variants share the same four-step structure and differ only in the Hessian-tracker and regularization-parameter modules (see Table 2 at the end of this section for a summary).

CEDISGREM (the prefix ‘‘Ce’’ stands for communication-efficient) reduces communication by compressing Hessian data. The dominant communication cost of DISGREM is the  $\frac{d(d+1)}{2}$ -dimensional Hessian increment  $\nabla^2 f_j(x_{j,k+1}) - \nabla^2 f_j(x_{j,k})$ . CEDISGREM replaces each symmetric Hessian increment  $\Delta H_{j,k} := \nabla^2 f_j(x_{j,k+1}) - \nabla^2 f_j(x_{j,k})$  by a compressed approximation  $\mathcal{C}(\Delta H_{j,k})$ . The implementation supports both element-wise Top- $k$  sparsification and low-rank symmetric truncation; the main experiments use Top- $k$  with a 10% element budget, while Appendix C compares the two choices. For the low-rank option, let  $\Delta H_{j,k} = V \text{diag}(\mu_1, \dots, \mu_d) V^\top$  with  $|\mu_1| \geq \dots \geq |\mu_d|$  and  $V = [v_1, \dots, v_d]$  orthogonal. Define the truncated approximation

$$\hat{\Delta} H_{j,k} := \sum_{\ell=1}^r \mu_\ell v_\ell v_\ell^\top = V_r \Lambda_r V_r^\top,$$

where  $V_r = [v_1, \dots, v_r] \in \mathbb{R}^{d \times r}$  and  $\Lambda_r = \text{diag}(\mu_1, \dots, \mu_r) \in \mathbb{R}^{r \times r}$ . This  $\hat{\Delta} H_{j,k}$  is the best rank- $r$  symmetric approximation of  $\Delta H_{j,k}$  in Frobenius norm, since the best rank- $r$  approximation of a symmetric matrix retains the  $r$  eigenpairs with largest absolute eigenvalues. Thus, transmitting  $(V_r, \Lambda_r)$  costs  $r(d+1)$  floats instead of  $\frac{d(d+1)}{2}$  floats per neighbor per round.

The truncation error satisfies

$$\begin{aligned} \left\| \Delta H_{j,k} - \hat{\Delta} H_{j,k} \right\|_F &= \left( \sum_{\ell=r+1}^d \mu_\ell^2 \right)^{1/2} \\ &\leq |\mu_{r+1}(\Delta H_{j,k})| \sqrt{d-r}, \end{aligned}$$

where  $\mu_{r+1}(\Delta H_{j,k})$  denotes the  $(r+1)$ -th largest absolute eigenvalue. For Top- $k$ ,  $\mathcal{C}(\Delta H_{j,k})$  retains the largest-magnitude entries and symmetrizes the result. The compression error can be viewed as an additional Hessian-tracker perturbation. In the experiments, both Top- $k$  and low-rank compression reduce communication with modest iteration overhead when the compression level is not too aggressive (Section 6.3).

*Remark 4.1.* The exact eigendecomposition of  $\Delta H_{j,k} \in \mathbb{R}^{d \times d}$  costs  $\mathcal{O}(d^3)$  per agent per iteration—the same order as the Newton-system solve. When  $d$  is large, randomized singular value decomposition (SVD) (cost  $\mathcal{O}(d^2 r)$ ) or Nyström-type approximations can replace the exact decomposition. The additional approximation error enters the tracker dispersion additively.

ADADISGREM introduces an adaptive scaling factor. When  $M$  is fixed, choosing a good value typically relies on problem-specific curvature information (see Section 4.5). ADADISGREM instead

updates a local scaling value  $\hat{M}_{i,k}$  from a secant ratio:

$$\hat{L}_{i,k} \leftarrow \frac{\|\nabla^2 f_i(x_{i,k}) - \nabla^2 f_i(x_{i,k-1})\|_2}{\|x_{i,k} - x_{i,k-1}\|},$$

$$\hat{M}_{i,k} \leftarrow \max(\gamma \hat{M}_{i,k-1}, \zeta \min(\hat{L}_{i,k}, \eta_c \hat{M}_{i,0})),$$

where  $\zeta \geq 1$  is a safety inflation factor,  $\gamma \in (0, 1)$  is the decay factor, and  $\eta_c > 0$  is the upper-bound parameter. If  $x_{i,k} = x_{i,k-1}$ , we set  $\hat{L}_{i,k} = 0$ . The vanishing regularizer becomes  $\lambda_{i,k} = \sqrt{\hat{M}_{i,k} \|\tilde{g}_{i,k}\|}$ . The decay factor allows  $\hat{M}_{i,k}$  to decrease when the local curvature scale is moderate, enabling larger Newton steps near the solution, while the upper bound damps isolated large secant ratios. The quantity  $\hat{L}_{i,k}$  is a per-iterate secant indicator, distinct from the static proxy  $H_{\max}^0 := \max_i \|\nabla^2 f_i(x_0)\|_2$  used to scale the baseline  $M$  (Section 4.5). In the experiments, ADADISGREM serves as an empirical parameter-selection variant of the fixed- $M$  method. Section 6.4 studies its robustness across a  $100\times$  range of initial  $\hat{M}_{i,0}$ .

CEADADISGREM applies both Hessian compression (Ce) and adaptive  $M$  (Ada) simultaneously. Because the compressed Hessian increments perturb the secant-based scaling rule, Section 6.3 reports this combined variant separately from the fixed- $M$  compression results.

Table 2 summarizes the full DISGREM family. All members share the core structure of Algorithm 1; differences are confined to the Hessian-tracker and regularization-parameter modules.

Table 2: The DISGREM algorithm family. All variants use the same four-step structure (Algorithm 1); differences are confined to the Hessian communication and the choice of  $M$ .

Variant	Hessian	$M$	Extra parameter(s)
DISGREM	exact tracking	fixed	$M$
CEDISGREM	compressed + lazy	fixed	$M$ , comp., budget, $K_{\text{lazy}}$
ADADISGREM	exact tracking	adaptive	$\hat{M}_{i,0}$ , $\gamma$ , $\zeta$ , $\eta_c$
CEADADISGREM	compressed + lazy	adaptive	Ada params, comp., budget, $K_{\text{lazy}}$

## 4.5 Practical guidelines for parameter selection

The theoretical convergence requires  $M \geq L_2$  (Theorem 5.20). When the Hessian Lipschitz constant  $L_2$  is unknown,  $M$  acts as a robustness parameter: larger values increase damping and ensure well-conditioning, though potentially slowing asymptotic convergence. A practical baseline choice is  $M = M_{\text{fac}} \cdot H_{\max}^0$ , where  $H_{\max}^0 := \max_i \|\nabla^2 f_i(x_0)\|_2$  is a readily computable baseline curvature proxy and  $M_{\text{fac}} \in [0.1, 15]$  is a tuning factor that scales with the problem’s ill-conditioning. ADADISGREM replaces this fixed choice by the online secant rule described above.

The communication depths are chosen by the logarithmic schedule

$$\tau_k = t_k = \left\lceil \frac{p \log(k+2) + c_{\text{mix}}}{-\log \rho} \right\rceil,$$

with a fixed constant  $c_{\text{mix}} \geq 0$ . In the numerical experiments we impose a maximum communication depth once the tested accuracy range has been reached.

For Hessian compression in CEDISGREM, Top- $k$  with a 10% element budget is used in the main experiments. For low-rank compression,  $r = \lceil d/5 \rceil$  serves as a robust nominal value, while  $r = 1$  often suffices for diagonally dominant objectives. To further reduce communication, the Hessian tracker update (step (D) of Algorithm 1) can be executed every  $K_{\text{lazy}}$ -th iteration. Reusing the previous Hessian for  $K_{\text{lazy}} \in \{5, 10\}$  consecutive steps reduces payload bytes with minimal impact on convergence for slowly varying problems.

## 5 Convergence analysis

Throughout this section we assume Assumptions 3.1 and 5.1, the parameter requirement  $M \geq L_2$ , and that Algorithm 1 is run with the initialization  $g_{i,0} = \nabla f_i(x_{i,0})$ ,  $H_{i,0} = \nabla^2 f_i(x_{i,0})$ . Complete proofs are collected in Appendix B, and the dispersion-decay and burn-in construction is detailed in Appendix A.

The convergence argument proceeds through the following chain of reductions. Averaging identities (§5.2) show that the average iterate evolves as  $\bar{x}_{k+1} = \bar{x}_k + \bar{s}_k$  and that tracked averages equal the averages of exact local gradients and Hessians evaluated at the current local iterates. Reference step and bridge bounds (§5.3–§5.4) introduce a “centralized reference” step  $s_k^{\text{ref}}$  and bound its gap from  $\bar{s}_k$  in terms of tracker dispersions. Stabilizer and step-dispersion control (§5.5–§5.6) relate the eigenvalue shift  $\delta_{i,k}$  and the step dispersion to gradient/Hessian tracker dispersions. These three ingredients are combined in §5.7 to verify that the average iterate satisfies an inexact Newton residual bound, from which a 3/2-recursion on the optimality gap (§5.8) yields the  $\mathcal{O}(\varepsilon^{-1})$  rate.

In summary, the logical dependency chain is: averaging identities  $\rightarrow$  reference step  $\rightarrow$  stabilizer/dispersion bounds  $\rightarrow$  inexact Newton condition (Proposition 5.14)  $\rightarrow$  3/2-recursion on the steady subsequence (Lemma 5.18)  $\rightarrow$  global complexity (Theorem 5.20). Appendix A supplies the burn-in index  $K_0(\varepsilon)$ .

The proof combines two independent stages (detailed in Remark 5.24 after the main theorem). The reader interested only in the final result may skip directly to Theorem 5.20.

### 5.1 Bounded trajectory and local constants

**Assumption 5.1** (Bounded iterates). *There exists a solution  $x_\star \in \arg \min f$  and a finite constant  $D > 0$  such that the iterates generated by Algorithm 1 satisfy*

$$\|\bar{x}_k - x_\star\| \leq D, \quad \|x_{i,k} - x_\star\| \leq D, \quad \|\tilde{x}_{i,k} - x_\star\| \leq D, \quad (5.1)$$

for all  $k \geq 0$  and all  $i \in \{1, \dots, N\}$ .

Under Assumption 5.1, we define all subsequent constants on the compact set  $\{x : \|x - x_\star\| \leq D\}$ . Since each  $\nabla f_i$  is globally  $L_1$ -Lipschitz, the Hessian bound

$$M_{H,\max} := L_1 \quad (5.2)$$

is valid for all iterates and is independent of the compact set.

*Remark 5.2.* Since each  $f_i$  is twice continuously differentiable (Assumption 3.1(i)) and the iterates are confined to a compact set by Assumption 5.1, the quantity  $\sup_{x \in \mathcal{B}} \max_{1 \leq i \leq N} \|\nabla^2 f_i(x)\|_2$  is automatically finite for any bounded  $\mathcal{B} \subset \mathbb{R}^d$ . No separate assumption is needed.

*Remark 5.3.* Prior decentralized second-order analyses [12, 13, 28] posit a bounded static heterogeneity constant  $\sigma_H := \sup_{\|x-x_\star\| \leq D} \frac{1}{\sqrt{N}} \|(I - (\frac{1}{N} \mathbf{1}\mathbf{1}^\top) \otimes I_{d^2}) \mathcal{H}(\mathbf{1} \otimes x)\|$ . We avoid this entirely: Hessian-tracker dispersion is controlled by an increment-based recursion (Appendix A, Lemma A.8) that tracks mismatch through Lipschitz-continuous differences  $\nabla^2 F(X_{k+1}) - \nabla^2 F(X_k)$ , so no accuracy floor linked to  $\sigma_H$  appears in the final bounds.

### 5.2 Averaging identities

The starting point of the analysis is that doubly stochastic mixing preserves averages, so the mean iterate and mean trackers evolve as if they were computed by a single “virtual agent.”

Define averages  $\bar{x}_k := \frac{1}{N} \sum_{i=1}^N x_{i,k}$  and similarly for other variables. Define pre-mixed averages

$$\begin{aligned}\tilde{x}_k &:= \frac{1}{N} \sum_{i=1}^N \tilde{x}_{i,k}, & \tilde{g}_k &:= \frac{1}{N} \sum_{i=1}^N \tilde{g}_{i,k}, \\ \tilde{H}_k &:= \frac{1}{N} \sum_{i=1}^N \tilde{H}_{i,k}.\end{aligned}$$

Define the average step  $\bar{s}_k := \frac{1}{N} \sum_{i=1}^N s_{i,k}$ .

**Lemma 5.4.** *For all  $k \geq 0$ ,  $\tilde{x}_k = \bar{x}_k$  and  $\tilde{x}_{k+1} = \bar{x}_k + \bar{s}_k$ .*

*Proof.* Immediate from  $W\mathbf{1} = \mathbf{1}$  (doubly stochastic), which gives  $\frac{1}{N}\mathbf{1}^\top(W^t \otimes I_d) = \frac{1}{N}\mathbf{1}^\top \otimes I_d$  for every integer  $t \geq 1$ .  $\square$

**Lemma 5.5.** *If Algorithm 1 is initialized by  $g_{i,0} = \nabla f_i(x_{i,0})$ , then for all  $k \geq 0$ ,*

$$\bar{g}_k := \frac{1}{N} \sum_{i=1}^N g_{i,k} = \frac{1}{N} \sum_{i=1}^N \nabla f_i(x_{i,k}), \quad \tilde{g}_k = \bar{g}_k.$$

*Proof.* By induction using  $W\mathbf{1} = \mathbf{1}$  and the telescoping form of the tracker update (step (D)).  $\square$

**Lemma 5.6.** *If Algorithm 1 is initialized by  $H_{i,0} = \nabla^2 f_i(x_{i,0})$ , then for all  $k \geq 0$ ,*

$$\bar{H}_k := \frac{1}{N} \sum_{i=1}^N H_{i,k} = \frac{1}{N} \sum_{i=1}^N \nabla^2 f_i(x_{i,k}), \quad \tilde{H}_k = \bar{H}_k.$$

*Proof.* The Hessian tracker has the same telescoping form as the gradient tracker in Lemma 5.5: multiplication by  $W$  preserves the block average, and the Hessian increment  $\nabla^2 f_i(x_{i,k+1}) - \nabla^2 f_i(x_{i,k})$  telescopes in the averaged update.  $\square$

### 5.3 Well-posed local solves and a reference step

With the averaging identities in hand, we next introduce the reference step  $s_k^{\text{ref}}$ : the Newton step that a centralized agent would compute using the averaged Hessian and gradient. The gap  $\|\bar{s}_k - s_k^{\text{ref}}\|$  then quantifies how much the decentralized updates deviate from this ideal step.

Algorithm 1 sets

$$\begin{aligned}\lambda_{i,k} &:= \sqrt{M \|\tilde{g}_{i,k}\|}, \\ \delta_{i,k} &:= \max\{0, -\lambda_{\min}(\tilde{H}_{i,k})\}, \\ \tilde{\lambda}_{i,k} &:= \lambda_{i,k} + \delta_{i,k}.\end{aligned}$$

Define

$$A_{i,k} := \tilde{H}_{i,k} + \tilde{\lambda}_{i,k}I,$$

When  $\tilde{g}_{i,k} \neq 0$ , the coefficient matrix is positive definite and Algorithm 1 sets  $s_{i,k} := -A_{i,k}^{-1} \tilde{g}_{i,k}$ . When  $\tilde{g}_{i,k} = 0$ , Algorithm 1 uses the convention  $s_{i,k} = 0$ . All inverse-based estimates below are stated on indices where the corresponding regularization lower bound is positive; in particular, Lemma 5.12 assumes  $\underline{\lambda}_k > 0$ . Define averaged quantities

$$\tilde{\lambda}_k := \frac{1}{N} \sum_{i=1}^N \tilde{\lambda}_{i,k}, \quad A_k^{\text{ref}} := \tilde{H}_k + \tilde{\lambda}_k I.$$

Whenever  $A_k^{\text{ref}}$  is nonsingular, the reference step is defined by  $s_k^{\text{ref}} = -(A_k^{\text{ref}})^{-1} \tilde{g}_k$ . In the analysis below this definition is used only on indices where the regularization lower bound is positive.

**Lemma 5.7.** *For all  $i, k$ , the local step satisfies*

$$M \|s_{i,k}\| \leq \lambda_{i,k} \quad \text{and hence} \quad L_2 \|s_{i,k}\| \leq \lambda_{i,k}.$$

**Lemma 5.8.** *For all  $k$ ,*

$$L_2 \|\bar{s}_k\| \leq \frac{1}{N} \sum_{i=1}^N \lambda_{i,k} \leq \tilde{\lambda}_k.$$

#### 5.4 Bridge bounds: tracked averages versus true quantities

The reference step uses the tracked averages  $\tilde{g}_k, \tilde{H}_k$  rather than the true gradient  $g_k := \nabla f(\bar{x}_k)$  and true Hessian  $\nabla^2 f(\bar{x}_k)$ . By Lemma 5.5,  $\tilde{g}_k = \frac{1}{N} \sum_{i=1}^N \nabla f_i(x_{i,k})$ , which coincides with  $\nabla f(\bar{x}_k)$  only at exact consensus ( $x_{i,k} = \bar{x}_k$  for all  $i$ ). Away from consensus the discrepancy is controlled by the bridge lemmas below, which quantify it in terms of the post-mixing spatial disagreement  $D(X_k)$ . All constants depending on iterate boundedness (e.g.,  $L_1, L_2$ ) are evaluated on the compact set fixed by Assumption 5.1.

The post-mixing disagreement (RMS) is  $D(X_k) = (\frac{1}{N} \sum_{i=1}^N \|x_{i,k} - \bar{x}_k\|^2)^{1/2}$ , i.e., the dispersion  $D(\cdot)$  defined in Section 3 applied to the stacked iterate  $X_k$ .

**Lemma 5.9.** *For every  $k$ ,*

$$\|\nabla f(\bar{x}_k) - \tilde{g}_k\| \leq L_1 D(X_k).$$

**Lemma 5.10.** *For every  $k$ ,*

$$\|\nabla^2 f(\bar{x}_k) - \tilde{H}_k\|_2 \leq L_2 D(X_k).$$

#### 5.5 The eigenvalue-shift stabilizer $\delta_{i,k}$

The stabilizer  $\delta_{i,k}$  makes the local coefficient matrix positive definite whenever  $\tilde{g}_{i,k} \neq 0$ . When  $\tilde{g}_{i,k} = 0$ , Algorithm 1 uses the convention  $s_{i,k} = 0$ . Therefore the local step is well posed in all cases. Because it acts as an additive bias in  $\lambda_{i,k}$ , we need to show that its average  $\bar{\delta}_k$  is controlled by quantities that vanish as consensus improves.

Define the stabilizer average

$$\bar{\delta}_k := \frac{1}{N} \sum_{i=1}^N \delta_{i,k}.$$

**Lemma 5.11.** *For every  $k$  and every  $i$ ,*

$$0 \leq \delta_{i,k} \leq \|\tilde{H}_{i,k} - \nabla^2 f(\bar{x}_k)\|_2.$$

Consequently,

$$\begin{aligned} \bar{\delta}_k &\leq \Delta_k^H + L_2 D(X_k), \\ \Delta_k^H &:= \frac{1}{N} \sum_{i=1}^N \|\tilde{H}_{i,k} - \tilde{H}_k\|_2. \end{aligned}$$

## 5.6 Step dispersion via a resolvent identity

The inexact Newton condition (Proposition 5.14 below) requires three quantities to be small: the step dispersion  $\|\bar{s}_k - s_k^{\text{ref}}\|$ , the gradient bridge error  $L_1 D(X_k)$ , and the Hessian bridge error  $L_2 D(X_k)$ . The latter two are already controlled by Lemmas 5.9–5.10; this subsection handles the first. The key tool is a resolvent identity that factorizes the difference of two linear-system solutions through their coefficient matrices.

Define dispersions

$$\begin{aligned}\Delta_k^g &:= \frac{1}{N} \sum_{i=1}^N \|\tilde{g}_{i,k} - \tilde{g}_k\|, \\ \Delta_k^\lambda &:= \frac{1}{N} \sum_{i=1}^N |\tilde{\lambda}_{i,k} - \tilde{\lambda}_k|, \\ \underline{\lambda}_k &:= \min_{1 \leq i \leq N} \tilde{\lambda}_{i,k}.\end{aligned}$$

**Lemma 5.12.** *For every  $k$  with  $\underline{\lambda}_k > 0$ ,*

$$\|\bar{s}_k - s_k^{\text{ref}}\| \leq \frac{1}{\underline{\lambda}_k} \Delta_k^g + \frac{\|\tilde{g}_k\|}{\underline{\lambda}_k \tilde{\lambda}_k} (\Delta_k^H + \Delta_k^\lambda).$$

**Lemma 5.13.** *If  $\tilde{g}_k \neq 0$  and the relative gradient dispersion condition*

$$\max_{1 \leq i \leq N} \|\tilde{g}_{i,k} - \tilde{g}_k\| \leq \alpha_d \|\tilde{g}_k\|, \quad \text{for some } \alpha_d \in (0, 1), \quad (5.3)$$

then

$$\Delta_k^\lambda \leq \frac{\sqrt{M}}{\sqrt{1 - \alpha_d}} \cdot \frac{\Delta_k^g}{\sqrt{\|\tilde{g}_k\|}} + 2\bar{\delta}_k. \quad (5.4)$$

## 5.7 Inexact regularized Newton condition for the average step

Collecting the bridge, stabilizer, and step-dispersion bounds, we verify that the average iterate  $\bar{x}_k$  satisfies a standard inexact regularized Newton condition once the burn-in phase is complete, that is, for  $k \geq K_0(\varepsilon)$ , where  $K_0$  is the burn-in index from Proposition A.15. This is the key step, as it permits invoking the one-step descent lemma from the centralized analysis.

Specifically, we define  $g_k := \nabla f(\bar{x}_k)$ ,  $\lambda_k := \tilde{\lambda}_k$ , and  $r_k := (\nabla^2 f(\bar{x}_k) + \lambda_k I)\bar{s}_k + g_k$ .

**Proposition 5.14.** *If the following hold at iteration  $k$  for some  $\eta \in (0, 1)$ :*

1. *Dispersion control:*

$$\|\bar{s}_k - s_k^{\text{ref}}\| \leq \frac{\eta}{8} \cdot \frac{\lambda_k}{M_{H,\max} + \lambda_k} \|\bar{s}_k\|.$$

2. *Gradient bridge accuracy:*

$$L_1 D(X_k) \leq \frac{\eta}{8} \lambda_k \|\bar{s}_k\|.$$

3. *Hessian bridge accuracy:*

$$L_2 D(X_k) \leq \frac{\eta}{8} \lambda_k.$$

then

$$\|r_k\| \leq \eta \lambda_k \|\bar{s}_k\|, \quad L_2 \|\bar{s}_k\| \leq \lambda_k.$$

## 5.8 Descent and global rates

The preceding subsections have established the four building blocks of the proof pipeline: the average iterate satisfies an inexact regularized Newton condition (Proposition 5.14) once the burn-in phase ends. The remaining descent step follows the centralized analysis of Mishchenko [5]: a one-step descent lemma yields a 3/2-power recursion on the optimality gap, from which the global complexity bound follows.

We introduce the optimality gap  $\Phi_k := f(\bar{x}_k) - f_*$ .

**Lemma 5.15.** *Assume*

$$\|(\nabla^2 f(\bar{x}_k) + \lambda_k I)\bar{s}_k + g_k\| \leq \eta \lambda_k \|\bar{s}_k\|, \quad L_2 \|\bar{s}_k\| \leq \lambda_k,$$

for some  $\eta \in (0, 5/6)$ . Then

$$f(\bar{x}_{k+1}) \leq f(\bar{x}_k) - \left(1 - \eta - \frac{1}{6}\right) \lambda_k \|\bar{s}_k\|^2.$$

**Lemma 5.16.** *Under the conditions of Lemma 5.15,*

$$\|g_{k+1}\| \leq \left(1 + \eta + \frac{1}{2}\right) \lambda_k \|\bar{s}_k\|.$$

We partition the iteration indices into *steady* iterations (where the gradient norm does not drop sharply) and *super-descent* iterations (where it drops by at least a factor of 4):

$$\begin{aligned} \mathcal{I} &:= \{k \geq 0 : \|g_{k+1}\| \geq \frac{1}{4} \|g_k\|\}, \\ \mathcal{S} &:= \{k \geq 0 : \|g_{k+1}\| < \frac{1}{4} \|g_k\|\}. \end{aligned}$$

The following lemma establishes a sharp decrease in the optimality gap during steady-descent iterations. The auxiliary requirement  $\lambda_k \leq C_\lambda \sqrt{\|g_k\|}$  is rigorously verified in Appendix B (Lemma B.1).

**Lemma 5.17.** *If Proposition 5.14 holds for all  $k$  with some  $\eta \leq 1/12$  and there exists  $C_\lambda > 0$  such that*

$$\lambda_k \leq C_\lambda \sqrt{\|g_k\|} \quad \text{for all } k \text{ with } g_k \neq 0.$$

Then there exists  $\nu > 0$  such that for all  $k \in \mathcal{I}$ ,

$$\Phi_k - \Phi_{k+1} \geq \nu \Phi_k^{3/2}.$$

**Lemma 5.18.** *If  $\Phi_{k+1} \leq \Phi_k - \nu \Phi_k^{3/2}$  for some  $\nu > 0$  and all  $k$ , then*

$$\Phi_k \leq \frac{4}{\nu^2 (k+2)^2}.$$

Throughout we use the logarithmic mixing schedule

$$\tau_k = t_k = \left\lceil \frac{p \log(k+2) + c_{\text{mix}}}{-\log \rho} \right\rceil, \quad k \geq 0, \quad (5.5)$$

where  $c_{\text{mix}} \geq 0$  is a fixed constant. Then  $\rho^{\tau_k} \leq e^{-c_{\text{mix}}}(k+2)^{-p}$ ; details and motivation are given in Appendix A.

*Remark 5.19.* The schedule (5.5) requires the spectral gap  $1-\rho$ , or equivalently,  $\rho = \|W - (\frac{1}{N}\mathbf{1}\mathbf{1}^\top)\|_2$ . Computing  $\rho$  exactly is a centralized operation; in a fully decentralized implementation one may use any certified upper bound  $\hat{\rho} \geq \rho$  available for the chosen weight matrix. Overestimating  $\rho$  increases each  $\tau_k$  by a constant factor but does not affect the  $\mathcal{O}(\varepsilon^{-1})$  iteration complexity. If only a rough network description is available, one may use a conservative upper bound; the asymptotic statement is unchanged.

**Theorem 5.20.** *If Assumptions 3.1 and 5.1 hold and  $M \geq L_2$ , then the following is true. Fix  $p \geq 3$  and run DISGREM with the logarithmic mixing schedule (5.5). Then for every target accuracy  $0 < \varepsilon \leq 1$ , there exist a finite burn-in index  $K_0(\varepsilon)$  (depending on the spectral gap, Lipschitz constants, initial dispersions, and  $\varepsilon$ ; see Proposition A.15) and a constant  $C_K > 0$  (independent of  $\varepsilon$ ) such that the total number of outer iterations to achieve  $\|\nabla f(\bar{x}_k)\| \leq \varepsilon$  satisfies*

$$K(\varepsilon) \leq K_0(\varepsilon) + C_K \varepsilon^{-1}.$$

*In particular, the post-burn-in phase requires at most  $\mathcal{O}(\varepsilon^{-1})$  iterations. Since  $p \geq 3$  implies  $K_0(\varepsilon) = \mathcal{O}(\varepsilon^{-1})$  by Remark 5.21, the total iteration complexity is  $K(\varepsilon) = \mathcal{O}(\varepsilon^{-1})$ , matching the centralized regularized Newton complexity of Mishchenko [5], and under the schedule (5.5), for a fixed connected network, the total number of neighbor communication rounds is  $\mathcal{O}(\varepsilon^{-1} \log(1/\varepsilon))$ . More explicitly, its dependence on the mixing rate is  $\mathcal{O}((1-\rho)^{-1} \varepsilon^{-1} \log(1/\varepsilon))$  as  $\rho \rightarrow 1$ .*

*Remark 5.21.* For  $0 < \varepsilon \leq 1$ , the direct verification of Proposition 5.14 uses the explicit step-dispersion estimate in Proposition A.15. Because  $\|\tilde{g}_k\| \gtrsim \varepsilon$ ,  $\|s_k^{\text{ref}}\| \gtrsim \varepsilon$ , and  $\lambda_k \gtrsim \sqrt{\varepsilon}$  on the burn-in tail, a conservative sufficient set of conditions for Item 1 is

$$\Delta_k^g = \mathcal{O}(\varepsilon^2), \quad \Delta_k^H = \mathcal{O}(\varepsilon^{3/2}), \quad D(X_k) = \mathcal{O}(\varepsilon^{3/2}),$$

up to constants. Since  $\Delta_k^g, \Delta_k^H = \mathcal{O}(k^{-(p-1)})$  by Proposition A.14, this gives the conservative burn-in estimate

$$K_0(\varepsilon) = \mathcal{O}(\varepsilon^{-2/(p-1)}).$$

If one keeps only  $p > 2$ , the same burn-in estimate gives the more general bound

$$K(\varepsilon) = \mathcal{O}\left(\varepsilon^{-1} + \varepsilon^{-2/(p-1)}\right).$$

In particular, for  $p \geq 3$ , the burn-in estimate is no larger than the  $\mathcal{O}(\varepsilon^{-1})$  post-burn-in term, and hence  $K(\varepsilon) = \mathcal{O}(\varepsilon^{-1})$ .

The dependence on the spectral gap enters through the mixing schedule:  $\tau_k = \lceil (p \log(k+2) + c_{\text{mix}})/(-\log \rho) \rceil$  implies that each outer iteration uses  $\mathcal{O}((1-\rho)^{-1} \log k)$  communication rounds; the constant  $c_{\text{mix}}$  affects only the constant. Here  $-1/\log \rho \approx (1-\rho)^{-1}$  for  $\rho$  near 1. The total communication-round budget is therefore

$$\mathcal{O}((1-\rho)^{-1} \varepsilon^{-1} \log(1/\varepsilon)),$$

exhibiting the same linear dependence on the inverse spectral gap as repeated gossip mixing. On very sparse graphs ( $\rho \rightarrow 1$ ), the per-iteration communication overhead grows, but the iteration count remains network-independent.

*Remark 5.22* ( $\varepsilon$ -independence of the algorithm). The algorithm is not restarted or retuned for a prescribed  $\varepsilon$ ; the logarithmic mixing schedule (5.5) is fixed independently of the target accuracy. The index  $K_0(\varepsilon)$  enters only in the complexity proof as the first index after which the scheduled consensus errors fall below accuracy-dependent thresholds.

*Remark 5.23* (Dimension dependence of the constants). The constants  $C_K$  and  $K_0(\varepsilon)$  in Theorem 5.20 depend on  $d, N, L_1, L_2, D, M$ , and the spectral gap  $1 - \rho$ . In particular, the Frobenius–spectral norm conversion in the dispersion bounds introduces a factor  $\sqrt{d}$ ; hence the iteration bound, while independent of  $\varepsilon$  up to  $\mathcal{O}(\varepsilon^{-1})$ , is not dimension-free.

*Remark 5.24*. The proof of Theorem 5.20 combines two independent analyses, distinct from the per-iteration reduction chain in Sections 5.2–5.8 (which is used in Stage 2). In Stage 1 (dispersion decay; Proposition A.14, Appendix A), the logarithmic schedule makes tracker dispersions decay polynomially on the bounded trajectory of Assumption 5.1. In Stage 2 (descent), once the consensus errors meet the burn-in requirements (after  $K_0(\varepsilon)$  iterations), the per-iteration chain verifies an inexact regularized Newton recursion (Proposition 5.14), and the 3/2-recursion (Lemma 5.18) gives  $\mathcal{O}(\varepsilon^{-1})$  further iterations. The two stages are self-contained and do not depend on each other’s conclusions.

## 5.9 Strong convexity and local superlinear convergence

The preceding results require only convexity. When the objective is locally strongly convex near the optimum, the stabilizer term  $\bar{\delta}_k$  becomes negligible relative to  $\|g_k\|$ , recovering the exact Newton regime and, with it, local  $Q$ -superlinear convergence.

**Assumption 5.25.** *The average objective  $f$  is  $\mu$ -strongly convex on the bounded set  $\{x : \|x - x_\star\| \leq D\}$  (where  $D$  is given by Assumption 5.1):  $\nabla^2 f(x) \succeq \mu I$  for all  $\|x - x_\star\| \leq D$ .*

**Lemma 5.26.** *If Assumptions 3.1, 5.1, and 5.25 hold, then the following is true. Fix any exponent  $\gamma > 0$ . Let*

$$G_g := \sup_{k \geq 0} \max_{1 \leq i \leq N} \|\tilde{g}_{i,k}\| \in [0, \infty),$$

*which is finite by Lemma A.9. Suppose that for all  $k$  large enough (and  $k \geq 1$ ) the mixing depths satisfy*

$$\max\{\rho^{\tau_k}, \rho^{t_{k-1}}\} \leq \frac{1}{C_\delta} \|g_k\|^{1+\gamma}, \quad (5.6)$$

*where  $C_\delta := \hat{C}_H + L_2(2D + \sqrt{G_g/M})$  and  $\hat{C}_H := B_H + 2\sqrt{d}L_2D$ , where  $B_H := \sup_{k \geq 0} D(\tilde{\mathcal{H}}_k) < \infty$  is the uniform Hessian-tracker dispersion bound from Lemma A.10. Then, for all sufficiently large  $k$ ,*

$$\bar{\delta}_k = o(\|g_k\|) \quad \text{and more precisely} \quad \bar{\delta}_k \leq \|g_k\|^{1+\gamma}.$$

**Theorem 5.27.** *Under the hypotheses of Theorem 5.20, suppose in addition that Assumption 5.25 holds, Proposition 5.14 holds for all sufficiently large  $k$  with some  $\eta \in (0, 1/12]$ , and there exists a post-burn-in tail on which  $\|g_k\| \rightarrow 0$  and a constant  $\gamma > 0$  such that, for all sufficiently large  $k$ ,*

$$\max\{\rho^{\tau_k}, \rho^{t_{k-1}}\} \leq \frac{1}{C_\delta} \|g_k\|^{1+\gamma}, \quad \Delta_k^g \leq C_g \|g_k\|^{1+\gamma} \quad (5.7)$$

*for some constant  $C_g > 0$ , then there exist constants  $C_{sc} > 0$  and  $k_{sc}$  such that, for all  $k \geq k_{sc}$ ,*

$$\|\nabla f(\bar{x}_{k+1})\| \leq C_{sc} \|\nabla f(\bar{x}_k)\|^{3/2}.$$

*Remark 5.28.* The logarithmic schedule in Theorem 5.20 is sufficient for the global  $\mathcal{O}(\varepsilon^{-1})$  rate. The local superlinear result uses the relative accuracy condition (5.7), which requires the consensus and tracking errors to decay relative to the current gradient norm along the local tail.

## 6 Numerical experiments

This section evaluates the practical performance of the DISGREM family using the logarithmic communication rule motivated by the analysis. All main convergence experiments report statistics over 20 independent Monte Carlo (MC) trials with randomized starting points and random Erdős–Rényi graphs. Four DISGREM variants are compared against six first- and second-order baselines on nine objectives spanning well-conditioned and ill-conditioned convex problems, real-data logistic regression, and four nonconvex objectives.

### 6.1 Experimental setup

We use  $N=10$  agents communicating over an Erdős–Rényi (ER) random graph with edge probability  $p_{\text{er}}=0.5$  (regenerated per trial). The Metropolis–Hastings doubly stochastic mixing matrix  $W$  yields spectral gap  $1-\rho \approx 0.08$  ( $\rho \approx 0.92$ ; typical range  $\rho \in [0.88, 0.96]$  across 20 trials), representing a moderately sparse topology. The analysis uses the same logarithmic depth for all tracked quantities. In the experiments, the vector mixing depths in the DISGREM family are chosen as

$$\tau_k = t_k = \min \left\{ 10, \left\lceil \frac{3 \log(k+2) + 2}{-\log \rho} \right\rceil \right\},$$

which is the logarithmic rule (5.5) with  $p = 3$  and  $c_{\text{mix}} = 2$ , implemented with a maximum depth of 10 over the tested tolerance range. This choice matches the smallest exponent covered by the  $\mathcal{O}(\varepsilon^{-1})$  total-complexity statement in Theorem 5.20; the maximum depth is sufficient for all tolerances reported below. For the full-matrix variants, Hessian pre-mixing is limited to three matrix rounds. For the communication-efficient variants, Hessian-matrix mixing is limited to two matrix rounds while vector mixing uses the full  $\tau_k$  and  $t_k$  depths. These matrix-round limits reduce payload while preserving the vector-mixing schedule used by the analysis. Baselines retain their standard consensus settings, and all comparisons report cumulative communication cost so that different per-iteration communication patterns are accounted for explicitly.

We compare ten methods in three groups. The proposed DISGREM family comprises four variants: DISGREM (Algorithm 1), CEDISGREM (communication-efficient Hessian tracking using Top- $k$  sparsification with a 10% nominal budget, with low-rank alternatives studied in Appendix C), ADADISGREM (adaptive  $M$  via secant-based Lipschitz estimation), and CEADADISGREM (adaptive + compressed). In the Ce variants, the lazy Hessian-update period and compression budget are adjusted with the current communication depth so that communication is reduced early while more Hessian information is retained as the requested consensus depth increases. The regularization scaling is  $M = M_{\text{fac}} \cdot H_{\text{max}}^0$  where  $H_{\text{max}}^0 = \max_i \|\nabla^2 f_i(x_0)\|_2$ ; per-function  $M_{\text{fac}}$  values are listed in Table 4. The adaptive variant ADADISGREM replaces this fixed scaling by online secant-based updates (Section 6.4).

Two first-order baselines are included: EXTRA [11] and DIGing [9]. Four second-order baselines complete the comparison: DQM [3], ESOM [28], SONATA [12], and Network-GIANT [13]. First-order baselines use a Lipschitz-scaled stepsize  $\alpha = \alpha_{\text{base}}/H_{\text{max}}^0$ ; for each function,  $\alpha_{\text{base}}$  is selected from  $\{0.01, 0.1, 0.5, 1.0\}$  as the value giving the fastest convergence without divergence over 5 preliminary runs (Table 4). Second-order baselines (DQM, ESOM, SONATA, Network-GIANT) use their published parameters; SONATA and Network-GIANT solve local subproblems to machine precision via a direct solver. The baselines use their standard consensus settings. Because the DISGREM family has a three-stage gossip structure and carries Hessian payloads, its per-iteration byte cost can exceed that of single-stage baselines; cross-method fairness is therefore assessed through the cumulative communication cost (MB) reported in Figure 2. We use *light, problem-class-level tuning*: the per-function  $M_{\text{fac}}$  for the proposed family and the per-function  $\alpha_{\text{base}}$  for

first-order baselines are both selected from small discrete grids via a handful of preliminary runs, while second-order baselines retain their published settings. Sensitivity sweeps in Appendix C (Figure 16) show that broad changes in the second-order baselines’ hyperparameters do not remove their stagnation on hard instances such as LOGSUMEXP. Code to reproduce all experiments is available at <https://github.com/huwei0121/DisGRem>.

We test on nine objective functions (Table 3); all synthetic functions use  $d=30$ , while the two logistic regression problems inherit  $d=22$  from the SVMGUIDE3 dataset. See Table 4 for per-function algorithmic parameters. Five objectives are convex: (i) RIDGE ( $\ell_2$ -regularized least squares,  $\lambda=10^{-3}$ ); (ii) QUADBAD (heterogeneous ill-conditioned quadratic,  $\kappa=10^3$ ); (iii) LOGSUMEXP (smooth approximation of the max function [32],  $\sigma=0.5$ ); (iv) HUBER (pseudo-Huber loss [33],  $\delta=1$ ); (v) LOGREG-REAL ( $\ell_2$ -regularized logistic regression on the SVMGUIDE3 LibSVM dataset [2],  $m=1243$ ,  $d=22$ ; a standard benchmark in decentralized optimization [11, 12]). To assess behavior beyond the convex setting, we also include four nonconvex objectives: (vi) LINLOG (piecewise quadratic-logarithmic loss with flat curvature regions); (vii) ROSENBROCK [34]; (viii) STYBLINSKI–TANG [35] (multimodal); (ix) LOGREG-NCVR (logistic regression with bounded nonconvex penalty  $\alpha \sum_k x_k^2/(1+x_k^2)$  [36] on SVMGUIDE3). On these nonconvex objectives, the eigenvalue-shift stabilizer  $\delta_{i,k}$  makes the local coefficient matrix positive definite whenever  $\tilde{g}_{i,k} \neq 0$ . When  $\tilde{g}_{i,k} = 0$ , Algorithm 1 uses the convention  $s_{i,k} = 0$ . Thus the algorithm remains well posed and operates as a damped Newton-like method; however, the convergence guarantees of Theorems 5.20–5.27 do not apply. The shift  $\delta_{i,k}$  plays two structurally similar but theoretically distinct roles: in the convex analysis it compensates for transient indefiniteness of tracked Hessian matrices (which are PSD in the exact case); on nonconvex objectives it additionally absorbs true negative curvature, acting as a Levenberg–Marquardt damping term. For convex objectives,  $f_{\text{ref}} := f^*$  (the global minimum, whose existence is guaranteed by coercivity). For nonconvex objectives,  $f_{\text{ref}}$  denotes the best value found by multi-start L-BFGS-B (50 restarts, tolerance  $10^{-15}$ ); it is not a certified global optimum.

We define the consensus residual

$$\text{cons}_k := D(X_k) = \sqrt{\frac{1}{N} \sum_{i=1}^N \|x_{i,k} - \bar{x}_k\|^2},$$

and the combo stopping criterion

$$\text{combo}_k := \|\nabla f(\bar{x}_k)\| + \text{cons}_k,$$

where  $\nabla f(\bar{x}_k) = \frac{1}{N} \sum_{i=1}^N \nabla f_i(\bar{x}_k)$  is the true gradient at the average iterate (computed offline, not from the tracker), ensuring a fair comparison across algorithms with different internal tracking mechanisms. Each algorithm runs to  $K_{\text{max}}$  iterations or until  $\text{combo}_k < 10^{-12}$ . We report four metrics: (a)  $\text{combo} = \min_k \text{combo}_k$ ; (b)  $\text{relF} = \min_k |f(\bar{x}_k) - f_{\text{ref}}|/|f(\bar{x}_0) - f_{\text{ref}}|$ ; (c) wall-clock time (seconds; for reference only—all implementations use Python/NumPy with comparable vectorization); (d) cumulative communication cost (MB), defined by summing the stage-wise directed neighbor-message payloads over all outer iterations (consistent with the accounting in Section 4.3). All convergence curves show the 20-run median with interquartile shading, after applying the standard running-best envelope to monotone accuracy metrics. Analytical gradients and Hessians are used for all functions. A run is deemed successful at threshold  $\varepsilon$  if it reaches  $\text{relF} \leq \varepsilon$  within  $K_{\text{max}}$  iterations without encountering NaN or overflow; for nonconvex problems,  $\text{relF}$  is computed relative to  $f_{\text{ref}}$ . Unless otherwise noted, the Hessian is updated every iteration ( $K_{\text{lazy}}=1$ ); Section 6.3 studies the effect of lazy updates.

The theoretical results correspond to the logarithmic rule without a maximum-depth restriction; the reported experiments use the displayed maximum depth because the tolerances in the figures and tables are reached within that range.

Table 3: Test function definitions. Each  $f_i: \mathbb{R}^d \rightarrow \mathbb{R}$  is the local objective of agent  $i$ . For synthetic problems (Ridge–LinLog), data  $(A_i, b_i)$  are independently generated per agent with i.i.d. Gaussian entries; for logistic regression, the SVMGUIDE3 dataset [2] ( $m=1243$ ,  $d=22$ ) is randomly partitioned across agents. Rosenbrock and Styblinski–Tang are homogeneous (all agents share the same  $f_i$ ).

Name	Local objective $f_i(x)$	Data / parameters
<i>Convex</i>		
Ridge	$\frac{1}{2}\ A_i x - y_i\ ^2 + \frac{\lambda}{2}\ x\ ^2$	$A_i \in \mathbb{R}^{150 \times d}$ , $y_i = A_i x_{\text{true}} + 0.05 \varepsilon_i$ , $\lambda = 10^{-3}$
QuadBad	$\frac{1}{2} x^\top Q_i x + b_i^\top x$	$Q_i$ diagonal, eigenvalues log-spaced in $[1, \chi_i]$ , $\chi_i \approx \kappa$ ; $b_i \sim \mathcal{N}(0, I)$
LogSumExp	$\sigma \log(\sum_{j=1}^p e^{(A_i^\top x - b_i)_j / \sigma})$	$A_i \in \mathbb{R}^{d \times p}$ , $p = \max(d+2, 12)$ , $\sigma = 0.5$
Huber	$\sum_{j=1}^p \delta^2 (\sqrt{1 + (r_j / \delta)^2} - 1)$ , $r = A_i x - b_i$	$A_i \in \mathbb{R}^{5 \times d}$ , $\delta = 1$
LogReg-real	$\frac{\iota}{2}\ x\ ^2 + \frac{1}{m_i} \sum_{j=1}^{m_i} \log(1 + e^{-b_j a_j^\top x})$	SVMGUIDE3 data split; $\iota = 10^{-2}$
<i>Nonconvex</i>		
LinLog	$\sum_{j=1}^d \ell((A_i x - b_i)_j)$ ; see <sup>†</sup> below	$A_i \in \mathbb{R}^{d \times d}$
Rosenbrock	$\sum_{j=1}^{d/2} [100(x_{2j} - x_{2j-1}^2)^2 + (x_{2j-1} - 1)^2]$	shared ( $f_i = f \ \forall i$ )
Styblinski	$\sum_{j=1}^d (x_j^4 - 16x_j^2 + 5x_j)$	shared ( $f_i = f \ \forall i$ )
LogReg-NCVR	$\frac{1}{m_i} \sum_{j=1}^{m_i} \log(1 + e^{-b_j a_j^\top x}) + \alpha \sum_{k=1}^d \frac{x_k^2}{1 + x_k^2}$	SVMGUIDE3 data split; $\alpha = 0.05$

<sup>†</sup>LinLog:  $\ell(r) = r^2/2$  for  $|r| \leq 1$ ;  $\ell(r) = \ln|r| + \frac{1}{2}$  for  $|r| > 1$ .

Table 4: Per-function experimental configuration.  $M_{\text{fac}}$ : regularization scaling for DISGREM ( $M = M_{\text{fac}} \cdot H_{\text{max}}^0$ );  $\alpha_{\text{base}}$ : stepsize coefficient for first-order baselines (actual step  $\alpha_{\text{base}}/H_{\text{max}}^0$ );  $K_{\text{max}}$ : iteration budget (shared by all algorithms); Decay: whether a  $1/\sqrt{k}$  stepsize decay is applied to first-order baselines (relevant only for nonconvex problems).

Function	$M_{\text{fac}}$	$\alpha_{\text{base}}$	$K_{\text{max}}$	Decay	Notes
Ridge	0.1	0.20	200	No	$\lambda = 10^{-3}$
QuadBad	0.1	0.10	1500	No	$\kappa = 10^3$
LogSumExp	5.0	0.30	400	No	
Huber	1.5	0.30	800	No	Pseudo-Huber, $\delta = 1$
LogReg-real	3.0	1.00	600	No	svmguide3, $d = 22$
LinLog	1.0	0.20	1500	No	Nonconvex
Rosenbrock	3.0	0.10	300	Yes	Nonconvex
Styblinski	15.0	0.05	100	Yes	Multimodal
LogReg-NCVR	3.0	1.00	1000	Yes	svmguide3, $d = 22$

## 6.2 Convergence benchmarks

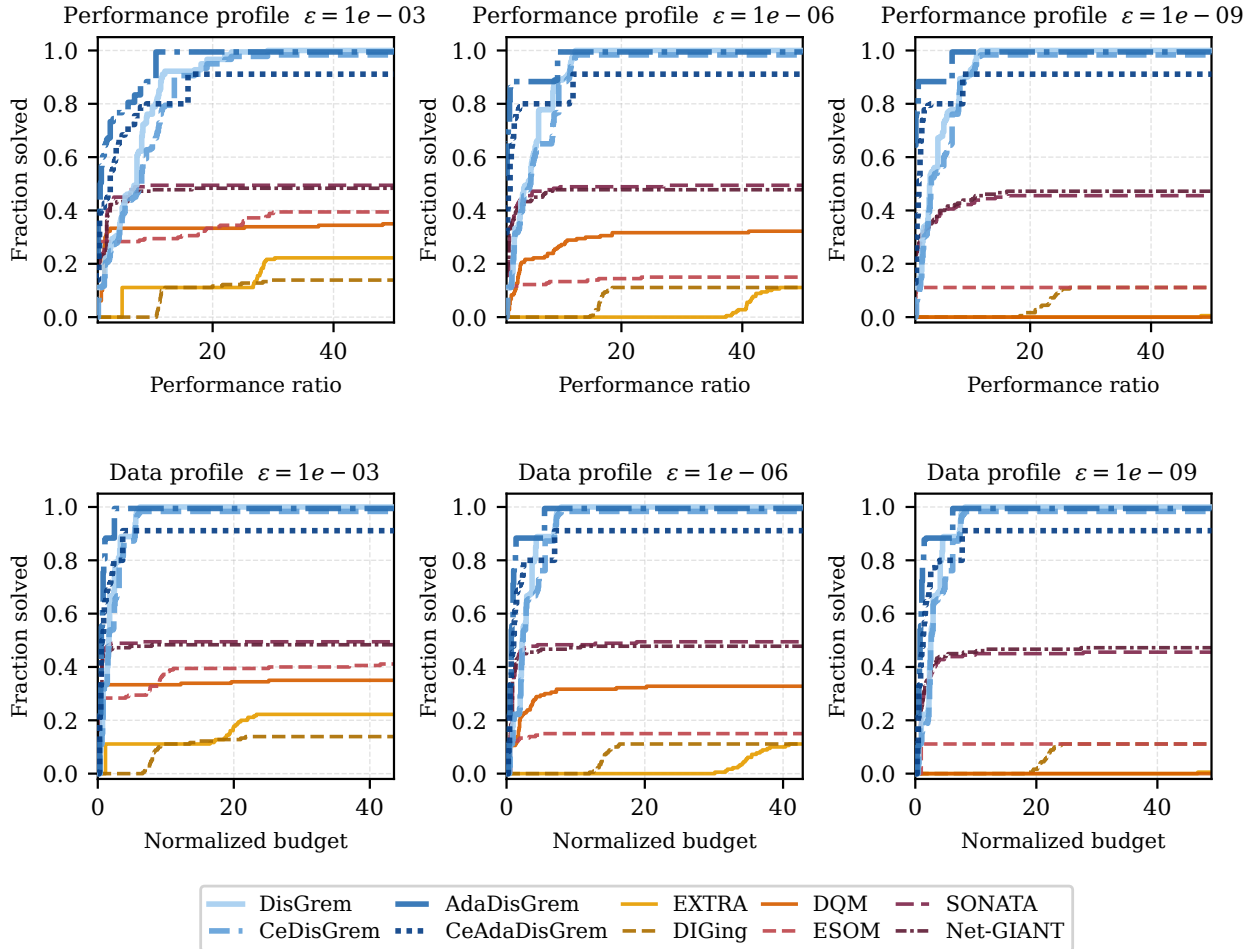


Figure 1: Iteration-budget profiles at three precision levels  $\varepsilon \in \{10^{-3}, 10^{-6}, 10^{-9}\}$ . Top: performance profiles; bottom: data profiles. A solver’s curve at ordinate  $\pi$  indicates it solves a  $\pi$ -fraction of the problem–MC instances within the given budget.

The main empirical finding is that the DISGREM family is consistently accurate across the full benchmark suite: it attains high accuracy on all nine test problems, whereas the baselines exhibit stagnation, divergence, or strong problem dependence on at least one instance (Figures 1–2).

Table 5 reports key numerical results on four representative functions covering both favorable and challenging cases; per-problem details follow.

Figure 3 shows relF versus iteration for all nine benchmark functions; additional metrics (combo, wall-clock time, communication cost) are collected in Appendix C, Figures 8–10.

We now detail the per-problem behavior. On the harder convex problems the accuracy gap is significant. On LogSumExp, the DISGREM family reaches  $\text{relF} \lesssim 10^{-12}$ , whereas every baseline stagnates above  $10^{-3}$  (first-order) or  $10^{-2}$  (SONATA, Net-GIANT). On Huber the proposed methods attain  $10^{-12}$ – $10^{-10}$ , well below the  $> 10^{-1}$  plateau of DQM/ESOM/SONATA. On ill-conditioned problems (QuadBad,  $\kappa=10^3$ ), the relF curve exhibits a clear two-phase pattern: an initial plateau of  $\sim 50$ – $100$  iterations during which the tracker dispersions contract but the objective barely decreases, followed by a rapid descent phase consistent with the  $\mathcal{O}(1/k^2)$  theoretical rate. This matches the predicted burn-in/descent structure of Theorem 5.20.

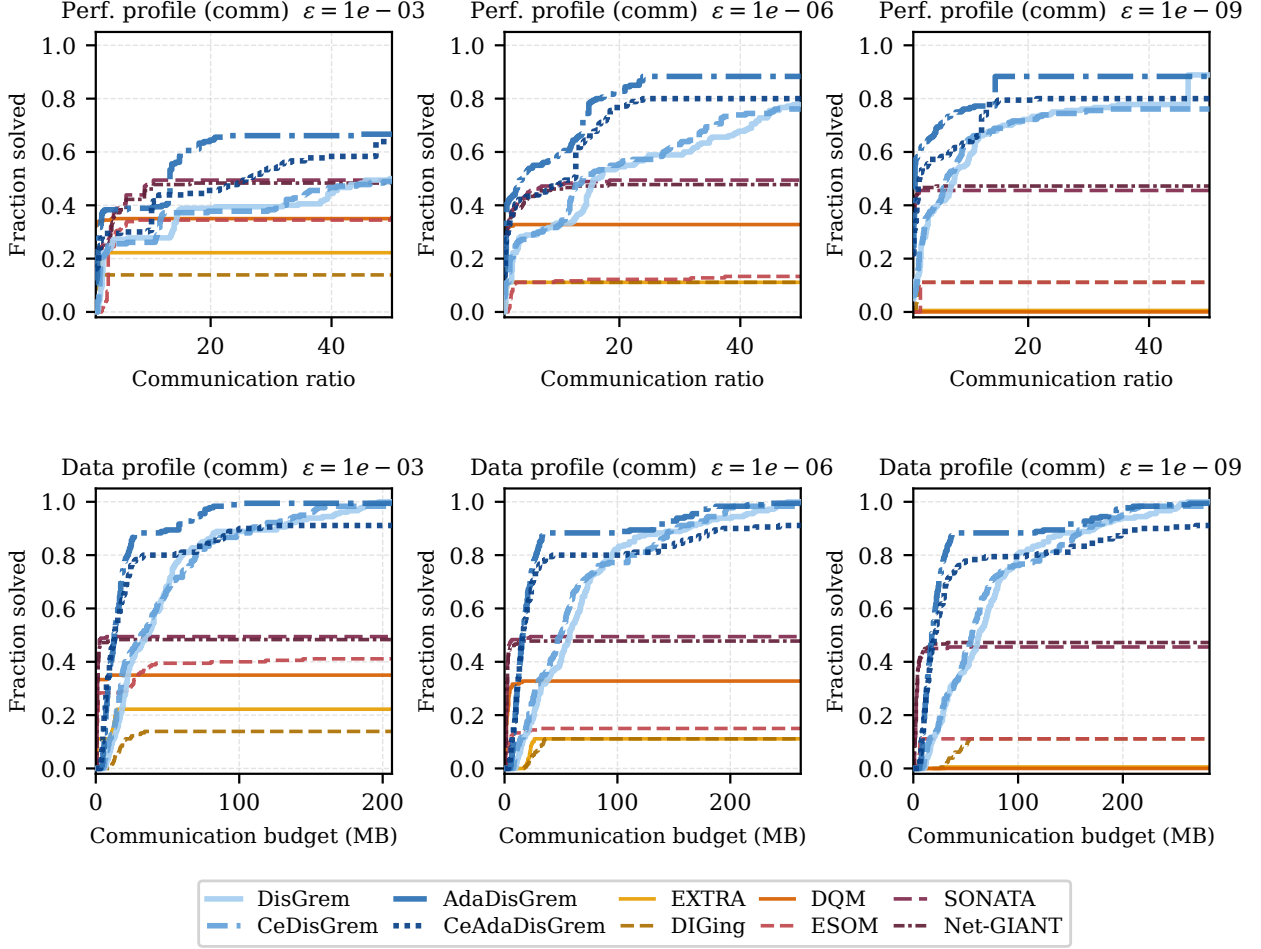


Figure 2: Communication-budget profiles at three precision levels  $\varepsilon \in \{10^{-3}, 10^{-6}, 10^{-9}\}$ . Top: performance profiles with cumulative communication cost (MB) as the ratio axis. Bottom: data profiles with communication cost on the  $\kappa$ -axis.

Table 5: Summary on four representative functions ( $N=10, 20$  MC runs; synthetic functions use  $d=30$ , and LOGREG-REAL uses  $d=22$ ). Column keys: Time (s),  $K$  (iterations), min(relF), Comm (MB).

Algorithm	HUBER ( $K_{\max}=800$ )				LOGSUMEXP ( $K_{\max}=400$ )				LINLOG ( $K_{\max}=1500$ )				STYBLINSKI-TANG ( $K_{\max}=100$ )			
	Time	$K$	min(relF)	MB	Time	$K$	min(relF)	MB	Time	$K$	min(relF)	MB	Time	$K$	min(relF)	MB
Proposed (DISGREM family)																
DISGREM	0.16	85	$3e^{-13}$	39	0.57	259	$1e^{-13}$	121	0.08	41	$2e^{-13}$	19	0.14	94	$7e^{-16}$	44
CEDISGREM	1.13	800	$2e^{-12}$	260	0.43	259	$1e^{-13}$	98	0.23	140	$1e^{-12}$	57	0.10	93	$1e^{-13}$	37
ADADISGREM	1.33	800	$4e^{-12}$	426	0.07	33	$9e^{-13}$	15	0.08	42	$6e^{-13}$	19	0.02	17	$5e^{-16}$	8
CEADADISGREM	1.21	800	$5e^{-10}$	313	0.07	35	$3e^{-13}$	13	0.26	156	$6e^{-13}$	64	0.02	18	$5e^{-16}$	7
First-order baselines																
EXTRA	5.9	800	$5e^{-3}$	8	3.5	400	$4e^{-1}$	4	16.9	1500	$7e^{-9}$	15	0.70	100	$7e^{-1}$	1
DIGing	6.0	800	$3e^{-4}$	25	3.3	400	$2e^{-1}$	12	10.3	989	$1e^{-12}$	31	0.72	100	$9e^{-1}$	3
Second-order baselines																
DQM	0.8	800	$2e^{-1}$	12	0.5	400	$3e^{-3}$	6	1.7	1500	$2e^0$	23	0.09	100	$2e^{-1}$	2
ESOM	1.4	800	$1e^{-1}$	74	0.7	400	$2e^{-3}$	37	3.5	1500	$1e^1$	139	0.19	100	$1e^1$	9
SONATA	1.0	800	$1e^{-1}$	37	0.5	400	$3e^{-2}$	19	2.3	1500	$1e^0$	69	0.03	12	$5e^{-16}$	1
Net-GIANT	1.0	800	$4e^{-2}$	37	0.6	400	$1e^{-2}$	19	2.5	1500	$1e^0$	69	0.01	12	$5e^{-16}$	1

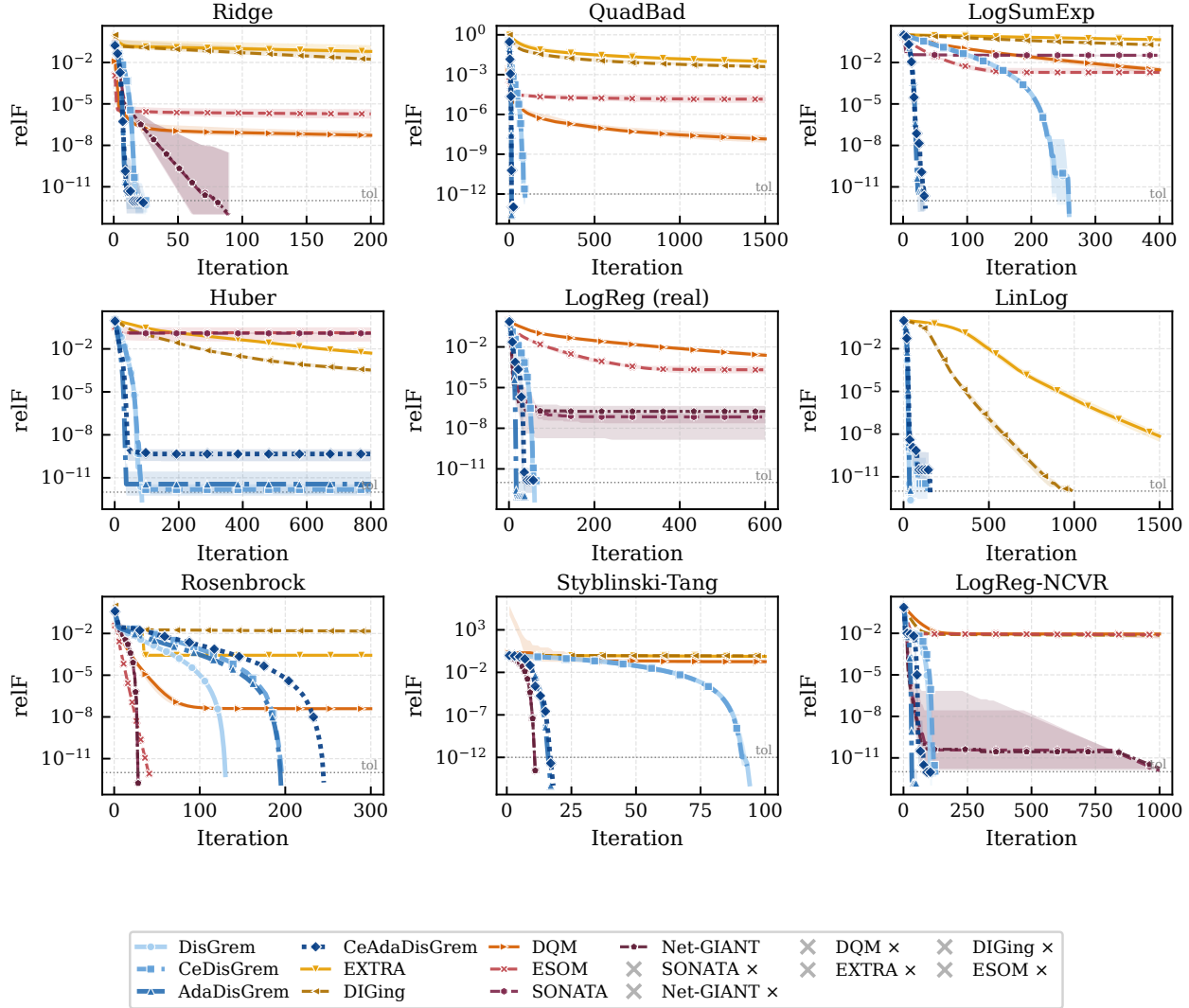


Figure 3: relF vs. iteration on all nine test functions ( $N=10, 20$  MC runs; synthetic objectives use  $d=30$ , whereas the two logistic-regression objectives use the  $d=22$  svmGUIDE3 feature dimension; logarithmic communication implementation). Solid curves: DISGREM family; dashed: baselines. Shaded bands: interquartile range. Legend entries marked by  $\times$  indicate algorithms whose median curve is not drawn because the corresponding runs terminated by NaN, overflow, or divergence.

We note two exceptions where individual baselines outperform. DIGing on LinLog reaches  $\text{relF} \approx 10^{-12}$ , comparable to the DISGREM family: LinLog exhibits very flat curvature regions where the Hessian-based regularization overestimates curvature, whereas DIGing’s simpler dynamics are less affected. However, DIGing is much slower in wall-clock time and fails on the majority of other functions. SONATA and Net-GIANT reach  $\sim 10^{-16}$  on Styblinski–Tang in 12 steps, but stagnate or diverge on Huber and LinLog ( $\text{relF} > 1$ ).

Regarding the adaptive versus fixed- $M$  trade-off, ADADISGREM is fastest on LogSumExp (33 versus 259 iterations for fixed- $M$  DISGREM) and Styblinski–Tang (17 versus 94 iterations), where the secant estimate quickly reduces the effective regularization scale. In summary, adaptation reduces the need for manually selecting a fixed  $M$  (Section 6.4) and often reduces the iteration count, although fixed  $M$  may still use less communication on some problems. Section 6.3 compares total communication volume to a target precision, the more informative metric given the  $\mathcal{O}(d^2)$

per-iteration Hessian payload of DISGREM.

Theorem 5.20 assumes convexity, yet the DISGREM family converges on all four nonconvex benchmarks in our tests: all four proposed variants reach  $\text{relF} \lesssim 10^{-12}$  on LinLog; all four variants achieve  $\text{relF} < 10^{-12}$  on Rosenbrock within 300 iterations; ADADISGREM attains  $\sim 10^{-16}$  on Styblinski–Tang in 17 steps; and the family converges to  $\sim 10^{-12}$  on LogReg-NCVR within 128 steps for the fixed- $M$  pair and within 114 steps for CEADADISGREM. These tests indicate that the regularization and eigenvalue shift provide useful damping beyond the convex regime analyzed in the theory.

### 6.3 Communication cost

The profiles in Section 6.2 use iteration count as the budget axis; here we take a communication-volume perspective. We focus on four representative functions (Ridge, LogSumExp, Huber, and LogReg-real) with 5 MC runs; the synthetic problems use  $d = 30$ , while LogReg-real uses the SVMGUIDE3 dimension  $d = 22$ .

#### 6.3.1 Benefit of communication-efficient (Ce) variants

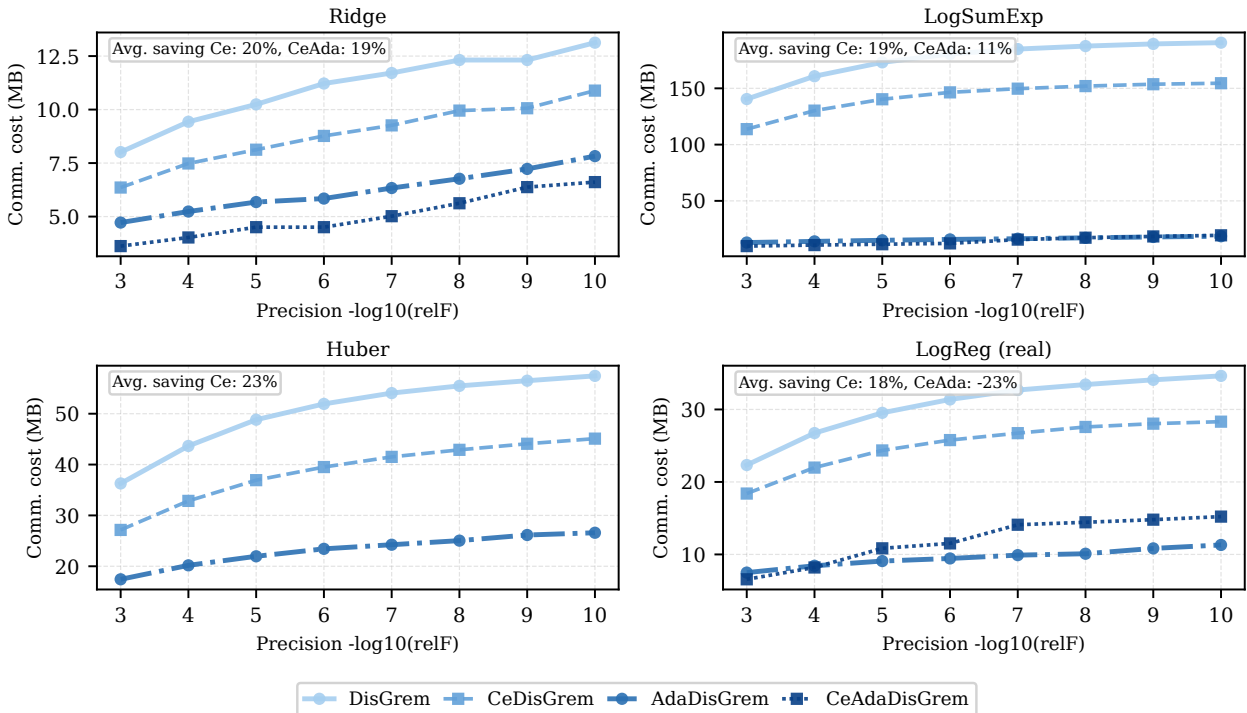


Figure 4: Communication cost (MB) to reach target precision  $\varepsilon \in \{10^{-3}, \dots, 10^{-10}\}$  for full vs. Ce variants. Missing markers: target not reached.

Figure 4 and Table 6 compare the total communication cost needed to reach precision levels  $\varepsilon \in \{10^{-3}, 10^{-6}, 10^{-8}, 10^{-10}\}$ . For the fixed- $M$  pair (DISGREM vs. CEDISGREM), the Ce variant saves about 18–25% communication across the four representative functions and the tested precision range.

For the adaptive pair (ADADISGREM vs. CEADADISGREM), the savings are more problem-dependent. At low precision, CEADADISGREM provides savings on Ridge, LogSumExp, and LogReg-real, but at high precision it can require more communication on LogReg-real; on Huber

Table 6: Communication savings (%) of Ce variants over their full counterparts at selected precision levels. Positive values indicate savings; negative values indicate that Ce requires more communication (due to slower convergence erasing per-iteration byte savings).

Function	Pair	$\varepsilon=10^{-3}$	$\varepsilon=10^{-6}$	$\varepsilon=10^{-8}$	$\varepsilon=10^{-10}$
Ridge	DISGREM $\rightarrow$ Ce	+21%	+22%	+19%	+17%
	ADADISGREM $\rightarrow$ Ce	+23%	+23%	+17%	+16%
LogSumExp	DISGREM $\rightarrow$ Ce	+19%	+19%	+19%	+19%
	ADADISGREM $\rightarrow$ Ce	+24%	+22%	-1%	-4%
Huber	DISGREM $\rightarrow$ Ce	+25%	+24%	+23%	+22%
	ADADISGREM $\rightarrow$ Ce	—	—	—	—
LogReg-real	DISGREM $\rightarrow$ Ce	+18%	+18%	+18%	+18%
	ADADISGREM $\rightarrow$ Ce	+12%	-22%	-43%	-35%

it does not reach the selected precision levels in this study. The fixed- $M$  pair therefore gives the clearest communication benefit, while compression can interfere with the adaptive scaling rule at high precision.

In summary, the Ce mechanism reliably reduces per-iteration payload (by compressing the  $\mathcal{O}(d^2)$  Hessian exchange), but total communication savings depend on the convergence-speed trade-off: with fixed  $M$ , savings of 18–25% are typical in the fixed- $M$  setting; with adaptive  $M$ , compression noise can still slow convergence enough to increase total bytes at high precision on some problems (Table 6).

### 6.3.2 $K_{\text{lazy}}$ and compression ablation

Appendix C (Figures 11–12) reports a full sweep of  $K_{\text{lazy}} \in \{1, 5, 10, 20, 40, 80\}$  and compression methods (Top- $k$ , Low-Rank). Moderate values  $K_{\text{lazy}} \in \{5, 10\}$  reduce communication by 40–60% on well-conditioned problems with negligible precision loss. Low-rank compression with  $r=d/5$  provides a good balance across all tested functions; aggressive compression ( $r=1$  or Top- $k$  at 5%) degrades convergence on Huber and LogSumExp.

## 6.4 Adaptive mechanism

We study the adaptive  $M$  mechanism of ADADISGREM on four representative functions (Ridge, LogSumExp, LogReg-real, LogReg-NCVR) with 5 Monte Carlo runs each.

Figure 5 shows the  $M$  trajectory. The adaptive estimate responds to the local curvature: it starts near or above the fixed baseline value, then decays as the iterate approaches stationarity, often below the conservative fixed values used for the fixed- $M$  method. Figure 6 compares ADADISGREM against five manually chosen fixed- $M$  settings spanning a  $100\times$  range: ADADISGREM is competitive with the best fixed choice on most functions while avoiding failures at aggressive fixed- $M$  choices. Furthermore, all initializations in  $[0.1M^*, 10M^*]$  converge to a common  $M$  trajectory within 50–100 iterations (Appendix C, Figure 13), showing that the adaptive dynamics, rather than the initial scale alone, drive its empirical performance.

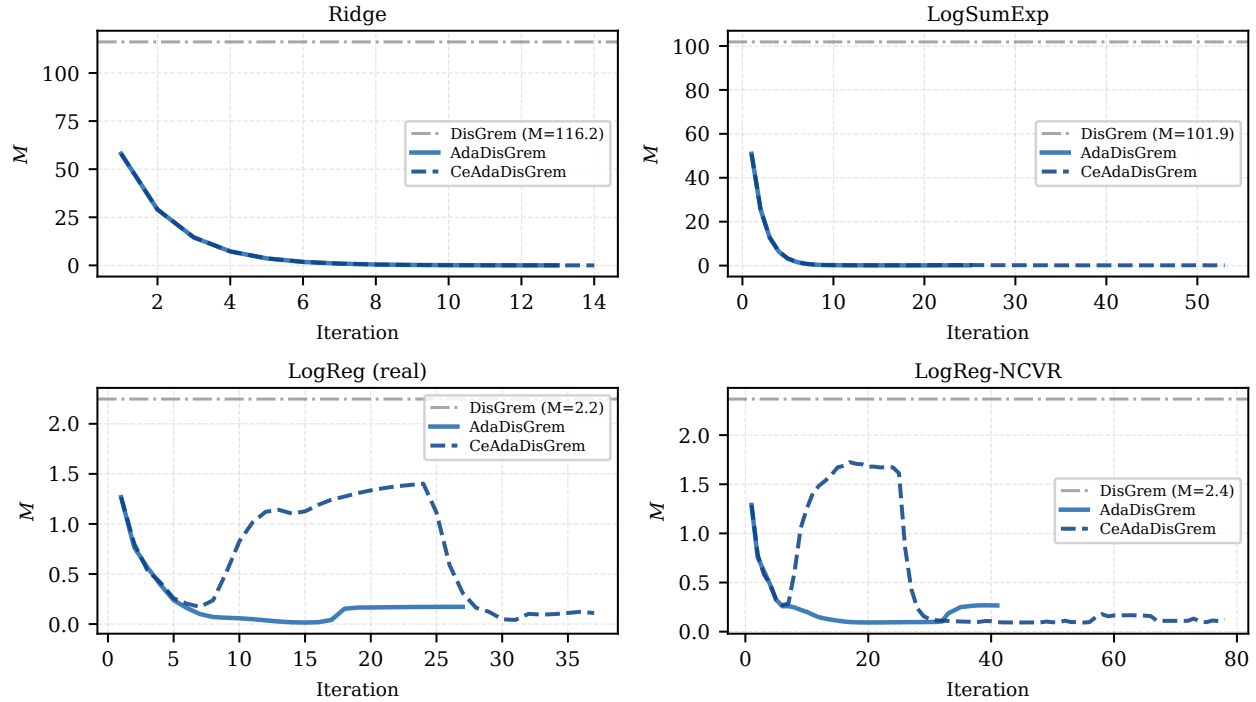


Figure 5: Regularization parameter  $M$  trajectory for ADADISGREM (solid) vs. the fixed  $M$  of DISGREM (dashed). Curves averaged over 5 MC runs.

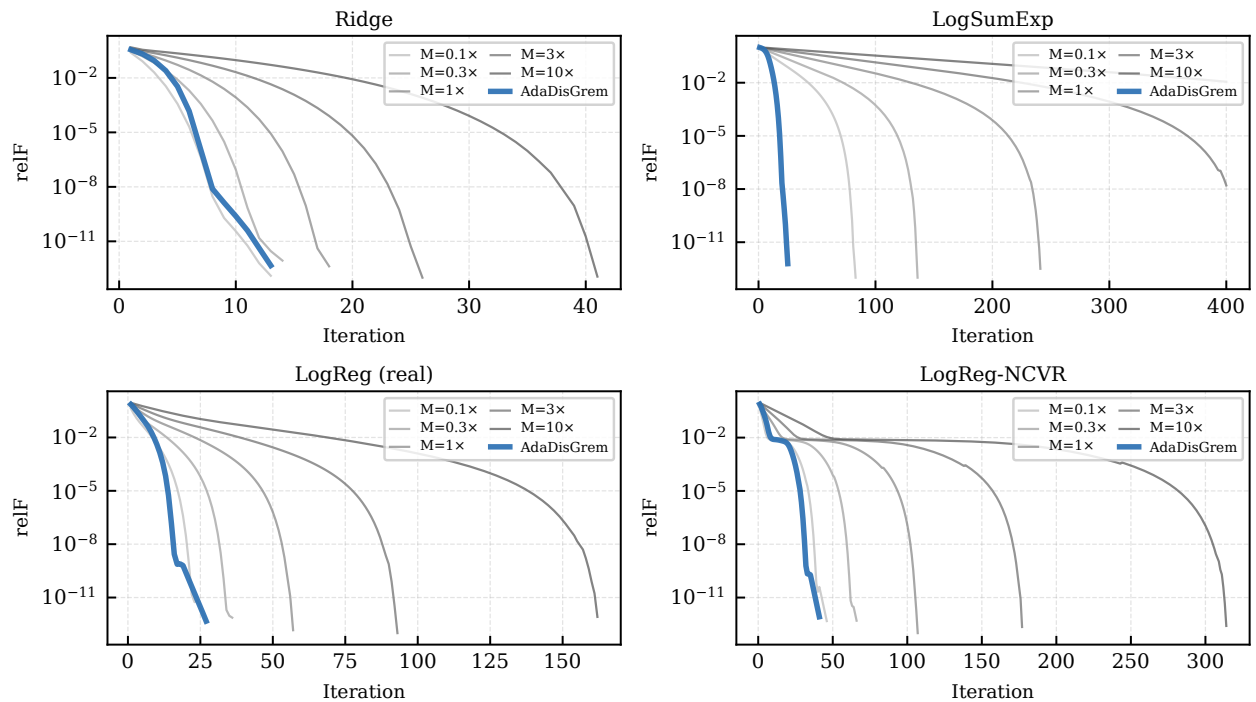


Figure 6: ADADISGREM (bold blue) vs. DISGREM at five fixed- $M$  values ( $0.1\times$ – $10\times$  the baseline  $M^*$ ; gray curves light-to-dark). The adaptive variant is competitive with the best fixed choice on most functions and avoids failures at aggressive fixed- $M$  choices.

## 6.5 Robustness

We investigate robustness along two complementary axes: (i) sensitivity to the starting point, and (ii) sensitivity to the key algorithmic parameter ( $M_{\text{fac}}$  for the DISGREM family, stepsize  $\alpha$  for first-order methods, penalty or regularization for second-order baselines). All runs use  $N=10$  and the same communication settings as the convergence benchmarks. All synthetic objectives use  $d=30$ , whereas the two logistic-regression objectives use the  $d=22$  SVMGUIDE3 feature dimension.

### 6.5.1 Starting-point robustness

Each algorithm is run from 100 independent random initial points sampled uniformly on a ball of radius  $r$  centered at the reference initialization. We test two regimes: *near* ( $r=1$ ) and *far* ( $r=3$ ). A run is counted as successful if it reaches  $\text{relF} < 10^{-6}$  within the iteration budget  $K_{\text{max}}$ . (This threshold is deliberately less stringent than the  $\text{combo} < 10^{-12}$  criterion used in the convergence benchmarks, meaning that iteration counts between the two sections are not directly comparable.) Table 7 reports success rates (%) across all nine functions and ten algorithms.

Table 7: Starting-point robustness: success rate (%) at two radii ( $r=1$  near,  $r=3$  far; 100 MC runs). Success:  $\text{relF} < 10^{-6}$ . Bold: best value in each row; “—”: 0%.

Function	DISGREM family				1st-order		2nd-order baselines			
	DG	CeDG	AdaDG	CeAdaDG	EXTRA	DIGing	DQM	ESOM	SON	N-GI
Near initialization ( $r=1$ )										
Ridge	<b>100</b>	<b>100</b>	<b>100</b>	<b>100</b>	—	—	<b>100</b>	59	<b>100</b>	<b>100</b>
QuadBad	<b>100</b>	<b>100</b>	<b>100</b>	<b>100</b>	—	—	98	—	1	1
LogSumExp	<b>100</b>	<b>100</b>	98	<b>100</b>	—	—	—	—	—	—
Huber	<b>100</b>	68	96	17	—	—	—	—	—	—
LinLog	99	<b>100</b>	99	<b>100</b>	<b>100</b>	<b>100</b>	—	—	—	—
LogReg-real	<b>100</b>	<b>100</b>	<b>100</b>	<b>100</b>	—	—	—	—	53	49
Rosenbrock	<b>100</b>	<b>100</b>	<b>100</b>	<b>100</b>	—	—	97	<b>100</b>	<b>100</b>	<b>100</b>
Styblinski	<b>100</b>	<b>100</b>	<b>100</b>	<b>100</b>	—	—	—	—	<b>100</b>	<b>100</b>
LogReg-NCVR	<b>100</b>	<b>100</b>	<b>100</b>	99	—	—	—	—	98	96
<i>Avg</i>	<i><b>100</b></i>	<i>96</i>	<i>99</i>	<i>91</i>	<i>11</i>	<i>11</i>	<i>33</i>	<i>18</i>	<i>50</i>	<i>50</i>
Far initialization ( $r=3$ )										
Ridge	<b>100</b>	<b>100</b>	<b>100</b>	<b>100</b>	—	—	<b>100</b>	59	<b>100</b>	<b>100</b>
QuadBad	<b>100</b>	<b>100</b>	<b>100</b>	<b>100</b>	—	—	98	1	1	1
LogSumExp	<b>100</b>	<b>100</b>	98	<b>100</b>	—	—	—	—	—	—
Huber	<b>100</b>	80	96	24	—	—	—	—	—	—
LinLog	99	<b>100</b>	99	<b>100</b>	89	<b>100</b>	—	—	—	—
LogReg-real	<b>100</b>	<b>100</b>	<b>100</b>	<b>100</b>	—	—	—	—	51	48
Rosenbrock	<b>100</b>	<b>100</b>	<b>100</b>	<b>100</b>	—	—	82	96	<b>100</b>	<b>100</b>
Styblinski	57	61	<b>100</b>	<b>100</b>	—	—	—	—	<b>100</b>	<b>100</b>
LogReg-NCVR	<b>100</b>	<b>100</b>	<b>100</b>	<b>100</b>	—	1	—	—	99	97
<i>Avg</i>	<i>95</i>	<i>93</i>	<i><b>99</b></i>	<i>92</i>	<i>10</i>	<i>11</i>	<i>31</i>	<i>17</i>	<i>50</i>	<i>50</i>

ADADISGREM is the most robust variant (about 99% average success, near and far), followed closely by DISGREM. Both maintain nearly identical rates across the two initialization radii, showing stable regions of convergence. The adaptive mechanism is especially valuable on Styblinski–Tang, where ADADISGREM and CEADADISGREM maintain 100% success even from far starts. Hessian compression has mild effects on most functions but reduces robustness on Huber, where CEADADISGREM succeeds on only 18–24% of trials. The drop is consistent with compression noise accumulating in the Hessian tracker and, for CEADADISGREM, perturbing the  $\hat{M}$  estimation.

The baselines are function-specific: first-order methods succeed only on LinLog; DQM only on Ridge/QuadBad/Rosenbrock; SONATA/Net-GIANT only on Ridge/Rosenbrock/Styblinski–Tang. Huber remains the hardest function for the compressed adaptive variant, due to its near-linear tails and flat curvature regions.

### 6.5.2 Parameter sensitivity

We sweep the key parameter ( $M_{\text{fac}}$  for the DISGREM family; stepsize  $\alpha$  for first-order methods; penalty/regularization for second-order baselines) over 10 values on four representative functions. Full curves are in Appendix C, Figures 14–16.

The DISGREM family converges across a wide range of  $M_{\text{fac}}$  on well-conditioned problems; only below a problem-dependent threshold does it diverge (e.g.,  $M_{\text{fac}} < 1$  on LogSumExp). First-order baselines are highly sensitive to  $\alpha$ : too large triggers divergence, too small causes stagnation, and even the best  $\alpha$  fails to break the  $\text{relF} > 10^{-1}$  barrier on LogSumExp. Second-order baselines exhibit moderate sensitivity; DQM and ESOM diverge for aggressive penalty values, while SONATA and Net-GIANT are more stable but stagnate on LogSumExp.

## 6.6 Scalability with problem dimension

To assess how the DISGREM family scales with problem dimension, we repeat the benchmark on three representative functions (Ridge, LogSumExp, Rosenbrock) at  $d = 30, 100,$  and  $200$ , keeping  $N = 10$  agents and the same logarithmic communication implementation as in Section 6.1, with 5 Monte Carlo runs (reduced from the 20 runs in Section 6.2 due to the higher per-run cost at  $d=200$ ; the deterministic objective functions ensure low inter-run variance, so the median curves are highly stable). We compare DISGREM, ADADISGREM, EXTRA, and SONATA.

Figure 7 reports  $\text{relF}$  versus iteration. On Ridge and Rosenbrock, the DISGREM family reaches  $\text{relF} \leq 10^{-12}$  within a similar iteration count across all three dimensions, suggesting an empirically near dimension-insensitive iteration count, consistent with the network-independent iteration bound of Theorem 5.20. On LogSumExp, the final accuracy degrades slightly at  $d = 200$ , yet DISGREM still outperforms both baselines by 3–5 orders of magnitude in  $\text{relF}$ . EXTRA stagnates above  $\text{relF} \sim 1$  on all problems regardless of dimension, while SONATA converges but requires substantially more iterations.

The per-iteration wall-clock time scales as  $\mathcal{O}(d^3)$ , because each agent solves a dense  $d \times d$  linear system (e.g., on RIDGE, the cumulative time for all 5 MC runs increases from 2.3 s at  $d=30$  to 118 s at  $d=200$ ). Since per-iteration communication volume is  $\mathcal{O}(d^2)$  (already analyzed in §4.3), the dominant bottleneck at high dimensions shifts from communication to local computation.

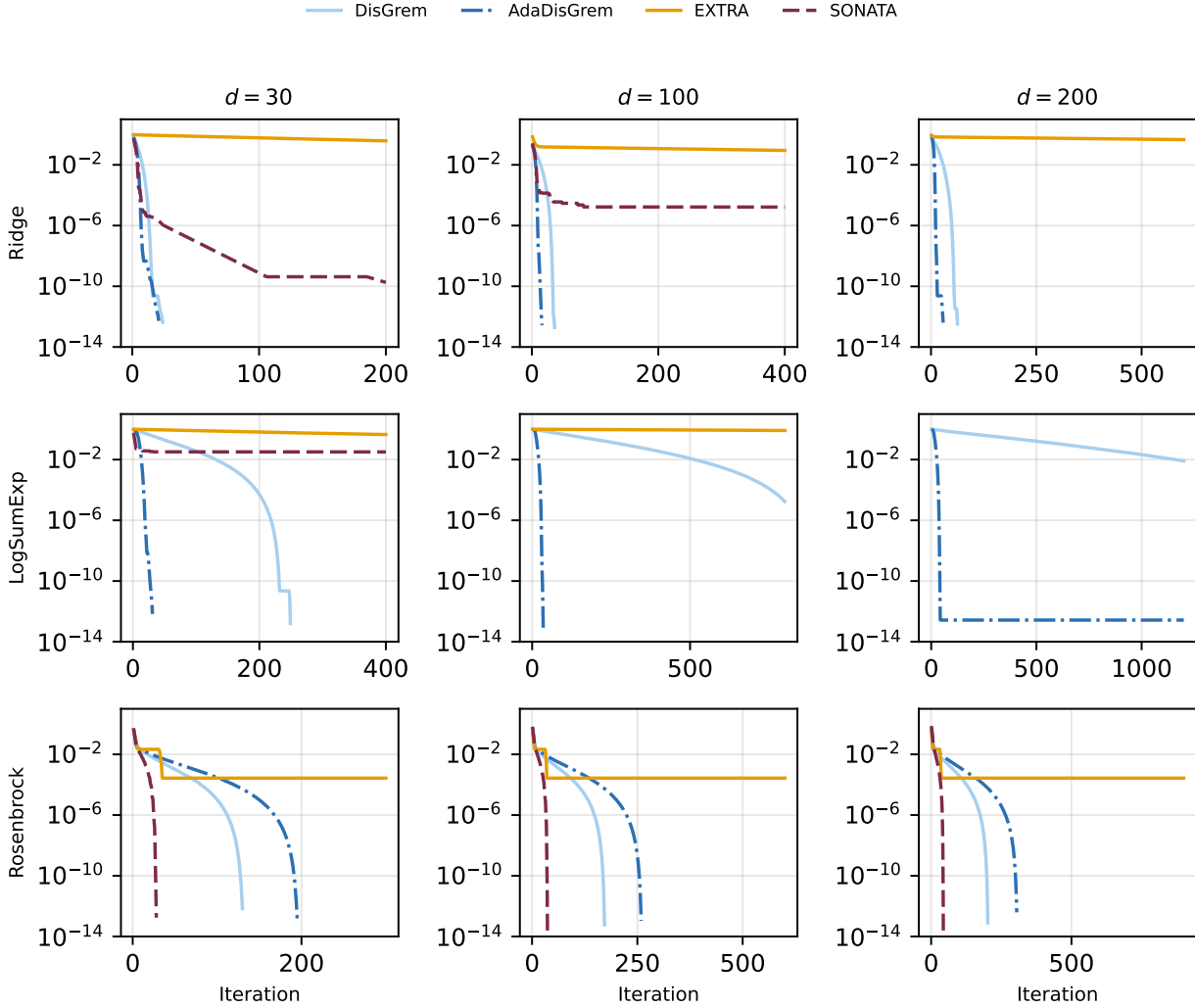


Figure 7: Dimension scalability: relF vs. iteration for  $d \in \{30, 100, 200\}$  on three functions (5 MC runs, median).

## 7 Conclusion and future directions

Under the bounded-trajectory and smoothness assumptions used in the analysis, DISGREM retains the centralized regularized Newton post-burn-in rate, with the burn-in order controlled by the scheduled consensus accuracy, in a fully decentralized setting without line search, stepsize tuning, or static Hessian-heterogeneity constants. Algorithmic stability is achieved by combining a local eigenvalue-shift stabilizer with a two-stage mixing protocol. Analytically, the key ingredients are a virtual reference-step construction—which reduces the decentralized dynamics to an inexact centralized update—and an increment-based dispersion analysis. By bounding tracker mismatch through Lipschitz differences rather than fixed heterogeneity constants, the consensus error becomes transient and imposes no accuracy floor. Under the logarithmic mixing schedule used in the analysis, with  $p \geq 3$ , the total communication cost for a fixed connected network is  $\mathcal{O}(\varepsilon^{-1} \log(1/\varepsilon))$  rounds. More explicitly, the dependence on the mixing rate is  $\mathcal{O}((1 - \rho)^{-1} \varepsilon^{-1} \log(1/\varepsilon))$  as  $\rho \rightarrow 1$ . The experiments use the corresponding implementation over the precision range reported in the figures and tables.

The experiments are consistent with the theoretical picture and provide three further findings. First, ADADISGREM attains the highest success rate (about 99% average over nine functions and two initialization radii) without choosing a separate fixed  $M$  for each problem. Second, Hessian compression (CEDISGREM) can reduce total communication in the fixed- $M$  regime, saving 18–25% at moderate precision in our tests, though compression noise can erode these savings at extremely high precision. Third, dimension-scalability experiments ( $d \in \{30, 100, 200\}$ ) demonstrate a nearly dimension-insensitive iteration count, consistent with the network-independent theoretical bound.

Future directions include a nonconvex extension, lower bounds for decentralized second-order methods with explicit spectral-gap dependence, and extensions to directed or time-varying graphs. The  $\mathcal{O}(d^3)$  cost of solving the local Newton system also motivates inversion-free variants based on iterative linear solvers [15] or inversion-free tracking [19], as well as stochastic or variance-reduced gradient and Hessian estimators for large-scale settings.

## Acknowledgments

The work of W. Hu, Y.-X. Yuan, and L. Zhang was supported in part by NSFC and the Chinese Academy of Sciences. The work of L. Zhang was also supported by the China Postdoctoral Science Foundation under Grant Nos. 2023T160670 and 2023M743720. The work of P. Xie was supported in part by the U.S. Department of Energy, Office of Science.

## References

- [1] C. Cartis, N. I. M. Gould, and Ph. L. Toint. Adaptive cubic regularisation methods for unconstrained optimization. Part I: motivation, convergence and numerical results. *Mathematical Programming*, 127:245–295, 2011.
- [2] C.-C. Chang and C.-J. Lin. LIBSVM: a library for support vector machines. *ACM Transactions on Intelligent Systems and Technology*, 2(3):27:1–27:27, 2011. Software available at <https://www.csie.ntu.edu.tw/~cjlin/libsvmtools/datasets/>.
- [3] M. Eisen, A. Mokhtari, and A. Ribeiro. Decentralized quasi-Newton methods. *IEEE Transactions on Signal Processing*, 65(10):2613–2628, 2017.
- [4] D. Jakovetić, J. Xavier, and J. M. F. Moura. Fast distributed gradient methods. *IEEE Transactions on Automatic Control*, 59(5):1131–1146, 2014.
- [5] K. Mishchenko. Regularized Newton method with global  $O(1/k^2)$  convergence. *SIAM Journal on Optimization*, 33(3):1440–1462, 2023.
- [6] A. Mokhtari, Q. Ling, and A. Ribeiro. Network Newton distributed optimization methods. *IEEE Transactions on Signal Processing*, 65(1):146–161, 2017.
- [7] J. Zhang, Q. Ling, and A. M.-C. So. A Newton tracking algorithm with exact linear convergence for decentralized consensus optimization. *IEEE Transactions on Signal and Information Processing over Networks*, 7:346–358, 2021.
- [8] A. Nedić and A. Ozdaglar. Distributed subgradient methods for multi-agent optimization. *IEEE Transactions on Automatic Control*, 54(1):48–61, 2009.

- [9] A. Nedić, A. Olshevsky, and W. Shi. Achieving geometric convergence for distributed optimization over time-varying graphs. *SIAM Journal on Optimization*, 27(4):2597–2633, 2017.
- [10] Y. Nesterov and B. T. Polyak. Cubic regularization of Newton method and its global performance. *Mathematical Programming*, 108:177–205, 2006.
- [11] W. Shi, Q. Ling, G. Wu, and W. Yin. EXTRA: an exact first-order algorithm for decentralized consensus optimization. *SIAM Journal on Optimization*, 25(2):944–966, 2015.
- [12] Y. Sun, G. Scutari, and D. P. Palomar. Distributed nonconvex optimization and learning based on successive convex approximation. *IEEE Transactions on Signal Processing*, 70:5900–5915, 2022.
- [13] A. Maritan, G. Sharma, L. Schenato, and S. Dey. Network-GIANT: fully distributed Newton-type optimization via harmonic Hessian consensus. *arXiv preprint arXiv:2305.07898*, 2023.
- [14] K. Yuan, B. Ying, and A. H. Sayed. Exact diffusion for distributed optimization and learning—Part I: algorithm development. *IEEE Transactions on Signal Processing*, 67(3):708–723, 2019.
- [15] D. Jakovetić, N. Krejić, and G. Malaspina. DINAS: Distributed inexact Newton method with adaptive step sizes. *Computational Optimization and Applications*, 91:683–715, 2025.
- [16] A. Daneshmand, G. Scutari, P. Dvurechensky, and A. Gasnikov. Newton method over networks is fast up to the statistical precision. In *Proceedings of the 38th International Conference on Machine Learning (ICML)*, volume 139 of PMLR, pp. 2398–2409, 2021.
- [17] S. Gratton, S. Jerad, and Ph. L. Toint. Yet another fast variant of Newton’s method for nonconvex optimization. *arXiv preprint arXiv:2302.10065*, 2023.
- [18] N. Doikov and Y. Nesterov. Gradient regularization of Newton method with Bregman distances. *Mathematical Programming*, 204:1–25, 2024.
- [19] G. Yuan, X. Li, and Q. Ling. INDO: INversion-free Distributed second-Order method for consensus optimization. *Optimization Online preprint*, 2022.
- [20] Z. Zhang, K. Che, S. Yang, et al. Communication-efficient distributed cubic Newton with compressed lazy Hessian. *Neural Networks*, 174:106212, 2024.
- [21] S. A. Alghunaim, E. K. Ryu, K. Yuan, and A. H. Sayed. Decentralized proximal gradient algorithms with linear convergence rates. *IEEE Transactions on Automatic Control*, 66(6):2787–2794, 2021.
- [22] D. Bajović, D. Jakovetić, N. Krejić, and N. Krklec Jerinkić. Newton-like method with diagonal correction for distributed optimization. *SIAM Journal on Optimization*, 27(2):1171–1203, 2017.
- [23] A. Beznosikov, P. Richtárik, M. Diskin, et al. Distributed methods with compressed communication for solving variational inequalities, with theoretical guarantees. In *Advances in Neural Information Processing Systems (NeurIPS)*, 35:14013–14029, 2022.
- [24] N. Doikov and Y. Nesterov. Local convergence of tensor methods. *Mathematical Programming*, 193:315–336, 2022.
- [25] N. Doikov, E. M. Chayti, and M. Jaggi. Second-order optimization with lazy Hessians. In *Proceedings of the International Conference on Machine Learning (ICML)*, 2023.

- [26] A. Koloskova, S. U. Stich, and M. Jaggi. Decentralized stochastic optimization and gossip algorithms with compressed communication. In Proceedings of the International Conference on Machine Learning (ICML), pp. 3478–3487, 2019.
- [27] H. Li and Z. Lin. Accelerated gradient tracking over time-varying graphs for decentralized optimization. *Journal of Machine Learning Research*, 25(274):1–52, 2024.
- [28] A. Mokhtari, W. Shi, Q. Ling, and A. Ribeiro. ESOM: A second-order method for exact decentralized optimization over networks. *IEEE Transactions on Signal and Information Processing over Networks*, 2(4):507–522, 2016.
- [29] S. Pu and A. Nedić. Distributed stochastic gradient tracking methods. *Mathematical Programming*, 187:409–457, 2021.
- [30] R. Xin and U. A. Khan. Distributed heavy-ball: a generalization and acceleration of first-order methods with gradient tracking. *IEEE Transactions on Automatic Control*, 65(6):2627–2633, 2020.
- [31] B. Li, S. Cen, Y. Chen, et al. Communication-efficient distributed optimization in networks with gradient tracking and variance reduction. *Journal of Machine Learning Research*, 21(180):1–51, 2020.
- [32] Y. Nesterov. Smooth minimization of non-smooth functions. *Mathematical Programming*, 103(1):127–152, 2005.
- [33] P. Charbonnier, L. Blanc-Féraud, G. Aubert, and M. Barlaud. Deterministic edge-preserving regularization in computed imaging. *IEEE Transactions on Image Processing*, 6(2):298–311, 1997.
- [34] H. H. Rosenbrock. An automatic method for finding the greatest or least value of a function. *The Computer Journal*, 3(3):175–184, 1960.
- [35] M. A. Styblinski and T. S. Tang. Experiments in nonconvex optimization: Stochastic approximation with function smoothing and simulated annealing. *Neural Networks*, 3(4):467–483, 1990.
- [36] D. Geman and C. Yang. Nonlinear image recovery with half-quadratic regularization. *IEEE Transactions on Image Processing*, 4(7):932–946, 1995.
- [37] P. Xie and Y. Yuan. A derivative-free optimization algorithm combining line-search and trust-region techniques. *Chinese Annals of Mathematics, Series B*, 44(5):719–734, 2023.
- [38] P. Xie and Y. Yuan. Derivative-free optimization with transformed objective functions (DFOTO) and the algorithm based on the least Frobenius norm updating quadratic model. *Journal of the Operations Research Society of China*, 13:327–363, 2025.
- [39] P. Xie and Y. Yuan. A derivative-free method using a new underdetermined quadratic interpolation model. *SIAM Journal on Optimization*, 35(2):1110–1133, 2025.
- [40] P. Xie and Y. Yuan. Least  $H^2$  norm updating of quadratic interpolation models for derivative-free trust-region algorithms. *IMA Journal of Numerical Analysis*, 46(1):21–50, 2026.

- [41] P. Xie and Y. Yuan. A new two-dimensional model-based subspace method for large-scale unconstrained derivative-free optimization: 2D-MoSub. *Optimization Methods and Software*, 41(1):118–150, 2026.
- [42] P. Xie and S. M. Wild. ReMU: Regional minimal updating for model-based derivative-free optimization. arXiv:2504.03606, 2025.
- [43] Y. He and P. Xie. Model-driven subspaces for large-scale optimization with local approximation strategy. arXiv:2509.08256, 2025.
- [44] P. Xie. A derivative-free trust-region method for optimization on the ellipsoid. *Journal of Physics: Conference Series*, 2620:012007, 2023.
- [45] P. Xie. Sufficient conditions for error distance reduction in the  $\ell^2$ -norm trust region between minimizers of local nonconvex multivariate quadratic approximates. *Journal of Computational and Applied Mathematics*, 453:116146, 2025.
- [46] P. Xie, Z. Zhou, and Z. Zhou. Objective value change and shape-based accelerated optimization for the neural network approximation. arXiv:2508.20290, 2025.
- [47] P. Xie and S. M. Wild. Barycenter of weight coefficient region of least weighted  $H^2$  norm updating quadratic models with vanishing trust-region radius. *SIAM NCC 2024, Early Career Travel Award*, 2024.
- [48] P. Xie. On the relationship between  $\Lambda$ -poisedness in derivative-free optimization and outliers in local outlier factor. arXiv:2407.17529, 2024.
- [49] L. Li, P. Xie, and L. Zhang. A novel numerical method tailored for unconstrained optimization problems. arXiv:2504.02832, 2025.
- [50] P. Xie. An efficient derivative-free method for finding multiple solutions. To be posted on arXiv, 2024.
- [51] L. Li, Y. Zhou, P. Xie, and H. Li. A spectral Levenberg–Marquardt–Deflation method for multiple solutions of semilinear elliptic systems. *Journal of Computational and Applied Mathematics*, 2025.
- [52] Y. Ye, L. Li, P. Xie, and H. Yu. An improved adaptive orthogonal basis deflation method for multiple solutions with applications to nonlinear elliptic equations in varying domains. *Journal of Computational Mathematics*, 2025.
- [53] P. Xie. Privacy-preserving black-box optimization (PBBO): Theory and the model-based algorithm DFOP. arXiv:2601.11570, 2025.
- [54] P. Xie et al. A novel local analysis of objectives approximated by neural network: L-Change. International Conference on Mathematical Theory of Deep Learning (MTDL), 2024.
- [55] K. J. Dzahini, S. M. Wild, and P. Xie. Optimization approaches for solving inverse problems must account for uncertainty in both data and downstream decisions. Position paper, Inverse Methods for Complex Systems under Uncertainty Workshop, Sponsored by the U.S. Department of Energy, Office of Science, Advanced Scientific Computing Research, 2025.
- [56] P. Xie and M. Tao. Parametric resonant control of macroscopic behaviors of multiple oscillators. In *2019 American Control Conference (ACC)*, pages 1898–1905, 2019.

- [57] P. Xie. A note on the invariant distribution of a stochastic dynamical system. 2024.
- [58] P. Xie. The modeling and optimization of a multi-dam system. *Applied and Computational Mathematics*, 13(5):140–152, 2024.

## A Dispersion recursions, burn-in analysis, and logarithmic mixing

### A.1 Basic inequalities

**Lemma A.1.** *Let  $h : \mathbb{R}^d \rightarrow \mathbb{R}$  have  $L_2$ -Lipschitz Hessian. Then for all  $x, s$ ,*

$$h(x + s) \leq h(x) + \langle \nabla h(x), s \rangle + \frac{1}{2} s^\top \nabla^2 h(x) s + \frac{L_2}{6} \|s\|^3.$$

**Lemma A.2.** *For any  $z \in \mathbb{R}^N$  and integer  $t \geq 1$ ,*

$$\left\| \left( W^t - \left( \frac{1}{N} \mathbf{1} \mathbf{1}^\top \right) \right) z \right\|_2 \leq \rho^t \|z\|_2.$$

Consequently, for any stacked  $Z \in \mathbb{R}^{Nd}$ ,

$$\left\| \left( \left( W^t - \left( \frac{1}{N} \mathbf{1} \mathbf{1}^\top \right) \right) \otimes I_d \right) Z \right\| \leq \rho^t \|Z\|.$$

**Lemma A.3.** *Let  $h$  be convex with  $L$ -Lipschitz gradient. Then for any minimizer  $x_*$ ,*

$$\|\nabla h(x)\|^2 \leq 2L(h(x) - h(x_*)).$$

This appendix develops the tracker-dispersion analysis in full detail, eliminating the non-vanishing heterogeneity constants present in prior work. The central idea is to bound tracker increments using Lipschitz continuity of differences  $\nabla F(X_{k+1}) - \nabla F(X_k)$  and  $\nabla^2 F(X_{k+1}) - \nabla^2 F(X_k)$ .

### A.2 Dispersion operators and a contraction identity

For  $Z = [z_1; \dots; z_N] \in \mathbb{R}^{Nd}$  define the (RMS) dispersion

$$D(Z) := \sqrt{\frac{1}{N} \sum_{i=1}^N \|z_i - \bar{z}\|^2} = \frac{1}{\sqrt{N}} \left\| \left( I - \left( \frac{1}{N} \mathbf{1} \mathbf{1}^\top \right) \right) \otimes I_d Z \right\|,$$

$$\bar{z} := \frac{1}{N} \sum_{i=1}^N z_i.$$

Since  $\|A\|_F = \|\text{vec}(A)\|_2$ , the standard vector dispersion  $D(\cdot)$  naturally applies to the stacked vectorized Hessians  $\mathcal{H} \in \mathbb{R}^{Nd^2}$ .

**Lemma A.4.** *For any stacked vectors  $Z \in \mathbb{R}^{Nd}$  and any integer  $t \geq 1$ ,*

$$D((W^t \otimes I_d)Z) \leq \rho^t D(Z).$$

Likewise, for any stacked matrices  $\mathcal{H} \in \mathbb{R}^{Nd^2}$ ,

$$D((W^t \otimes I_{d^2})\mathcal{H}) \leq \rho^t D(\mathcal{H}).$$

*Proof.* We prove the vector case; the matrix case follows identically with  $I_d$  replaced by  $I_{d^2}$ . Let  $Z^\perp := ((I - (\frac{1}{N}\mathbf{1}\mathbf{1}^\top)) \otimes I_d)Z$ . Since  $W$  is doubly stochastic,  $W^\top (\frac{1}{N}\mathbf{1}\mathbf{1}^\top) = (\frac{1}{N}\mathbf{1}\mathbf{1}^\top)$  and  $(\frac{1}{N}\mathbf{1}\mathbf{1}^\top)W^\top = (\frac{1}{N}\mathbf{1}\mathbf{1}^\top)$ , hence  $I - (\frac{1}{N}\mathbf{1}\mathbf{1}^\top)W^\top = (W^\top - (\frac{1}{N}\mathbf{1}\mathbf{1}^\top))$ . Therefore

$$\begin{aligned} & (I - (\frac{1}{N}\mathbf{1}\mathbf{1}^\top)) \otimes I_d (W^\top \otimes I_d) Z \\ &= ((W^\top - (\frac{1}{N}\mathbf{1}\mathbf{1}^\top)) \otimes I_d) Z = ((W^\top - (\frac{1}{N}\mathbf{1}\mathbf{1}^\top)) \otimes I_d) Z^\perp, \end{aligned}$$

because  $(W^\top - (\frac{1}{N}\mathbf{1}\mathbf{1}^\top)) (\frac{1}{N}\mathbf{1}\mathbf{1}^\top) = 0$  implies  $(W^\top - (\frac{1}{N}\mathbf{1}\mathbf{1}^\top)) = (W^\top - (\frac{1}{N}\mathbf{1}\mathbf{1}^\top))I - (\frac{1}{N}\mathbf{1}\mathbf{1}^\top)$ . Taking norms and using Lemma A.2 gives

$$\begin{aligned} \|(I - (\frac{1}{N}\mathbf{1}\mathbf{1}^\top)) \otimes I_d (W^\top \otimes I_d) Z\| &= \|((W^\top - (\frac{1}{N}\mathbf{1}\mathbf{1}^\top)) \otimes I_d) Z^\perp\| \\ &\leq \|W^\top - (\frac{1}{N}\mathbf{1}\mathbf{1}^\top)\|_2 \|Z^\perp\| \leq \rho^t \|Z^\perp\|. \end{aligned}$$

Divide by  $\sqrt{N}$  to obtain the claim.  $\square$

### A.3 A uniform step bound

**Lemma A.5.** *For every  $k \geq 0$  and  $i \in \{1, \dots, N\}$ ,*

$$\|s_{i,k}\| \leq \sqrt{\frac{\|\tilde{g}_{i,k}\|}{M}}.$$

*Consequently, using the boundedness from Assumption 5.1,*

$$\|x_{i,k+1} - x_{i,k}\| \leq 2D \quad \text{and} \quad \|X_{k+1} - X_k\| \leq 2\sqrt{N}D,$$

where  $X_k = [x_{1,k}; \dots; x_{N,k}]$ .

*Proof.* Fix  $i, k$ . The local linear system is

$$(\tilde{H}_{i,k} + (\lambda_{i,k} + \delta_{i,k})I)s_{i,k} = -\tilde{g}_{i,k}.$$

By definition of  $\delta_{i,k}$ , the matrix  $\tilde{H}_{i,k} + \delta_{i,k}I$  is PSD, hence

$$\tilde{H}_{i,k} + (\lambda_{i,k} + \delta_{i,k})I \succeq \lambda_{i,k}I.$$

Taking norms, we obtain

$$\lambda_{i,k}\|s_{i,k}\| \leq \|(\tilde{H}_{i,k} + (\lambda_{i,k} + \delta_{i,k})I)s_{i,k}\| = \|\tilde{g}_{i,k}\|.$$

If  $\tilde{g}_{i,k} = 0$ , then  $s_{i,k} = 0$  and the bound holds. Otherwise divide by  $\lambda_{i,k} > 0$ :

$$\|s_{i,k}\| \leq \frac{\|\tilde{g}_{i,k}\|}{\lambda_{i,k}} = \frac{\|\tilde{g}_{i,k}\|}{\sqrt{M\|\tilde{g}_{i,k}\|}} = \sqrt{\frac{\|\tilde{g}_{i,k}\|}{M}}.$$

For the second part, Assumption 5.1 gives  $\|x_{i,k}\| \leq \|x_\star\| + D$  and in particular  $\|x_{i,k+1} - x_{i,k}\| \leq \|x_{i,k+1} - x_\star\| + \|x_{i,k} - x_\star\| \leq 2D$ . Summing squares yields  $\|X_{k+1} - X_k\| \leq 2\sqrt{N}D$ .  $\square$

#### A.4 Primal dispersion recursion (explicit)

Recall the stacked post-mixing update is

$$X_{k+1} = (W^{t_k} \otimes I_d)(\tilde{X}_k + S_k), \quad \tilde{X}_{k+1} = (W^{\tau_{k+1}} \otimes I_d)X_{k+1}.$$

**Lemma A.6.** *For all  $k \geq 0$ ,*

$$D(\tilde{X}_{k+1}) \leq \rho^{\tau_{k+1}} \rho^{t_k} \left( D(\tilde{X}_k) + \frac{\|S_k\|}{\sqrt{N}} \right).$$

Also,

$$D(X_{k+1}) \leq \rho^{t_k} \left( D(\tilde{X}_k) + \frac{\|S_k\|}{\sqrt{N}} \right).$$

*Proof.* By Lemma A.4 applied to  $Z = \tilde{X}_k + S_k$ ,

$$D(X_{k+1}) = D((W^{t_k} \otimes I_d)(\tilde{X}_k + S_k)) \leq \rho^{t_k} D(\tilde{X}_k + S_k).$$

Next we bound  $D(\tilde{X}_k + S_k)$  by the triangle inequality in the Hilbert space:

$$\begin{aligned} D(\tilde{X}_k + S_k) &= \frac{1}{\sqrt{N}} \left\| \left( I - \left( \frac{1}{N} \mathbf{1}\mathbf{1}^\top \right) \otimes I_d \right) (\tilde{X}_k + S_k) \right\| \\ &\leq \frac{1}{\sqrt{N}} \left\| \left( I - \left( \frac{1}{N} \mathbf{1}\mathbf{1}^\top \right) \otimes I_d \right) \tilde{X}_k \right\| \\ &\quad + \frac{1}{\sqrt{N}} \left\| \left( I - \left( \frac{1}{N} \mathbf{1}\mathbf{1}^\top \right) \otimes I_d \right) S_k \right\|. \end{aligned}$$

The first term equals  $D(\tilde{X}_k)$ . For the second,  $\left\| \left( I - \left( \frac{1}{N} \mathbf{1}\mathbf{1}^\top \right) \otimes I_d \right) S_k \right\| \leq \|S_k\|$ , hence it is bounded by  $\|S_k\|/\sqrt{N}$ . This proves the post-mixing inequality. Finally, apply Lemma A.4 to the pre-mixing step:  $D(\tilde{X}_{k+1}) \leq \rho^{\tau_{k+1}} D(X_{k+1})$  and combine.  $\square$

#### A.5 Gradient-tracker dispersion recursion (increment-based, fully expanded)

Write stacked variables

$$\begin{aligned} G_k &:= [g_{1,k}; \dots; g_{N,k}], \quad \tilde{G}_k := [\tilde{g}_{1,k}; \dots; \tilde{g}_{N,k}], \\ \Delta \nabla F_k &:= \nabla F(X_{k+1}) - \nabla F(X_k). \end{aligned}$$

Algorithm 1 implies the stacked recursion

$$\begin{aligned} G_{k+1} &= (W^{t_k} \otimes I_d)(\tilde{G}_k + \Delta \nabla F_k), \\ \tilde{G}_{k+1} &= (W^{\tau_{k+1}} \otimes I_d)G_{k+1}. \end{aligned} \tag{A.1}$$

**Lemma A.7.** *For all  $k \geq 0$ ,*

$$D(\tilde{G}_{k+1}) \leq \rho^{\tau_{k+1}} \rho^{t_k} \left( D(\tilde{G}_k) + \frac{L_1}{\sqrt{N}} \|X_{k+1} - X_k\| \right). \tag{A.2}$$

*In particular, using Lemma A.5,*

$$D(\tilde{G}_{k+1}) \leq \rho^{\tau_{k+1}} \rho^{t_k} \left( D(\tilde{G}_k) + 2L_1 D \right). \tag{A.3}$$

*Proof.* Starting from (A.1), substitute  $G_{k+1}$  into  $\tilde{G}_{k+1}$ :

$$\begin{aligned}\tilde{G}_{k+1} &= (W^{\tau_{k+1}} \otimes I_d)(W^{t_k} \otimes I_d)(\tilde{G}_k + \Delta \nabla F_k) \\ &= (W^{\tau_{k+1} + t_k} \otimes I_d)(\tilde{G}_k + \Delta \nabla F_k).\end{aligned}$$

Let  $m := \tau_{k+1} + t_k$  and  $Z := \tilde{G}_k + \Delta \nabla F_k$ . Apply  $(I - (\frac{1}{N} \mathbf{1} \mathbf{1}^\top) \otimes I_d)$  and use  $I - (\frac{1}{N} \mathbf{1} \mathbf{1}^\top) W^m = W^m - (\frac{1}{N} \mathbf{1} \mathbf{1}^\top)$ :

$$(I - (\frac{1}{N} \mathbf{1} \mathbf{1}^\top) \otimes I_d) \tilde{G}_{k+1} = ((W^m - (\frac{1}{N} \mathbf{1} \mathbf{1}^\top)) \otimes I_d) Z.$$

The projection entering the contraction is explicit because

$$W^m - (\frac{1}{N} \mathbf{1} \mathbf{1}^\top) = (W^m - (\frac{1}{N} \mathbf{1} \mathbf{1}^\top))(I - (\frac{1}{N} \mathbf{1} \mathbf{1}^\top)),$$

and therefore

$$\begin{aligned}D(\tilde{G}_{k+1}) &= \frac{1}{\sqrt{N}} \|((W^m - (\frac{1}{N} \mathbf{1} \mathbf{1}^\top)) \otimes I_d)((I - (\frac{1}{N} \mathbf{1} \mathbf{1}^\top) \otimes I_d) Z)\| \\ &\leq \rho^m D(Z).\end{aligned}$$

Next, the triangle inequality for projected RMS dispersions gives

$$D(Z) \leq D(\tilde{G}_k) + D(\Delta \nabla F_k) \leq D(\tilde{G}_k) + \frac{1}{\sqrt{N}} \|\Delta \nabla F_k\|,$$

where the last inequality uses  $\|(I - (\frac{1}{N} \mathbf{1} \mathbf{1}^\top) \otimes I_d) \Delta \nabla F_k\| \leq \|\Delta \nabla F_k\|$ . It remains to bound  $\|\Delta \nabla F_k\|$ . By block structure,

$$\begin{aligned}\|\Delta \nabla F_k\|^2 &= \sum_{i=1}^N \|\nabla f_i(x_{i,k+1}) - \nabla f_i(x_{i,k})\|^2 \\ &\leq \sum_{i=1}^N (L_1 \|x_{i,k+1} - x_{i,k}\|)^2 = L_1^2 \|X_{k+1} - X_k\|^2.\end{aligned}$$

Taking square roots gives  $\|\Delta \nabla F_k\| \leq L_1 \|X_{k+1} - X_k\|$  and yields (A.2). Finally, Lemma A.5 gives  $\|X_{k+1} - X_k\| \leq 2\sqrt{N}D$ , which proves (A.3).  $\square$

## A.6 Hessian-tracker dispersion recursion (increment-based, fully expanded)

Define stacked Hessian trackers  $\mathcal{H}_k := [H_{1,k}; \dots; H_{N,k}] \in \mathbb{R}^{Nd^2}$  and  $\tilde{\mathcal{H}}_k := [\tilde{H}_{1,k}; \dots; \tilde{H}_{N,k}]$ . Define the stacked Hessian increment

$$\Delta \nabla^2 F_k := \nabla^2 F(X_{k+1}) - \nabla^2 F(X_k),$$

viewed as a block vector in  $\mathbb{R}^{Nd^2}$  with Frobenius norm per block. The Hessian-tracker recursion is

$$\begin{aligned}\mathcal{H}_{k+1} &= (W^{t_k} \otimes I_{d^2})(\tilde{\mathcal{H}}_k + \Delta \nabla^2 F_k), \\ \tilde{\mathcal{H}}_{k+1} &= (W^{\tau_{k+1}} \otimes I_{d^2}) \mathcal{H}_{k+1}.\end{aligned}\tag{A.4}$$

**Lemma A.8.** *For all  $k \geq 0$ ,*

$$D(\tilde{\mathcal{H}}_{k+1}) \leq \rho^{\tau_{k+1}} \rho^{t_k} \left( D(\tilde{\mathcal{H}}_k) + \frac{\sqrt{d} L_2}{\sqrt{N}} \|X_{k+1} - X_k\| \right).\tag{A.5}$$

*In particular, using Lemma A.5,*

$$D(\tilde{\mathcal{H}}_{k+1}) \leq \rho^{\tau_{k+1}} \rho^{t_k} \left( D(\tilde{\mathcal{H}}_k) + 2\sqrt{d} L_2 D \right).\tag{A.6}$$

*Proof.* Applying the projected mixing identity used in Lemma A.7, now with block dimension  $d^2$ , gives

$$\tilde{\mathcal{H}}_{k+1} = (W^{\tau_{k+1}} \otimes I_{d^2}) \mathcal{H}_{k+1} \implies D(\tilde{\mathcal{H}}_{k+1}) \leq \rho^{\tau_{k+1}} D(\mathcal{H}_{k+1}),$$

where we used Lemma A.4. From the linear tracker update,

$$\mathcal{H}_{k+1} = (W^{t_k} \otimes I_{d^2})(\tilde{\mathcal{H}}_k + \Delta \nabla^2 F_k),$$

hence Lemma A.4 yields

$$\begin{aligned} D(\mathcal{H}_{k+1}) &\leq \rho^{t_k} D(\tilde{\mathcal{H}}_k + \Delta \nabla^2 F_k) \\ &\leq \rho^{t_k} \left( D(\tilde{\mathcal{H}}_k) + \frac{1}{\sqrt{N}} \|\Delta \nabla^2 F_k\|_F \right). \end{aligned}$$

Combining the last two displays yields (A.5) once  $\|\Delta \nabla^2 F_k\|_F$  is bounded. By block structure and the inequality  $\|A\|_F \leq \sqrt{d} \|A\|_2$ ,

$$\begin{aligned} \|\Delta \nabla^2 F_k\|_F^2 &= \sum_{i=1}^N \|\nabla^2 f_i(x_{i,k+1}) - \nabla^2 f_i(x_{i,k})\|_F^2 \\ &\leq \sum_{i=1}^N d \|\nabla^2 f_i(x_{i,k+1}) - \nabla^2 f_i(x_{i,k})\|_2^2. \end{aligned}$$

Using  $L_2$ -Lipschitzness of  $\nabla^2 f_i$ ,

$$\|\nabla^2 f_i(x_{i,k+1}) - \nabla^2 f_i(x_{i,k})\|_2 \leq L_2 \|x_{i,k+1} - x_{i,k}\|,$$

hence

$$\begin{aligned} \|\Delta \nabla^2 F_k\|_F^2 &\leq \sum_{i=1}^N d L_2^2 \|x_{i,k+1} - x_{i,k}\|^2 \\ &= d L_2^2 \|X_{k+1} - X_k\|^2. \end{aligned}$$

Taking square roots gives  $\|\Delta \nabla^2 F_k\|_F \leq \sqrt{d} L_2 \|X_{k+1} - X_k\|$ , which yields (A.5). Finally use Lemma A.5 to obtain (A.6).  $\square$

## A.7 Uniform tracker bounds and post-mixing primal decay

**Lemma A.9.** *If Assumptions 3.1 and 5.1 hold and  $\tau_k, t_k \geq 1$  for all  $k$ , then there exists a finite constant  $B_G > 0$  such that*

$$\sup_{k \geq 0} D(\tilde{G}_k) \leq B_G,$$

and consequently there exists a finite constant  $G_g > 0$  such that

$$\sup_{k \geq 0} \max_{1 \leq i \leq N} \|\tilde{g}_{i,k}\| \leq G_g.$$

*Proof.* From (A.3) we have

$$D(\tilde{G}_{k+1}) \leq \rho^{\tau_{k+1}} \rho^{t_k} (D(\tilde{G}_k) + 2L_1 D) \leq \rho^2 (D(\tilde{G}_k) + 2L_1 D),$$

since  $\tau_{k+1}, t_k \geq 1$  and  $\rho \in [0, 1)$ . Set  $q := \rho^2 \in [0, 1)$  and  $b := 2L_1 D$ . Unrolling yields

$$D(\tilde{G}_k) \leq q^k D(\tilde{G}_0) + \frac{qb}{1-q} \quad \forall k \geq 0,$$

so we may take  $B_G := D(\tilde{G}_0) + \frac{qb}{1-q}$ . Next, Lemma 5.5 and the iterate boundedness from Assumption 5.1 imply that  $\|\tilde{g}_k\| = \|\bar{g}_k\| = \|\frac{1}{N} \sum_{i=1}^N \nabla f_i(x_{i,k})\|$  is uniformly bounded on the level set; let  $G_{\text{avg}} := \sup_{k \geq 0} \|\tilde{g}_k\| < \infty$ . For any  $i$ ,

$$\|\tilde{g}_{i,k}\| \leq \|\tilde{g}_k\| + \|\tilde{g}_{i,k} - \tilde{g}_k\| \leq G_{\text{avg}} + \sqrt{N} D(\tilde{G}_k) \leq G_{\text{avg}} + \sqrt{N} B_G.$$

Thus we may take  $G_g := G_{\text{avg}} + \sqrt{N} B_G$ .  $\square$

For later reference, we record the uniform gradient bound from Lemma A.9:

$$G_g := \sup_{k \geq 0} \max_{1 \leq i \leq N} \|\tilde{g}_{i,k}\| < \infty, \quad (\text{A.7})$$

where finiteness follows from Lemma A.9.

**Lemma A.10.** *If Assumptions 3.1 and 5.1 hold and  $\tau_k, t_k \geq 1$  for all  $k$ , then there exists a finite constant  $B_H > 0$  such that*

$$\sup_{k \geq 0} D(\tilde{\mathcal{H}}_k) \leq B_H.$$

Consequently, there exists a finite constant  $G_H > 0$  such that

$$\sup_{k \geq 0} \max_{1 \leq i \leq N} \|\tilde{H}_{i,k}\|_2 \leq G_H, \quad \sup_{k \geq 0} \bar{\delta}_k \leq G_H.$$

*Proof.* From Lemma A.8 and  $\tau_{k+1}, t_k \geq 1$ , we have

$$D(\tilde{\mathcal{H}}_{k+1}) \leq \rho^{\tau_{k+1}} \rho^{t_k} \left( D(\tilde{\mathcal{H}}_k) + 2\sqrt{d} L_2 D \right) \leq \rho^2 \left( D(\tilde{\mathcal{H}}_k) + 2\sqrt{d} L_2 D \right).$$

Let  $q := \rho^2 \in [0, 1)$  and  $b_H := 2\sqrt{d} L_2 D$ . Unrolling yields

$$D(\tilde{\mathcal{H}}_k) \leq q^k D(\tilde{\mathcal{H}}_0) + \frac{qb_H}{1-q} \quad \forall k \geq 0,$$

so we may take  $B_H := D(\tilde{\mathcal{H}}_0) + qb_H/(1-q)$ .

Next, by Lemma 5.6,  $\tilde{H}_k = \bar{H}_k = \frac{1}{N} \sum_{i=1}^N \nabla^2 f_i(x_{i,k})$ , hence  $\|\tilde{H}_k\|_2 \leq M_{H,\text{max}}$ . For any  $i$ ,

$$\|\tilde{H}_{i,k}\|_2 \leq \|\tilde{H}_k\|_2 + \|\tilde{H}_{i,k} - \tilde{H}_k\|_2 \leq M_{H,\text{max}} + \sqrt{N} B_H.$$

Define  $G_H := M_{H,\text{max}} + \sqrt{N} B_H$ .

Finally,  $\delta_{i,k} = \max\{0, -\lambda_{\min}(\tilde{H}_{i,k})\} \leq \|\tilde{H}_{i,k}\|_2 \leq G_H$ , and averaging yields  $\bar{\delta}_k \leq G_H$ .  $\square$

**Lemma A.11.** *For all  $k \geq 0$ ,*

$$D(X_{k+1}) \leq \rho^{t_k} \left( D(\tilde{X}_k) + \frac{\|S_k\|}{\sqrt{N}} \right).$$

*Proof.* Recall  $X_{k+1} = (W^{t_k} \otimes I_d)(\tilde{X}_k + S_k)$  and that  $D(Z) = \|Z^\perp\|/\sqrt{N}$  with  $Z^\perp := ((I - (\frac{1}{N} \mathbf{1}\mathbf{1}^\top)) \otimes I_d)Z$ . Since  $(W^{t_k} - (\frac{1}{N} \mathbf{1}\mathbf{1}^\top))$  annihilates consensus components, we have

$$(X_{k+1})^\perp = ((W^{t_k} - (\frac{1}{N} \mathbf{1}\mathbf{1}^\top)) \otimes I_d)(\tilde{X}_k + S_k),$$

and by Lemma A.2 (applied in stacked form) and the triangle inequality,

$$\|(X_{k+1})^\perp\| \leq \rho^{t_k} \|(\tilde{X}_k + S_k)^\perp\| \leq \rho^{t_k} (\|\tilde{X}_k^\perp\| + \|S_k^\perp\|) \leq \rho^{t_k} (\|\tilde{X}_k^\perp\| + \|S_k\|).$$

Divide by  $\sqrt{N}$  to obtain the claim.  $\square$

**Lemma A.12.** *Under Assumptions 3.1 and 5.1 and schedule (A.8), there exists a constant  $C_X^+ > 0$  such that for all  $k \geq 0$ ,*

$$D(X_k) \leq \frac{C_X^+}{(k+1)^p}.$$

*Proof.* From Lemma A.11 and  $\rho^{tk} \leq e^{-c_{\text{mix}}(k+2)^{-p}} \leq (k+2)^{-p}$  under (A.8), it remains to bound  $D(\tilde{X}_k)$  and  $\|S_k\|/\sqrt{N}$  uniformly. By Assumption 5.1, each  $\tilde{x}_{i,k}$  is a convex combination of  $\{x_{j,k}\}$ , hence  $\|\tilde{x}_{i,k} - x_\star\| \leq D$  and

$$D(\tilde{X}_k) \leq \max_{1 \leq i \leq N} \|\tilde{x}_{i,k} - \bar{x}_k\| \leq \max_i \|\tilde{x}_{i,k} - x_\star\| + \|\bar{x}_k - x_\star\| \leq 2D.$$

Moreover, Lemma A.5 yields  $\|S_k\|/\sqrt{N} \leq \sqrt{G_g/M}$ , where  $G_g$  is defined in (A.7). Therefore,

$$D(X_{k+1}) \leq (k+2)^{-p} \left( 2D + \sqrt{\frac{G_g}{M}} \right),$$

and the claim follows with  $C_X^+ := 2D + \sqrt{G_g/M}$  after shifting indices.  $\square$

## A.8 Polynomial decay under a logarithmic schedule

Fix  $p > 2$  and set the logarithmic schedule

$$\tau_k = t_k = \left\lceil \frac{p \log(k+2) + c_{\text{mix}}}{-\log \rho} \right\rceil, \quad k \geq 0, \quad (\text{A.8})$$

so that  $\rho^{\tau_k} = \rho^{t_k} \leq e^{-c_{\text{mix}}(k+2)^{-p}}$ .

**Lemma A.13.** *Let  $\{u_k\}_{k \geq 0}$  satisfy  $u_{k+1} \leq a_k(u_k + b)$  with  $b \geq 0$ , where  $a_k \leq q < 1$  for all  $k$  and  $a_k \leq (k+2)^{-p}$  for all  $k$  with  $p > 2$ . Then there exists  $C > 0$  such that  $u_k \leq C/(k+2)^{p-1}$  for all  $k \geq 0$ .*

*Proof.* Since  $a_k \leq q < 1$ , we have  $u_{k+1} \leq q(u_k + b)$  and hence by induction

$$u_k \leq q^k u_0 + \sum_{j=0}^{k-1} q^{k-j} q b \leq u_0 + \frac{q b}{1-q} =: u_{\text{max}}, \quad \forall k \geq 0.$$

Since  $a_k \leq (k+2)^{-p}$ , for every  $k \geq 0$  we have

$$u_{k+1} \leq a_k(u_k + b) \leq \frac{u_{\text{max}} + b}{(k+2)^p} \leq \frac{u_{\text{max}} + b}{(k+2)^{p-1}}.$$

Since  $(k+3)/(k+2) \leq 2$  for all  $k \geq 0$ , we obtain  $u_{k+1} \leq 2^{p-1}(u_{\text{max}} + b)/(k+3)^{p-1}$ . For  $k = 0$ , the base case  $u_0 \leq u_{\text{max}} \leq C/2^{p-1}$  holds by definition. The claim follows with  $C := 2^{p-1}(u_{\text{max}} + b)$ .  $\square$

**Proposition A.14.** *Under Assumptions 3.1 and 5.1 and schedule (A.8), there exist constants  $C_X, C_G, C_H > 0$  such that for all  $k \geq 0$ ,*

$$D(\tilde{X}_k) \leq \frac{C_X}{(k+2)^{p-1}}, \quad D(\tilde{G}_k) \leq \frac{C_G}{(k+2)^{p-1}}, \quad D(\tilde{\mathcal{H}}_k) \leq \frac{C_H}{(k+2)^{p-1}}.$$

*Proof.* Apply Lemma A.13 to the recursion in Lemma A.6 and the bounds (A.3) and (A.6), using the bounded forcing constants  $b_X := \sup_k \|S_k\|/\sqrt{N} < \infty$  (Lemma A.5),  $b_G := 2L_1 D$ , and  $b_H := 2\sqrt{d} L_2 D$ .  $\square$

## A.9 Burn-in conditions for Proposition 5.14

We now establish that for every target accuracy  $0 < \varepsilon \leq 1$ , there exists a finite index  $K_0(\varepsilon)$  such that whenever  $\|g_k\| \geq \varepsilon$  and  $k \geq K_0(\varepsilon)$ , the three hypotheses of Proposition 5.14 are satisfied with  $\eta = 1/12$ .

**Proposition A.15.** *Fix  $p > 2$  and the schedule (A.8). For every  $0 < \varepsilon \leq 1$  there exists an integer  $K_0(\varepsilon) \geq 0$  such that for every  $k \geq K_0(\varepsilon)$  with  $\|g_k\| = \|\nabla f(\bar{x}_k)\| \geq \varepsilon$ , all three items of Proposition 5.14 hold with  $\eta := 1/12$ .*

**Moreover (auxiliary conditions).** *With the same choice of  $K_0(\varepsilon)$ , we may further guarantee that for all  $k \geq K_0(\varepsilon)$ ,*

$$\Delta_k^g \leq \varepsilon^2, \quad \Delta_k^H \leq \varepsilon^{3/2}, \quad D(X_k) \leq \varepsilon^{3/2}, \quad \bar{\delta}_k \leq (1 + L_2)\varepsilon^{3/2}, \quad (\text{A.9})$$

where  $\Delta_k^g := \frac{1}{N} \sum_{i=1}^N \|\tilde{g}_{i,k} - \tilde{g}_k\|$ ,  $\Delta_k^H := \frac{1}{N} \sum_{i=1}^N \|\tilde{H}_{i,k} - \tilde{H}_k\|_2$ , and  $\bar{\delta}_k := \frac{1}{N} \sum_{i=1}^N \delta_{i,k}$ .

*Proof.* Fix  $0 < \varepsilon \leq 1$  and set  $\eta := 1/12$ . We will produce an explicit index  $K_0(\varepsilon)$  such that for every  $k \geq K_0(\varepsilon)$  with  $\|g_k\| \geq \varepsilon$ , all three conditions of Proposition 5.14 hold.

**Step 1: post-mixing disagreement and bridge terms.** Recall  $D(X_k) = \|X_k^\perp\|/\sqrt{N}$ . By Lemma A.12, there exists  $C_X^+ > 0$  such that for all  $k \geq 0$ ,

$$D(X_k) \leq \frac{C_X^+}{(k+1)^p}. \quad (\text{A.10})$$

Therefore, for all  $k \geq 0$ ,

$$L_1 D(X_k) \leq \frac{L_1 C_X^+}{(k+1)^p}, \quad L_2 D(X_k) \leq \frac{L_2 C_X^+}{(k+1)^p}. \quad (\text{A.11})$$

**Step 2: tracker dispersions.** From Proposition A.14, there exist constants  $C_G, C_H > 0$  such that for all  $k \geq 0$ ,

$$D(\tilde{G}_k) \leq \frac{C_G}{(k+2)^{p-1}}, \quad D(\tilde{\mathcal{H}}_k) \leq \frac{C_H}{(k+2)^{p-1}}. \quad (\text{A.12})$$

By Cauchy–Schwarz and  $\|\cdot\|_2 \leq \|\cdot\|_F$ ,

$$\Delta_k^g = \frac{1}{N} \sum_{i=1}^N \|\tilde{g}_{i,k} - \tilde{g}_k\| \leq \sqrt{\frac{1}{N} \sum_{i=1}^N \|\tilde{g}_{i,k} - \tilde{g}_k\|^2} = D(\tilde{G}_k),$$

and

$$\begin{aligned} \Delta_k^H &= \frac{1}{N} \sum_{i=1}^N \|\tilde{H}_{i,k} - \tilde{H}_k\|_2 \\ &\leq \frac{1}{N} \sum_{i=1}^N \|\tilde{H}_{i,k} - \tilde{H}_k\|_F \\ &\leq D(\tilde{\mathcal{H}}_k). \end{aligned}$$

Hence, using Proposition A.14,

$$\Delta_k^g \leq \frac{C_G}{(k+2)^{p-1}}, \quad \Delta_k^H \leq \frac{C_H}{(k+2)^{p-1}}. \quad (\text{A.13})$$

**Step 3: a usable lower bound on the reference step.** Assume  $\|g_k\| \geq \varepsilon$  and suppose  $k$  is large enough such that  $L_1 D(X_k) \leq \varepsilon/2$ . Then Lemma 5.9 implies  $\|\tilde{g}_k\| \geq \varepsilon/2$ . Moreover, since  $A_k^{\text{ref}} \preceq (M_{H,\max} + \tilde{\lambda}_k)I$ ,

$$\|s_k^{\text{ref}}\| \geq \frac{\|\tilde{g}_k\|}{M_{H,\max} + \tilde{\lambda}_k} \geq \frac{\varepsilon/2}{M_{H,\max} + \sqrt{MG_g} + G_H} =: \underline{s}(\varepsilon),$$

where we used  $\tilde{\lambda}_k = \frac{1}{N} \sum_{i=1}^N (\lambda_{i,k} + \delta_{i,k}) \leq \sqrt{MG_g} + G_H$ , with  $G_g$  from (A.7) and  $G_H$  from Lemma A.10.

**Step 4: ensure dispersion control (Item 1).** We first verify the relative dispersion condition (5.3) with  $\alpha_d = 1/2$ . Since  $D(\tilde{G}_k) = \sqrt{\frac{1}{N} \sum_{i=1}^N \|\tilde{g}_{i,k} - \tilde{g}_k\|^2}$ , we have

$$\max_{1 \leq i \leq N} \|\tilde{g}_{i,k} - \tilde{g}_k\| \leq \sqrt{N} D(\tilde{G}_k).$$

From Step 3, for all  $k$  large enough with  $\|g_k\| \geq \varepsilon$  we have  $\|\tilde{g}_k\| \geq \varepsilon/2$ . Thus, choosing  $k$  large enough so that  $\sqrt{N} D(\tilde{G}_k) \leq \frac{1}{2} \|\tilde{g}_k\|$ , condition (5.3) holds with  $\alpha_d = 1/2$ . Using Lemma 5.12 and Lemma 5.13 with  $\alpha_d := 1/2$ , for all sufficiently large  $k$  with  $\|g_k\| \geq \varepsilon$  we have

$$\|\bar{s}_k - s_k^{\text{ref}}\| \leq \frac{6}{\sqrt{M\varepsilon}} \Delta_k^g + \frac{2}{M} \Delta_k^H + \frac{4}{M} \bar{\delta}_k.$$

To make this estimate quantitative, set

$$B_\lambda := M_{H,\max} + \sqrt{MG_g} + G_H, \quad \theta := \frac{\eta\sqrt{M}}{64B_\lambda^2}.$$

Once the relative dispersion condition holds, Step 5 gives  $\lambda_k \geq \frac{1}{2} \sqrt{M\varepsilon}$ ; Step 3 gives  $\|s_k^{\text{ref}}\| \geq \varepsilon/(2B_\lambda)$ , and  $\lambda_k \leq \sqrt{MG_g} + G_H$  gives  $M_{H,\max} + \lambda_k \leq B_\lambda$ . Hence

$$\frac{\eta}{16} \cdot \frac{\lambda_k}{M_{H,\max} + \lambda_k} \|s_k^{\text{ref}}\| \geq \theta \varepsilon^{3/2}.$$

Using Lemma 5.11,  $\bar{\delta}_k \leq \Delta_k^H + L_2 D(X_k)$ , the estimate above is therefore implied by the explicit sufficient conditions

$$\Delta_k^g \leq a_g \varepsilon^2, \quad \Delta_k^H \leq a_H \varepsilon^{3/2}, \quad D(X_k) \leq a_X \varepsilon^{3/2},$$

where

$$a_g := \frac{\theta\sqrt{M}}{18}, \quad a_H := \frac{\theta M}{18}, \quad a_X := \frac{\theta M}{12 \max\{L_2, 1\}}.$$

Indeed, these three inequalities bound

$$\frac{6}{\sqrt{M\varepsilon}} \Delta_k^g + \frac{2}{M} \Delta_k^H + \frac{4}{M} \bar{\delta}_k \leq \frac{6}{\sqrt{M\varepsilon}} \Delta_k^g + \frac{6}{M} \Delta_k^H + \frac{4L_2}{M} D(X_k) \leq \theta \varepsilon^{3/2}.$$

Define  $K_1(\varepsilon)$  as any index such that, for every  $k \geq K_1(\varepsilon)$ ,

$$\sqrt{N} D(\tilde{G}_k) \leq \frac{\varepsilon}{4}, \quad \Delta_k^g \leq a_g \varepsilon^2, \quad \Delta_k^H \leq a_H \varepsilon^{3/2}, \quad D(X_k) \leq a_X \varepsilon^{3/2}.$$

Such an index exists by (A.10) and (A.13), and its order is still  $\mathcal{O}(\varepsilon^{-2/(p-1)})$  because  $0 < \varepsilon \leq 1$ . Consequently, for all  $k \geq K_1(\varepsilon)$  with  $\|g_k\| \geq \varepsilon$ ,

$$\|\bar{s}_k - s_k^{\text{ref}}\| \leq \frac{\eta}{16} \cdot \frac{\lambda_k}{M_{H,\max} + \lambda_k} \|s_k^{\text{ref}}\|.$$

This implies  $\|s_k^{\text{ref}}\| \leq 2\|\bar{s}_k\|$  by the triangle inequality, and hence Item 1 of Proposition 5.14 holds.

**Step 5: ensure Items 2–3.** After the relative dispersion condition has been enforced with  $\alpha_d = 1/2$ , Step 3 gives  $\|\tilde{g}_{i,k}\| \geq \frac{1}{2}\|\tilde{g}_k\| \geq \varepsilon/4$  for every  $i$ . Hence

$$\lambda_k = \frac{1}{N} \sum_{i=1}^N (\sqrt{M\|\tilde{g}_{i,k}\|} + \delta_{i,k}) \geq \frac{1}{2}\sqrt{M\varepsilon}.$$

Since  $\|s_k^{\text{ref}}\| \leq 2\|\bar{s}_k\|$ , it is enough to ensure

$$L_1 D(X_k) \leq \frac{\eta}{16} \lambda_k \|s_k^{\text{ref}}\|, \quad L_2 D(X_k) \leq \frac{\eta}{8} \lambda_k.$$

By (A.11) and  $\|s_k^{\text{ref}}\| \geq \underline{s}(\varepsilon)$ , there exists  $K_2(\varepsilon)$  such that both inequalities hold for all  $k \geq K_2(\varepsilon)$ .

**Step 6: enforce the auxiliary burn-in bounds.** By (A.13),  $\Delta_k^g \leq \frac{C_G}{(k+2)^{p-1}}$ . Define

$$K_\Delta(\varepsilon) := \min \left\{ k \geq 0 : \frac{C_G}{(k+2)^{p-1}} \leq \varepsilon^2, \frac{C_H}{(k+2)^{p-1}} \leq \varepsilon^{3/2} \right\}.$$

Then for all  $k \geq K_\Delta(\varepsilon)$ , we have  $\Delta_k^g \leq \varepsilon^2$  and  $\Delta_k^H \leq \varepsilon^{3/2}$ .

**Step 7: enforce the post-mixing and stabilizer bounds.** Define

$$K_\delta(\varepsilon) := \min \left\{ k \geq 1 : \frac{C_X^+}{(k+1)^p} \leq \varepsilon^{3/2} \right\}.$$

Then for all  $k \geq K_\delta(\varepsilon)$ , we have  $D(X_k) \leq \varepsilon^{3/2}$ . Lemma 5.11 and Step 6 further give  $\bar{\delta}_k \leq \Delta_k^H + L_2 D(X_k) \leq (1 + L_2)\varepsilon^{3/2}$ .

Finally set

$$K_0(\varepsilon) := \max\{K_1(\varepsilon), K_2(\varepsilon), K_\Delta(\varepsilon), K_\delta(\varepsilon)\}.$$

Then for every  $k \geq K_0(\varepsilon)$  with  $\|g_k\| \geq \varepsilon$ , all three items of Proposition 5.14 hold with  $\eta = 1/12$ , and (A.9) also holds.  $\square$

**Theorem A.16.** *If the hypotheses of Theorem 5.20 hold and  $0 < \varepsilon \leq 1$ , then*

$$\sum_{k=0}^{K(\varepsilon)-1} (\tau_k + 2t_k) = \mathcal{O}\left((1-\rho)^{-1}(K_0(\varepsilon) + \varepsilon^{-1}) \log(K_0(\varepsilon) + \varepsilon^{-1})\right).$$

*In particular, since Theorem 5.20 assumes  $p \geq 3$ ,*

$$\sum_{k=0}^{K(\varepsilon)-1} (\tau_k + 2t_k) = \mathcal{O}\left((1-\rho)^{-1}\varepsilon^{-1} \log(1/\varepsilon)\right).$$

*For a fixed connected network, this reduces to  $\mathcal{O}(\varepsilon^{-1} \log(1/\varepsilon))$ .*

*Remark A.17.* For  $0 < \varepsilon \leq 1$ , the burn-in index  $K_0(\varepsilon)$  in Theorem 5.20 is determined by the direct verification of the three conditions in Proposition 5.14. In Step 4 of Proposition A.15, the estimate

$$\|\bar{s}_k - s_k^{\text{ref}}\| \leq \frac{6}{\sqrt{M\varepsilon}}\Delta_k^g + \frac{2}{M}\Delta_k^H + \frac{4}{M}\bar{\delta}_k$$

is compared with an Item 1 target of order  $\lambda_k \|s_k^{\text{ref}}\| = \Omega(\varepsilon^{3/2})$ . A conservative sufficient condition is therefore

$$\Delta_k^g = \mathcal{O}(\varepsilon^2), \quad \Delta_k^H = \mathcal{O}(\varepsilon^{3/2}), \quad D(X_k) = \mathcal{O}(\varepsilon^{3/2}),$$

up to constants, where  $\bar{\delta}_k \leq \Delta_k^H + L_2 D(X_k)$ . Under the logarithmic schedule (A.8) with  $\tau_k, t_k = \lceil (p \log(k+2) + c_{\text{mix}})/(-\log \rho) \rceil$ , Proposition A.14 yields  $D(\tilde{G}_k), D(\tilde{\mathcal{H}}_k) = \mathcal{O}(k^{-(p-1)})$ . It therefore suffices, conservatively, to choose  $k$  so that  $k^{-(p-1)} \lesssim \varepsilon^2$ , giving

$$K_0(\varepsilon) = \mathcal{O}(\varepsilon^{-2/(p-1)}).$$

If one keeps only  $p > 2$ , this gives the more general total iteration bound

$$K(\varepsilon) = \mathcal{O}\left(\varepsilon^{-1} + \varepsilon^{-2/(p-1)}\right).$$

In particular, for  $p \geq 3$ , the burn-in estimate is no larger than the  $\mathcal{O}(\varepsilon^{-1})$  post-burn-in term. Hence the total iteration complexity in Theorem 5.20 and the communication complexity in Theorem A.16 become

$$K(\varepsilon) = \mathcal{O}(\varepsilon^{-1}), \quad \sum_{k=0}^{K(\varepsilon)-1} (\tau_k + 2t_k) = \mathcal{O}((1-\rho)^{-1}\varepsilon^{-1} \log(1/\varepsilon)),$$

with the latter reducing to  $\mathcal{O}(\varepsilon^{-1} \log(1/\varepsilon))$  for a fixed connected network.

## B Proofs

*Proof of Lemma A.1.* Fix  $x, s$  and define  $\phi(t) := h(x+ts)$  for  $t \in [0, 1]$ . Then  $\phi'(t) = \langle \nabla h(x+ts), s \rangle$  and  $\phi''(t) = s^\top \nabla^2 h(x+ts)s$ . By  $L_2$ -Lipschitzness of  $\nabla^2 h$ ,

$$\begin{aligned} |\phi''(t) - \phi''(0)| &= |s^\top (\nabla^2 h(x+ts) - \nabla^2 h(x))s| \\ &\leq \|\nabla^2 h(x+ts) - \nabla^2 h(x)\|_2 \|s\|^2 \\ &\leq L_2 t \|s\|^3. \end{aligned}$$

Hence  $\phi''(t) \leq \phi''(0) + L_2 t \|s\|^3$ . Integrating twice,

$$\begin{aligned} \phi(1) &= \phi(0) + \phi'(0) + \int_0^1 (1-t)\phi''(t) dt \\ &\leq \phi(0) + \phi'(0) + \int_0^1 (1-t)(\phi''(0) + L_2 t \|s\|^3) dt. \end{aligned}$$

Compute  $\int_0^1 (1-t) dt = \frac{1}{2}$  and  $\int_0^1 (1-t)t dt = \frac{1}{6}$  to obtain

$$\phi(1) \leq \phi(0) + \phi'(0) + \frac{1}{2}\phi''(0) + \frac{L_2}{6}\|s\|^3.$$

Substitute  $\phi(0) = h(x)$ ,  $\phi'(0) = \langle \nabla h(x), s \rangle$ , and  $\phi''(0) = s^\top \nabla^2 h(x)s$ . □

*Proof of Lemma A.2.* Because  $W$  is symmetric and doubly stochastic, it is diagonalizable with eigenvalues  $1 = \lambda_1 > \lambda_2 \geq \dots \geq \lambda_N \geq -1$  and eigenvector  $\mathbf{1}$  for  $\lambda_1$ . The projector  $\left(\frac{1}{N}\mathbf{1}\mathbf{1}^\top\right) = \frac{1}{N}\mathbf{1}\mathbf{1}^\top$  is the orthogonal projector onto  $\text{span}\{\mathbf{1}\}$  and satisfies  $W\left(\frac{1}{N}\mathbf{1}\mathbf{1}^\top\right) = \left(\frac{1}{N}\mathbf{1}\mathbf{1}^\top\right)W = \left(\frac{1}{N}\mathbf{1}\mathbf{1}^\top\right)$ . We show  $W^t - \left(\frac{1}{N}\mathbf{1}\mathbf{1}^\top\right) = (W - \left(\frac{1}{N}\mathbf{1}\mathbf{1}^\top\right))^t$  by induction: for  $t = 1$  trivial. If true for  $t$ , then

$$\begin{aligned} (W - \left(\frac{1}{N}\mathbf{1}\mathbf{1}^\top\right))^{t+1} &= (W - \left(\frac{1}{N}\mathbf{1}\mathbf{1}^\top\right))^t (W - \left(\frac{1}{N}\mathbf{1}\mathbf{1}^\top\right)) \\ &= (W^t - \left(\frac{1}{N}\mathbf{1}\mathbf{1}^\top\right)) (W - \left(\frac{1}{N}\mathbf{1}\mathbf{1}^\top\right)) \\ &= W^{t+1} - W^t \left(\frac{1}{N}\mathbf{1}\mathbf{1}^\top\right) - \left(\frac{1}{N}\mathbf{1}\mathbf{1}^\top\right) W + \left(\frac{1}{N}\mathbf{1}\mathbf{1}^\top\right)^2 \\ &= W^{t+1} - \left(\frac{1}{N}\mathbf{1}\mathbf{1}^\top\right), \end{aligned}$$

using  $W^t\left(\frac{1}{N}\mathbf{1}\mathbf{1}^\top\right) = \left(\frac{1}{N}\mathbf{1}\mathbf{1}^\top\right)$ ,  $\left(\frac{1}{N}\mathbf{1}\mathbf{1}^\top\right)W = \left(\frac{1}{N}\mathbf{1}\mathbf{1}^\top\right)$ , and  $\left(\frac{1}{N}\mathbf{1}\mathbf{1}^\top\right)^2 = \left(\frac{1}{N}\mathbf{1}\mathbf{1}^\top\right)$ . Thus  $\|W^t - \left(\frac{1}{N}\mathbf{1}\mathbf{1}^\top\right)\|_2 = \|(W - \left(\frac{1}{N}\mathbf{1}\mathbf{1}^\top\right))^t\|_2 \leq \|W - \left(\frac{1}{N}\mathbf{1}\mathbf{1}^\top\right)\|_2^t = \rho^t$ . For stacked vectors,  $\|(A \otimes I_d)\|_2 = \|A\|_2$ .  $\square$

*Proof of Lemma A.3.* By  $L$ -smoothness,

$$h(y) \leq h(x) + \langle \nabla h(x), y - x \rangle + \frac{L}{2} \|y - x\|^2.$$

Choose  $y = x - \frac{1}{L}\nabla h(x)$  to obtain

$$h\left(x - \frac{1}{L}\nabla h(x)\right) \leq h(x) - \frac{1}{2L} \|\nabla h(x)\|^2.$$

Since  $x_\star$  minimizes  $h$ ,  $h(x_\star) \leq h\left(x - \frac{1}{L}\nabla h(x)\right)$ . Rearranging yields the claim.  $\square$

*Proof of Lemma 5.4.* Because  $W^{\tau_k}$  is doubly stochastic,

$$\tilde{x}_k = \frac{1}{N} \sum_{i=1}^N \sum_{j=1}^N [W^{\tau_k}]_{ij} x_{j,k} = \frac{1}{N} \sum_{j=1}^N \left( \sum_{i=1}^N [W^{\tau_k}]_{ij} \right) x_{j,k} = \frac{1}{N} \sum_{j=1}^N x_{j,k} = \bar{x}_k.$$

Similarly,  $W^{t_k}$  is doubly stochastic and  $y_{i,k+1} = \tilde{x}_{i,k} + s_{i,k}$ , hence

$$\begin{aligned} \bar{x}_{k+1} &= \frac{1}{N} \sum_{i=1}^N x_{i,k+1} = \frac{1}{N} \sum_{i=1}^N \sum_{j=1}^N [W^{t_k}]_{ij} y_{j,k+1} \\ &= \frac{1}{N} \sum_{j=1}^N y_{j,k+1} = \tilde{x}_k + \bar{s}_k = \bar{x}_k + \bar{s}_k. \end{aligned}$$

$\square$

*Proof of Lemma 5.5.* Average the tracker update in Algorithm 1:

$$\bar{g}_{k+1} = \frac{1}{N} \sum_{i=1}^N g_{i,k+1} = \frac{1}{N} \sum_{i=1}^N \sum_{j=1}^N [W^{t_k}]_{ij} \left( \tilde{g}_{j,k} + \nabla f_j(x_{j,k+1}) - \nabla f_j(x_{j,k}) \right).$$

Swap sums and use column-stochasticity  $\sum_{i=1}^N [W^{t_k}]_{ij} = 1$ :

$$\bar{g}_{k+1} = \frac{1}{N} \sum_{j=1}^N \left( \tilde{g}_{j,k} + \nabla f_j(x_{j,k+1}) - \nabla f_j(x_{j,k}) \right)$$

$$= \tilde{g}_k + \frac{1}{N} \sum_{j=1}^N (\nabla f_j(x_{j,k+1}) - \nabla f_j(x_{j,k})).$$

Pre-mixing preserves averages, hence  $\tilde{g}_k = \bar{g}_k$ . Starting from

$$\bar{g}_0 = \frac{1}{N} \sum_{i=1}^N \nabla f_i(x_{i,0}),$$

induction gives  $\bar{g}_k = N^{-1} \sum_{i=1}^N \nabla f_i(x_{i,k})$  for all  $k$ , and thus  $\tilde{g}_k = \bar{g}_k$ .  $\square$

*Proof of Lemma 5.6.* Repeating the analysis in the proof of Lemma 5.5 with gradients replaced by Hessians yields the claim. Averaging the Hessian update gives

$$\bar{H}_{k+1} = \tilde{H}_k + \frac{1}{N} \sum_{i=1}^N (\nabla^2 f_i(x_{i,k+1}) - \nabla^2 f_i(x_{i,k})),$$

and  $\tilde{H}_k = \bar{H}_k$ . Induction yields  $\bar{H}_k = \frac{1}{N} \sum_{i=1}^N \nabla^2 f_i(x_{i,k})$ .  $\square$

*Proof of Lemma 5.7.* If  $\tilde{g}_{i,k} = 0$ , Algorithm 1 sets  $s_{i,k} = 0$  and  $\lambda_{i,k} = 0$ , so the claim is immediate. Assume henceforth that  $\tilde{g}_{i,k} \neq 0$ , so  $\lambda_{i,k} > 0$ . As in Appendix A, the local system satisfies  $(\tilde{H}_{i,k} + (\lambda_{i,k} + \delta_{i,k})I) \succeq \lambda_{i,k}I$ . Thus  $\lambda_{i,k}\|s_{i,k}\| \leq \|\tilde{g}_{i,k}\|$ . Since  $\lambda_{i,k}^2 = M\|\tilde{g}_{i,k}\|$ , we have  $\lambda_{i,k}\|s_{i,k}\| \leq \lambda_{i,k}^2/M$ , hence  $M\|s_{i,k}\| \leq \lambda_{i,k}$ . Using  $M \geq L_2$  gives  $L_2\|s_{i,k}\| \leq \lambda_{i,k}$ .  $\square$

*Proof of Lemma 5.8.* From Lemma 5.7,  $M\|s_{i,k}\| \leq \lambda_{i,k}$  for all  $i$ , hence

$$\frac{1}{N} \sum_{i=1}^N \lambda_{i,k} \geq \frac{M}{N} \sum_{i=1}^N \|s_{i,k}\| \geq M \left\| \frac{1}{N} \sum_{i=1}^N s_{i,k} \right\| = M\|\bar{s}_k\|,$$

using  $\left\| \frac{1}{N} \sum_{i=1}^N s_i \right\| \leq \frac{1}{N} \sum_{i=1}^N \|s_i\|$ . Since  $M \geq L_2$ ,  $L_2\|\bar{s}_k\| \leq \frac{1}{N} \sum_{i=1}^N \lambda_{i,k}$ . Finally  $\tilde{\lambda}_k = \frac{1}{N} \sum_{i=1}^N (\lambda_{i,k} + \delta_{i,k}) \geq \frac{1}{N} \sum_{i=1}^N \lambda_{i,k}$ .  $\square$

*Proof of Lemma 5.9.* By Lemma 5.5,  $\tilde{g}_k = \frac{1}{N} \sum_{i=1}^N \nabla f_i(x_{i,k})$ . Therefore

$$\begin{aligned} \|\nabla f(\bar{x}_k) - \tilde{g}_k\| &= \left\| \frac{1}{N} \sum_{i=1}^N (\nabla f_i(\bar{x}_k) - \nabla f_i(x_{i,k})) \right\| \\ &\leq \frac{1}{N} \sum_{i=1}^N \|\nabla f_i(\bar{x}_k) - \nabla f_i(x_{i,k})\|. \end{aligned}$$

The  $L_1$ -Lipschitzness of  $\nabla f_i$  implies  $\|\nabla f_i(\bar{x}_k) - \nabla f_i(x_{i,k})\| \leq L_1\|x_{i,k} - \bar{x}_k\|$ . Averaging this inequality and applying Cauchy–Schwarz gives

$$\frac{1}{N} \sum_{i=1}^N \|x_{i,k} - \bar{x}_k\| \leq \sqrt{\frac{1}{N} \sum_{i=1}^N \|x_{i,k} - \bar{x}_k\|^2} = D(X_k).$$

Combining this bound with the preceding display yields the claim.  $\square$

*Proof of Lemma 5.10.* By Lemma 5.6,  $\tilde{H}_k = \frac{1}{N} \sum_{i=1}^N \nabla^2 f_i(x_{i,k})$ . Thus

$$\nabla^2 f(\bar{x}_k) - \tilde{H}_k = \frac{1}{N} \sum_{i=1}^N (\nabla^2 f_i(\bar{x}_k) - \nabla^2 f_i(x_{i,k})),$$

and so

$$\begin{aligned} & \|\nabla^2 f(\bar{x}_k) - \tilde{H}_k\|_2 \\ & \leq \frac{1}{N} \sum_{i=1}^N \|\nabla^2 f_i(\bar{x}_k) - \nabla^2 f_i(x_{i,k})\|_2 \\ & \leq \frac{L_2}{N} \sum_{i=1}^N \|x_{i,k} - \bar{x}_k\|. \end{aligned}$$

Cauchy–Schwarz applied to the last average gives  $\|\nabla^2 f(\bar{x}_k) - \tilde{H}_k\|_2 \leq L_2 D(X_k)$ .  $\square$

*Proof of Lemma 5.11.* Let  $A := \tilde{H}_{i,k}$  and  $B := \nabla^2 f(\bar{x}_k) \succeq 0$ . By Weyl’s inequality,

$$\lambda_{\min}(A) \geq \lambda_{\min}(B) - \|A - B\|_2 \geq -\|A - B\|_2.$$

Therefore  $-\lambda_{\min}(A) \leq \|A - B\|_2$ , and since  $\delta_{i,k} = \max\{0, -\lambda_{\min}(A)\}$ , we obtain  $0 \leq \delta_{i,k} \leq \|A - B\|_2$ , proving the first claim. For the second,

$$\|A - B\|_2 \leq \|A - \tilde{H}_k\|_2 + \|\tilde{H}_k - B\|_2.$$

Averaging over  $i$  gives  $\bar{\delta}_k \leq \Delta_k^H + \|\tilde{H}_k - \nabla^2 f(\bar{x}_k)\|_2$ , and Lemma 5.10 gives the stated bound.  $\square$

*Proof of Lemma 5.12.* Fix  $k$  and abbreviate  $A_i := A_{i,k}$ ,  $A := A_k^{\text{ref}}$ ,  $\tilde{g}_i := \tilde{g}_{i,k}$ ,  $\tilde{g} := \tilde{g}_k$ . Then  $s_i = -A_i^{-1} \tilde{g}_i$  and  $s^{\text{ref}} = -A^{-1} \tilde{g}$ . Decompose:

$$s_i - s^{\text{ref}} = -A_i^{-1}(\tilde{g}_i - \tilde{g}) + (A^{-1} - A_i^{-1})\tilde{g}.$$

Since  $A_i \succeq \tilde{\lambda}_{i,k} I \succeq \underline{\lambda}_k I$ , we have  $\|A_i^{-1}\|_2 \leq 1/\underline{\lambda}_k$ . Thus

$$\|s_i - s^{\text{ref}}\| \leq \frac{1}{\underline{\lambda}_k} \|\tilde{g}_i - \tilde{g}\| + \|A^{-1} - A_i^{-1}\|_2 \|\tilde{g}\|.$$

Use the resolvent identity  $A^{-1} - A_i^{-1} = A_i^{-1}(A_i - A)A^{-1}$  to get

$$\|A^{-1} - A_i^{-1}\|_2 \leq \|A_i^{-1}\|_2 \|A_i - A\|_2 \|A^{-1}\|_2 \leq \frac{1}{\underline{\lambda}_k} \cdot \frac{1}{\tilde{\lambda}_k} \|A_i - A\|_2,$$

since  $A \succeq \tilde{\lambda}_k I$  implies  $\|A^{-1}\|_2 \leq 1/\tilde{\lambda}_k$ . Furthermore,

$$A_i - A = (\tilde{H}_{i,k} - \tilde{H}_k) + (\tilde{\lambda}_{i,k} - \tilde{\lambda}_k)I,$$

so  $\|A_i - A\|_2 \leq \|\tilde{H}_{i,k} - \tilde{H}_k\|_2 + |\tilde{\lambda}_{i,k} - \tilde{\lambda}_k|$ . Combining the resolvent bound with the estimate on  $\|A_i - A\|_2$ , and then averaging over  $i$  using  $\|\bar{s} - s^{\text{ref}}\| \leq \frac{1}{N} \sum_{i=1}^N \|s_i - s^{\text{ref}}\|$ , gives the claim.  $\square$

*Proof of Lemma 5.13.* Write  $\tilde{\lambda}_{i,k} - \tilde{\lambda}_k = (\lambda_{i,k} - \bar{\lambda}_k) + (\delta_{i,k} - \bar{\delta}_k)$ , where  $\bar{\lambda}_k := \frac{1}{N} \sum_{i=1}^N \lambda_{i,k}$ . Then

$$\Delta_k^\lambda = \frac{1}{N} \sum_{i=1}^N |\tilde{\lambda}_{i,k} - \tilde{\lambda}_k| \leq \underbrace{\frac{1}{N} \sum_{i=1}^N |\lambda_{i,k} - \bar{\lambda}_k|}_{=:T_1} + \underbrace{\frac{1}{N} \sum_{i=1}^N |\delta_{i,k} - \bar{\delta}_k|}_{=:T_2}.$$

**Step 1: bound  $T_2$ .** Since  $\delta_{i,k} \geq 0$ , a standard counting argument yields

$$\sum_{i=1}^N |\delta_{i,k} - \bar{\delta}_k| = 2 \sum_{i: \delta_{i,k} > \bar{\delta}_k} (\delta_{i,k} - \bar{\delta}_k) \leq 2 \sum_{i: \delta_{i,k} > \bar{\delta}_k} \delta_{i,k} \leq 2 \sum_{i=1}^N \delta_{i,k} = 2N\bar{\delta}_k,$$

so  $T_2 \leq 2\bar{\delta}_k$ .

**Step 2: bound  $T_1$ .** For any scalars  $\{u_i\}$  with  $\bar{u} = \frac{1}{N} \sum_{i=1}^N u_i$ ,  $|u_i - \bar{u}| = |\frac{1}{N} \sum_{j=1}^N (u_i - u_j)| \leq \frac{1}{N} \sum_{j=1}^N |u_i - u_j|$ . Averaging over  $i$  gives

$$T_1 \leq \frac{1}{N^2} \sum_{i=1}^N \sum_{j=1}^N |\lambda_{i,k} - \lambda_{j,k}|.$$

Let  $a_i := \|\tilde{g}_{i,k}\|$ . Then

$$|\lambda_{i,k} - \lambda_{j,k}| = \sqrt{M} |\sqrt{a_i} - \sqrt{a_j}| = \sqrt{M} \frac{|a_i - a_j|}{\sqrt{a_i} + \sqrt{a_j}}.$$

Moreover  $|a_i - a_j| \leq \|\tilde{g}_{i,k} - \tilde{g}_{j,k}\|$ . By triangle inequality,  $\|\tilde{g}_{i,k} - \tilde{g}_{j,k}\| \leq \|\tilde{g}_{i,k} - \tilde{g}_k\| + \|\tilde{g}_{j,k} - \tilde{g}_k\|$ , hence

$$\frac{1}{N^2} \sum_{i=1}^N \sum_{j=1}^N \|\tilde{g}_{i,k} - \tilde{g}_{j,k}\| \leq \frac{1}{N^2} \sum_{i=1}^N \sum_{j=1}^N (\|\tilde{g}_{i,k} - \tilde{g}_k\| + \|\tilde{g}_{j,k} - \tilde{g}_k\|) = 2\Delta_k^g.$$

Under (5.3),  $a_i \geq \|\tilde{g}_k\| - \|\tilde{g}_{i,k} - \tilde{g}_k\| \geq (1 - \alpha_d)\|\tilde{g}_k\|$  for all  $i$ , so  $\sqrt{a_i} + \sqrt{a_j} \geq 2\sqrt{(1 - \alpha_d)\|\tilde{g}_k\|}$ . Therefore

$$T_1 \leq \sqrt{M} \cdot \frac{2\Delta_k^g}{2\sqrt{(1 - \alpha_d)\|\tilde{g}_k\|}} = \frac{\sqrt{M}}{\sqrt{1 - \alpha_d}} \cdot \frac{\Delta_k^g}{\sqrt{\|\tilde{g}_k\|}}.$$

The displayed estimate for  $T_1$  and the Step 1 bound  $T_2 \leq 2\bar{\delta}_k$  give the stated bound on  $\Delta_k^\lambda$ .  $\square$

*Proof of Proposition 5.14.* Write

$$r_k = (\nabla^2 f(\bar{x}_k) + \lambda_k I) \bar{s}_k + g_k.$$

Add and subtract the reference step:

$$r_k = (\nabla^2 f(\bar{x}_k) + \lambda_k I) (\bar{s}_k - s_k^{\text{ref}}) + (\nabla^2 f(\bar{x}_k) + \lambda_k I) s_k^{\text{ref}} + g_k.$$

Using  $(\tilde{H}_k + \lambda_k I) s_k^{\text{ref}} = -\tilde{g}_k$ , we have

$$(\nabla^2 f(\bar{x}_k) + \lambda_k I) s_k^{\text{ref}} + g_k = (\nabla^2 f(\bar{x}_k) - \tilde{H}_k) s_k^{\text{ref}} + (g_k - \tilde{g}_k).$$

Therefore

$$r_k = (\nabla^2 f(\bar{x}_k) + \lambda_k I) (\bar{s}_k - s_k^{\text{ref}}) + (\nabla^2 f(\bar{x}_k) - \tilde{H}_k) s_k^{\text{ref}} + (g_k - \tilde{g}_k).$$

Take norms:

$$\begin{aligned} \|r_k\| &\leq \|\nabla^2 f(\bar{x}_k) + \lambda_k I\|_2 \|\bar{s}_k - s_k^{\text{ref}}\| \\ &\quad + \|\nabla^2 f(\bar{x}_k) - \tilde{H}_k\|_2 \|s_k^{\text{ref}}\| + \|g_k - \tilde{g}_k\|. \end{aligned}$$

By the global Hessian bound (5.2),  $\|\nabla^2 f(\bar{x}_k)\|_2 \leq M_{H,\max}$ , hence  $\|\nabla^2 f(\bar{x}_k) + \lambda_k I\|_2 \leq M_{H,\max} + \lambda_k$ . Item 1 of Proposition 5.14 implies

$$\begin{aligned} &\|\nabla^2 f(\bar{x}_k) + \lambda_k I\|_2 \|\bar{s}_k - s_k^{\text{ref}}\| \\ &\leq (M_{H,\max} + \lambda_k) \cdot \frac{\eta}{8} \cdot \frac{\lambda_k}{M_{H,\max} + \lambda_k} \|\bar{s}_k\| = \frac{\eta}{8} \lambda_k \|\bar{s}_k\|. \end{aligned}$$

Next, item (3) and Lemma 5.10 imply  $\|\nabla^2 f(\bar{x}_k) - \tilde{H}_k\|_2 \leq \frac{\eta}{8} \lambda_k$ . Moreover,

$$\|s_k^{\text{ref}}\| \leq \|\bar{s}_k\| + \|\bar{s}_k - s_k^{\text{ref}}\| \leq \left(1 + \frac{\eta}{8}\right) \|\bar{s}_k\| \leq \frac{9}{8} \|\bar{s}_k\|,$$

since  $\eta \leq 1/12$  implies  $1 + \eta/8 \leq 9/8$ . Therefore the second term is bounded by

$$\|\nabla^2 f(\bar{x}_k) - \tilde{H}_k\|_2 \|s_k^{\text{ref}}\| \leq \frac{\eta}{8} \lambda_k \cdot \frac{9}{8} \|\bar{s}_k\| = \frac{9\eta}{64} \lambda_k \|\bar{s}_k\|.$$

Finally, item (2) and Lemma 5.9 imply  $\|g_k - \tilde{g}_k\| \leq \frac{\eta}{8} \lambda_k \|\bar{s}_k\|$ . Summing yields

$$\|r_k\| \leq \left(\frac{\eta}{8} + \frac{9\eta}{64} + \frac{\eta}{8}\right) \lambda_k \|\bar{s}_k\| = \frac{25\eta}{64} \lambda_k \|\bar{s}_k\| \leq \eta \lambda_k \|\bar{s}_k\|.$$

The inequality  $L_2 \|\bar{s}_k\| \leq \lambda_k$  is Lemma 5.8.  $\square$

*Proof of Lemma 5.15.* Apply Lemma A.1 to  $f$  at  $(\bar{x}_k, \bar{s}_k)$ :

$$f(\bar{x}_k + \bar{s}_k) \leq f(\bar{x}_k) + \langle g_k, \bar{s}_k \rangle + \frac{1}{2} \bar{s}_k^\top \nabla^2 f(\bar{x}_k) \bar{s}_k + \frac{L_2}{6} \|\bar{s}_k\|^3.$$

Let  $d_k := (\nabla^2 f(\bar{x}_k) + \lambda_k I) \bar{s}_k + g_k$ . Then  $\langle g_k, \bar{s}_k \rangle = -\bar{s}_k^\top \nabla^2 f(\bar{x}_k) \bar{s}_k - \lambda_k \|\bar{s}_k\|^2 + \langle d_k, \bar{s}_k \rangle$ . Substitute:

$$f(\bar{x}_{k+1}) \leq f(\bar{x}_k) - \frac{1}{2} \bar{s}_k^\top \nabla^2 f(\bar{x}_k) \bar{s}_k - \lambda_k \|\bar{s}_k\|^2 + \langle d_k, \bar{s}_k \rangle + \frac{L_2}{6} \|\bar{s}_k\|^3.$$

Since  $\nabla^2 f(\bar{x}_k) \succeq 0$ , drop the nonpositive term. Also  $\langle d_k, \bar{s}_k \rangle \leq \|d_k\| \|\bar{s}_k\| \leq \eta \lambda_k \|\bar{s}_k\|^2$  and  $L_2 \|\bar{s}_k\| \leq \lambda_k$  implies  $\frac{L_2}{6} \|\bar{s}_k\|^3 \leq \frac{1}{6} \lambda_k \|\bar{s}_k\|^2$ . Combining the residual, cubic-remainder, and nonpositive-Hessian bounds yields the claim.  $\square$

*Proof of Lemma 5.16.* By the integral form of Taylor's theorem,

$$\nabla f(\bar{x}_k + \bar{s}_k) = g_k + \nabla^2 f(\bar{x}_k) \bar{s}_k + e_k, \quad \|e_k\| \leq \frac{L_2}{2} \|\bar{s}_k\|^2.$$

The definition  $d_k = (\nabla^2 f(\bar{x}_k) + \lambda_k I) \bar{s}_k + g_k$  gives  $g_k + \nabla^2 f(\bar{x}_k) \bar{s}_k = -\lambda_k \bar{s}_k + d_k$ . Thus

$$\|g_{k+1}\| \leq \lambda_k \|\bar{s}_k\| + \|d_k\| + \|e_k\| \leq \lambda_k \|\bar{s}_k\| + \eta \lambda_k \|\bar{s}_k\| + \frac{L_2}{2} \|\bar{s}_k\|^2.$$

Finally  $L_2 \|\bar{s}_k\| \leq \lambda_k$  implies  $\frac{L_2}{2} \|\bar{s}_k\|^2 \leq \frac{1}{2} \lambda_k \|\bar{s}_k\|$ .  $\square$

**Lemma B.1.** *If Assumptions 3.1 and 5.1 hold and the schedule (A.8) is used, then the following is true. Fix any  $0 < \varepsilon \leq 1$  and let  $K_0(\varepsilon)$  be as in Proposition A.15. Then there exists a constant  $C_\lambda > 0$  such that for all  $k \geq K_0(\varepsilon)$  with  $\|g_k\| \geq \varepsilon$ ,*

$$\lambda_k \leq C_\lambda \sqrt{\|g_k\|}.$$

*Proof.* Recall  $\lambda_k = \tilde{\lambda}_k = \frac{1}{N} \sum_{i=1}^N (\lambda_{i,k} + \delta_{i,k})$  with  $\lambda_{i,k} = \sqrt{M \|\tilde{g}_{i,k}\|}$  and  $\delta_{i,k} \geq 0$ . By Jensen's inequality (concavity of  $x \mapsto \sqrt{x}$ ),

$$\frac{1}{N} \sum_{i=1}^N \sqrt{\|\tilde{g}_{i,k}\|} \leq \sqrt{\frac{1}{N} \sum_{i=1}^N \|\tilde{g}_{i,k}\|}.$$

Moreover, by the triangle inequality and the definition of  $\Delta_k^g$ ,

$$\frac{1}{N} \sum_{i=1}^N \|\tilde{g}_{i,k}\| \leq \|\tilde{g}_k\| + \Delta_k^g.$$

By Lemma 5.9,  $\|\tilde{g}_k - g_k\| \leq L_1 D(X_k)$ . Using Item 2 of Proposition 5.14 (which holds for all  $k \geq K_0(\varepsilon)$  with  $\|g_k\| \geq \varepsilon$ ), together with  $\|(\nabla^2 f(\bar{x}_k) + \lambda_k I)\bar{s}_k\| = \|g_k - r_k\| \geq \lambda_k \|\bar{s}_k\|$  and  $\|r_k\| \leq \eta \lambda_k \|\bar{s}_k\|$ , we obtain  $(1 - \eta)\lambda_k \|\bar{s}_k\| \leq \|g_k\|$  and hence

$$L_1 D(X_k) \leq \frac{\eta}{8} \lambda_k \|\bar{s}_k\| \leq \frac{\eta}{8(1 - \eta)} \|g_k\|.$$

Therefore,

$$\|\tilde{g}_k\| \leq \|g_k\| + L_1 D(X_k) \leq \left(1 + \frac{\eta}{8(1 - \eta)}\right) \|g_k\|.$$

In addition, Proposition A.15 ensures  $\Delta_k^g \leq \varepsilon^2 \leq \varepsilon \leq \|g_k\|$  for all  $k \geq K_0(\varepsilon)$  with  $\|g_k\| \geq \varepsilon$ . Thus,

$$\frac{1}{N} \sum_{i=1}^N \|\tilde{g}_{i,k}\| \leq \left(2 + \frac{\eta}{8(1 - \eta)}\right) \|g_k\|.$$

Hence,

$$\lambda_k = \frac{1}{N} \sum_{i=1}^N (\sqrt{M \|\tilde{g}_{i,k}\|} + \delta_{i,k}) \leq \sqrt{M} \sqrt{\frac{1}{N} \sum_{i=1}^N \|\tilde{g}_{i,k}\|} + \bar{\delta}_k \leq C_0 \sqrt{\|g_k\|} + \bar{\delta}_k,$$

with  $C_0 := \sqrt{M(2 + \frac{\eta}{8(1 - \eta)})}$ . Finally, Proposition A.15 also ensures  $\bar{\delta}_k \leq (1 + L_2)\varepsilon^{3/2}$  on the same index set. Since  $0 < \varepsilon \leq 1$  and  $\|g_k\| \geq \varepsilon$ , we have  $\varepsilon^{3/2} \leq \sqrt{\varepsilon} \leq \sqrt{\|g_k\|}$ . Absorbing this term into the constant yields  $\lambda_k \leq (C_0 + 1 + L_2)\sqrt{\|g_k\|}$ , completing the proof.  $\square$

*Proof of Lemma 5.17.* Assume  $\eta \leq 1/12$ , so  $c_d := 1 - \eta - \frac{1}{6} \geq \frac{3}{4}$  in Lemma 5.15. Also from Lemma 5.16,  $C_g := 1 + \eta + \frac{1}{2} \leq 2$ . For  $k \in \mathcal{I}$ ,  $\|g_{k+1}\| \geq \frac{1}{4}\|g_k\|$  and  $\|g_{k+1}\| \leq C_g \lambda_k \|\bar{s}_k\|$  imply  $\|\bar{s}_k\| \geq \|g_k\|/(4C_g \lambda_k)$ . Then Lemma 5.15 yields

$$\Phi_k - \Phi_{k+1} \geq c_d \lambda_k \|\bar{s}_k\|^2 \geq c_d \lambda_k \left(\frac{\|g_k\|}{4C_g \lambda_k}\right)^2 = \frac{c_d}{16C_g^2} \frac{\|g_k\|^2}{\lambda_k}.$$

By the additional assumption in Lemma 5.17, we have  $\lambda_k \leq C_\lambda \sqrt{\|g_k\|}$ . Therefore,

$$\frac{\|g_k\|^2}{\lambda_k} \geq \frac{1}{C_\lambda} \|g_k\|^{3/2}.$$

Finally, convexity and the bounded level set imply  $\Phi_k \leq \langle g_k, \bar{x}_k - x_\star \rangle \leq D\|g_k\|$ , hence  $\|g_k\|^{3/2} \geq D^{-3/2} \Phi_k^{3/2}$ . Collect constants into  $\nu$ .  $\square$

*Proof of Lemma 5.18.* If  $\Phi_k = 0$  for some  $k$ , then  $\Phi_{k'} = 0$  for all  $k' \geq k$  and the claim is trivial. Assume  $\Phi_k > 0$  for all  $k$ .

From  $\Phi_{k+1} \leq \Phi_k - \nu \Phi_k^{3/2} = \Phi_k(1 - \nu\sqrt{\Phi_k})$ , we consider two cases.

Case 1:  $\nu\sqrt{\Phi_k} \geq 1$ . Then  $\Phi_{k+1} \leq 0$ . Since  $\Phi_{k+1} \geq 0$ , we must have  $\Phi_{k+1} = 0$ , contradicting  $\Phi_{k+1} > 0$ . Hence this case cannot occur under the assumption  $\Phi_k > 0$ .

Therefore, necessarily  $\nu\sqrt{\Phi_k} \in (0, 1)$  for all  $k$ .

Let  $\psi_k := \Phi_k^{-1/2}$ . Then

$$\begin{aligned}\psi_{k+1} &= \Phi_{k+1}^{-1/2} \geq \Phi_k^{-1/2} (1 - \nu\sqrt{\Phi_k})^{-1/2} \\ &= \psi_k (1 - u_k)^{-1/2}, \quad u_k := \nu\sqrt{\Phi_k} \in (0, 1).\end{aligned}$$

Using convexity of  $(1 - u)^{-1/2}$  on  $[0, 1)$  and  $(1 - u)^{-1/2} \geq 1 + \frac{1}{2}u$ , we obtain

$$\psi_{k+1} \geq \psi_k \left(1 + \frac{1}{2}u_k\right) = \psi_k + \frac{\nu}{2}.$$

The positive-sequence case also implies  $\nu\sqrt{\Phi_0} < 1$ , hence  $\psi_0 = \Phi_0^{-1/2} > \nu$ . Therefore,

$$\psi_k \geq \psi_0 + \frac{\nu}{2}k > \nu + \frac{\nu}{2}k = \frac{\nu}{2}(k + 2),$$

and hence

$$\Phi_k = \psi_k^{-2} \leq \frac{4}{\nu^2(k + 2)^2}.$$

□

*Proof of Theorem 5.20.* We establish the  $\mathcal{O}(\varepsilon^{-1})$  post-burn-in rate by deriving the 3/2-recursion only along the pre-hitting tail. Concretely, fix  $\eta \leq 1/12$  and let  $K_0 = K_0(\varepsilon)$  be the burn-in index from Proposition A.15, so that Proposition 5.14 holds for every shifted index before the first hitting time. Define  $\Phi_k := f(\bar{x}_k) - f_\star$  and  $g_k := \nabla f(\bar{x}_k)$ . Set

$$\hat{x}_j := \bar{x}_{K_0+j}, \quad \hat{g}_j := g_{K_0+j}, \quad \hat{\Phi}_j := \Phi_{K_0+j}, \quad j \geq 0.$$

Let

$$J_\varepsilon := \inf\{j \geq 0 : \|\hat{g}_j\| \leq \varepsilon\},$$

with  $J_\varepsilon = \infty$  if the set is empty. All post-burn-in estimates below are applied only for shifted indices  $0 \leq j < J_\varepsilon$ . For notational economy, the shifted sequence is relabeled as  $(\bar{x}_k, g_k, \Phi_k)$ .

**Step 0: descent along the shifted sequence.** By Proposition A.15, the hypotheses of Lemma 5.15 hold at every shifted index before the first hitting time. Hence, with  $c_d := 1 - \eta - \frac{1}{6} > 0$ ,

$$\hat{\Phi}_{j+1} \leq \hat{\Phi}_j - c_d \lambda_{K_0+j} \|\bar{s}_{K_0+j}\|^2 \leq \hat{\Phi}_j, \quad 0 \leq j < J_\varepsilon. \quad (\text{B.1})$$

Since we seek the first shifted index  $j$  with  $\|\hat{g}_j\| \leq \varepsilon$ , this is exactly the range needed for the complexity bound.

**Step 1: a uniform gradient growth bound.** Let  $r_k := (\nabla^2 f(\bar{x}_k) + \lambda_k I) \bar{s}_k + g_k$  as defined in the paper. For every shifted index before the first hitting time, Proposition 5.14 gives  $\|r_k\| \leq \eta \lambda_k \|\bar{s}_k\|$ . Moreover,

$$\lambda_k \|\bar{s}_k\| \leq \|(\nabla^2 f(\bar{x}_k) + \lambda_k I) \bar{s}_k\| = \|g_k - r_k\| \leq \|g_k\| + \|r_k\| \leq \|g_k\| + \eta \lambda_k \|\bar{s}_k\|.$$

Rearranging yields

$$\lambda_k \|\bar{s}_k\| \leq \frac{1}{1 - \eta} \|g_k\|, \quad 0 \leq k < J_\varepsilon. \quad (\text{B.2})$$

By Lemma 5.16, again only at shifted indices before the first hitting time,

$$\|g_{k+1}\| \leq C_g \lambda_k \|\bar{s}_k\|, \quad C_g := 1 + \eta + \frac{1}{2}.$$

Combining with (B.2) gives the uniform growth bound

$$\|g_{k+1}\| \leq \kappa_{\text{inc}} \|g_k\|, \quad \kappa_{\text{inc}} := \frac{C_g}{1-\eta}. \quad (\text{B.3})$$

Since  $\eta \leq 1/12$ , we have  $C_g \leq 2$  and thus  $\kappa_{\text{inc}} \leq 24/11 < 4$ .

**Step 2: decay along the steady-step subsequence.** Recall the index sets

$$\mathcal{I} := \{k \geq 0 : \|g_{k+1}\| \geq \frac{1}{4}\|g_k\|\}, \quad \mathcal{S} := \{k \geq 0 : \|g_{k+1}\| < \frac{1}{4}\|g_k\|\}.$$

Fix  $k < J_\varepsilon$ . Let  $n_k := |\mathcal{I} \cap \{0, 1, \dots, k-1\}|$  be the number of steady indices among the first  $k$  iterations. List these indices increasingly as  $0 \leq i_0 < i_1 < \dots < i_{n_k-1} \leq k-1$  (if  $n_k = 0$  skip this step). Define the subsequence  $u_j := \Phi_{i_j}$ . By Lemma 5.17, for each steady index  $i_j \in \mathcal{I}$ ,

$$\Phi_{i_j} - \Phi_{i_{j+1}} \geq \nu \Phi_{i_j}^{3/2} = \nu u_j^{3/2}.$$

Since  $i_{j+1} \geq i_j + 1$  and  $\Phi_k$  is nonincreasing along the indices before termination, we have

$$u_{j+1} = \Phi_{i_{j+1}} \leq \Phi_{i_j+1} \leq \Phi_{i_j} - \nu \Phi_{i_j}^{3/2} = u_j - \nu u_j^{3/2}.$$

Applying Lemma 5.18 to this pre-hitting subsequence yields

$$u_j \leq \frac{4}{\nu^2(j+2)^2} \quad \text{whenever } i_j < J_\varepsilon. \quad (\text{B.4})$$

**Step 3: two-case bound yielding  $\mathcal{O}(\varepsilon^{-1})$  iteration complexity.** Let  $m_k := |\mathcal{S} \cap \{0, 1, \dots, k-1\}| = k - n_k$ . We consider two cases.

Case 1:  $n_k \geq k/2$ . For  $k \geq 2$ , this implies  $n_k \geq 1$ , so the last steady index  $i_{n_k-1}$  is well defined. By monotonicity,  $\Phi_k \leq \Phi_{i_{n_k-1}} = u_{n_k-1}$ , and (B.4) gives

$$\Phi_k \leq \frac{4}{\nu^2(n_k+1)^2} \leq \frac{16}{\nu^2(k+2)^2}.$$

The finitely many cases  $k < 2$  are absorbed into the final constant.

Case 2:  $n_k < k/2$  (hence  $m_k > k/2$ ). For every sharp index  $\ell \in \mathcal{S}$ , we have  $\|g_{\ell+1}\| \leq \frac{1}{4}\|g_\ell\|$  by definition. For every other index, we have the growth bound (B.3). Therefore, after  $k$  iterations,

$$\|g_k\| \leq \kappa_{\text{inc}}^{n_k} \left(\frac{1}{4}\right)^{m_k} \|g_0\| \leq \kappa_{\text{inc}}^{k/2} \left(\frac{1}{4}\right)^{k/2} \|g_0\| = \left(\frac{\kappa_{\text{inc}}}{4}\right)^{k/2} \|g_0\|.$$

Since  $\kappa_{\text{inc}}/4 < 1$ , the bounded level set and convexity imply

$$\Phi_k = f(\bar{x}_k) - f_\star \leq \langle g_k, \bar{x}_k - x_\star \rangle \leq \|\bar{x}_k - x_\star\| \|g_k\| \leq D \|g_k\|.$$

Therefore,

$$\Phi_k \leq D G_\star \left(\frac{\kappa_{\text{inc}}}{4}\right)^{k/2}, \quad G_\star := \sup_{\ell \geq 0} \|g_\ell\| < \infty.$$

The finiteness of  $G_\star$  follows from Assumption 5.1 and the Lipschitz continuity of  $\nabla f$  on the bounded trajectory. Because  $\sup_{k \geq 0} (k+2)^2 \left(\frac{\kappa_{\text{inc}}}{4}\right)^{k/2} < \infty$ , there exists a finite constant  $C_{\text{exp}} > 0$  such that

$$\Phi_k \leq \frac{C_{\text{exp}}}{(k+2)^2} \quad 0 \leq k < J_\varepsilon.$$

Combining both cases, there exists  $C_\Phi > 0$  such that

$$\Phi_k \leq \frac{C_\Phi}{(k+2)^2} \quad 0 \leq k < J_\varepsilon,$$

which proves the pre-hitting  $\Phi_k = \mathcal{O}(1/k^2)$  estimate.

**Step 4: gradient rate and  $\varepsilon$ -complexity.** By Lemma A.3 with  $h = f$  and  $L = L_1$ ,

$$\|g_k\|^2 \leq 2L_1\Phi_k \leq \frac{2L_1C_\Phi}{(k+2)^2},$$

hence  $\|g_k\| \leq \sqrt{2L_1C_\Phi}/(k+2) = \mathcal{O}(1/k)$ . For every  $j < J_\varepsilon$ ,  $\|g_j\| \leq \sqrt{2L_1C_\Phi}/(j+2)$ . Consequently, if

$$j \geq \frac{\sqrt{2L_1C_\Phi}}{\varepsilon} - 2 = \mathcal{O}(\varepsilon^{-1}).$$

then  $j$  cannot remain before the first hitting time. Thus the first shifted hitting time satisfies this same  $\mathcal{O}(\varepsilon^{-1})$  bound.

**Step 5: total complexity with burn-in.** Let  $K(\varepsilon)$  be the first original iteration where  $\|g_k\| \leq \varepsilon$ . Translating the shifted-index bound back to the original index, it takes at most  $\mathcal{O}(\varepsilon^{-1})$  additional steps after  $K_0(\varepsilon)$ . Thus, the total iteration complexity is bounded by:

$$K(\varepsilon) \leq K_0(\varepsilon) + C_K \varepsilon^{-1},$$

for some constant  $C_K > 0$ . This completes the proof of the global rate.  $\square$

*Proof of Lemma 5.26.* From Lemma 5.11,  $\bar{\delta}_k \leq \Delta_k^H + L_2D(X_k)$ .

**Bound  $\Delta_k^H$ .** By Jensen's inequality and  $\|\cdot\|_2 \leq \|\cdot\|_F$ ,

$$\Delta_k^H \leq D(\tilde{\mathcal{H}}_k).$$

We apply the Hessian-tracker dispersion recursion (Lemma A.8), noting that  $\mathcal{H}_k$  is obtained from  $\tilde{\mathcal{H}}_{k-1}$  via the post-mixing update at iteration  $k-1$ :

$$\begin{aligned} D(\tilde{\mathcal{H}}_k) &\leq \rho^{\tau_k} D(\mathcal{H}_k) \\ &\leq \rho^{\tau_k} \rho^{t_{k-1}} (D(\tilde{\mathcal{H}}_{k-1}) + 2\sqrt{d}L_2D) \\ &\leq \rho^{\tau_k} (B_H + 2\sqrt{d}L_2D), \end{aligned}$$

where  $B_H := \sup_{j \geq 0} D(\tilde{\mathcal{H}}_j) < \infty$  is the uniform bound established in Lemma A.10. In particular, since  $B_H$  is finite, we obtain

$$\Delta_k^H \leq \rho^{\tau_k} (B_H + 2\sqrt{d}L_2D) =: \hat{C}_H \rho^{\tau_k}.$$

**Bound  $D(X_k)$ .** By Lemma A.11,

$$D(X_k) \leq \rho^{t_{k-1}} \left( D(\tilde{X}_{k-1}) + \frac{\|S_{k-1}\|}{\sqrt{N}} \right).$$

Moreover,  $D(\tilde{X}_{k-1}) \leq 2D$  and Lemma A.5 gives  $\|S_{k-1}\|/\sqrt{N} \leq \sqrt{G_g/M}$ . Thus

$$D(X_k) \leq \rho^{t_{k-1}} \left( 2D + \sqrt{\frac{G_g}{M}} \right).$$

Therefore,

$$\bar{\delta}_k \leq \hat{C}_H \rho^{\tau_k} + L_2 \rho^{t_{k-1}} \left( 2D + \sqrt{\frac{G_g}{M}} \right) \leq C_\delta \max\{\rho^{\tau_k}, \rho^{t_{k-1}}\}.$$

Using (5.6), we obtain  $\bar{\delta}_k \leq \|g_k\|^{1+\gamma}$  for all sufficiently large  $k$ .  $\square$

*Proof of Theorem 5.27.* Let  $x_k := \bar{x}_k$ ,  $g_k := \nabla f(x_k)$ , and  $H_k := \nabla^2 f(x_k)$ . Under Assumption 5.25, for all  $k$  we have  $H_k \succeq \mu I$  on the level set.

By definition,  $r_k := (H_k + \lambda_k I)\bar{s}_k + g_k$  and Proposition 5.14 gives for all large  $k$

$$(H_k + \lambda_k I)\bar{s}_k = -g_k + r_k, \quad \|r_k\| \leq \eta \lambda_k \|\bar{s}_k\|, \quad L_2 \|\bar{s}_k\| \leq \lambda_k,$$

with  $\eta \in (0, 1/12]$ . Under (5.7) and the bound  $D(X_k) \leq \rho^{t_{k-1}}(2D + \sqrt{G_g/M})$  (see Lemma A.11 and Lemma A.5), we have  $D(X_k) = \mathcal{O}(\|g_k\|^{1+\gamma})$ . Moreover, Lemma 5.26 gives  $\bar{\delta}_k = \mathcal{O}(\|g_k\|^{1+\gamma})$ . By the same Jensen argument as in Lemma B.1,

$$\lambda_k \leq \sqrt{M} \sqrt{\|\tilde{g}_k\| + \Delta_k^g} + \bar{\delta}_k.$$

The bridge bound gives  $\|\tilde{g}_k\| \leq \|g_k\| + L_1 D(X_k)$ . The second condition in (5.7) gives  $\Delta_k^g = \mathcal{O}(\|g_k\|^{1+\gamma})$ . Since the theorem assumes  $\|g_k\| \rightarrow 0$  along the local post-burn-in tail, the preceding estimates imply

$$\lambda_k \leq C \sqrt{\|g_k\| + \mathcal{O}(\|g_k\|^{1+\gamma})} + \mathcal{O}(\|g_k\|^{1+\gamma}) = \mathcal{O}(\sqrt{\|g_k\|}).$$

Therefore  $\lambda_k \rightarrow 0$ , and hence  $\eta \lambda_k \leq \mu/2$  for all sufficiently large  $k$ .

Since  $H_k + \lambda_k I \succeq \mu I$ ,

$$\mu \|\bar{s}_k\| \leq \|(H_k + \lambda_k I)\bar{s}_k\| = \|g_k - r_k\| \leq \|g_k\| + \eta \lambda_k \|\bar{s}_k\|.$$

Therefore  $\|\bar{s}_k\| \leq \frac{2}{\mu} \|g_k\|$  for all sufficiently large  $k$ .

Using  $g_{k+1} = g_k + H_k \bar{s}_k + e_k$  with  $\|e_k\| \leq \frac{L_2}{2} \|\bar{s}_k\|^2$  and  $g_k + H_k \bar{s}_k = -\lambda_k \bar{s}_k + r_k$ ,

$$\|g_{k+1}\| \leq (1 + \eta) \lambda_k \|\bar{s}_k\| + \frac{L_2}{2} \|\bar{s}_k\|^2 \leq \mathcal{O}(\|g_k\|^{3/2}) + \mathcal{O}(\|g_k\|^2) = \mathcal{O}(\|g_k\|^{3/2}),$$

which proves the claim.  $\square$

*Proof of Theorem A.16.* Under (A.8),  $\tau_k = t_k = \lceil (p \log(k+2) + c_{\text{mix}})/(-\log \rho) \rceil \leq c_0 + c_1(1 - \rho)^{-1} \log(k+2)$ , using  $-1/\log \rho = \Theta((1 - \rho)^{-1})$  as  $\rho \rightarrow 1$ . Hence

$$\sum_{k=0}^{K(\varepsilon)-1} (\tau_k + 2t_k) = \mathcal{O}\left((1 - \rho)^{-1} K(\varepsilon) \log(K(\varepsilon) + 2)\right).$$

Combining with Theorem 5.20 yields the claim.  $\square$

## C Supplementary experiments

This appendix collects additional experimental figures that support the main results in Section 6. All settings are identical to those described in Section 6.1 unless stated otherwise.

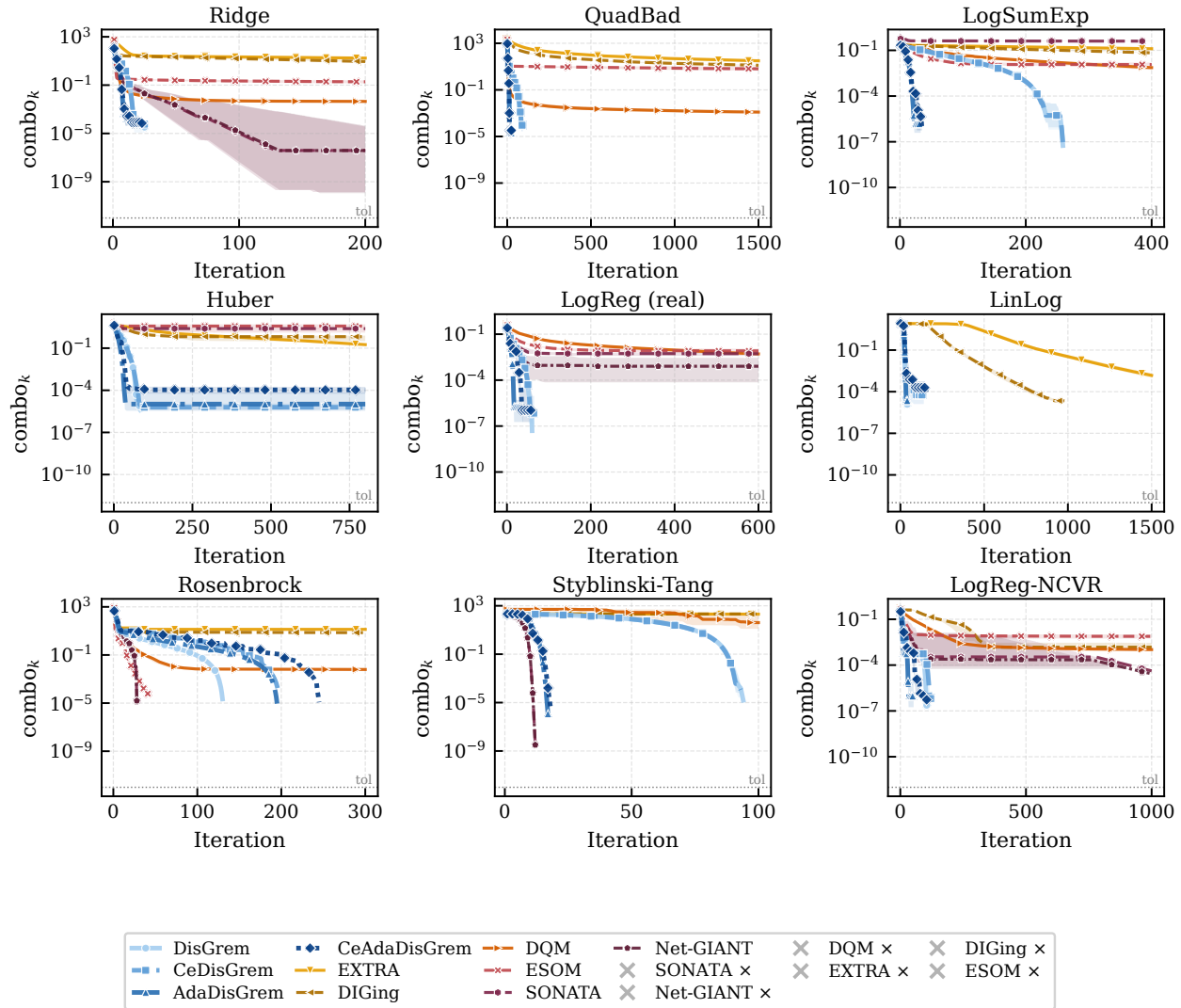


Figure 8: Composite optimality ( $\text{combo} = \|\nabla f(\bar{x}_k)\| + \text{cons}_k$ ) vs. iteration for all nine functions. Same setting as Figure 3;  $\times$  legend entries indicate runs terminated by NaN, overflow, or divergence.

### C.1 Additional per-problem convergence curves

The relF-vs.-iteration panel for all nine functions is already shown in Figure 3 of the main text. Below we collect the remaining metrics.

### C.2 Communication ablation details

### C.3 Adaptive mechanism details

### C.4 Parameter sensitivity sweeps

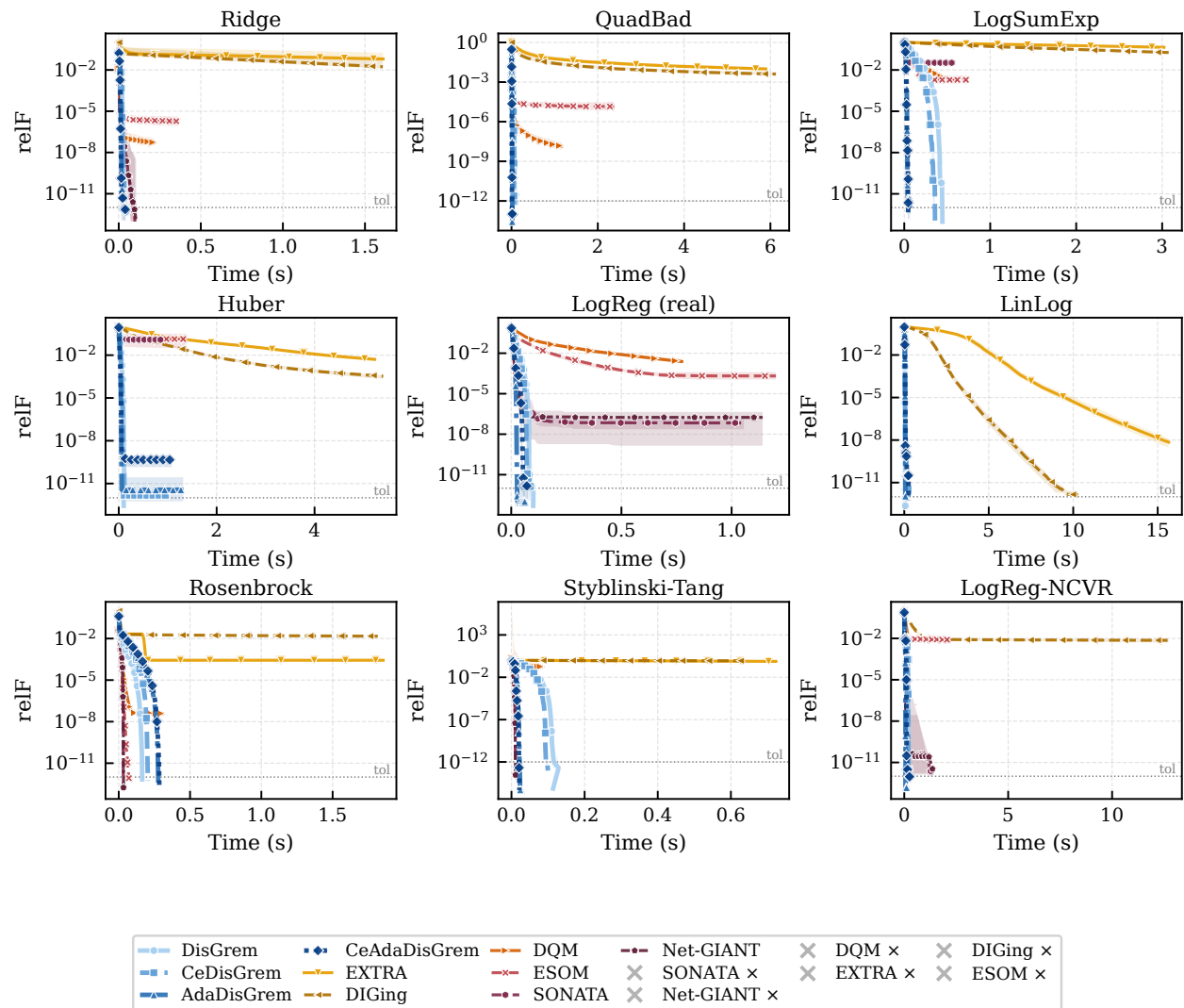


Figure 9: relF vs. wall-clock time (seconds) for all nine functions.

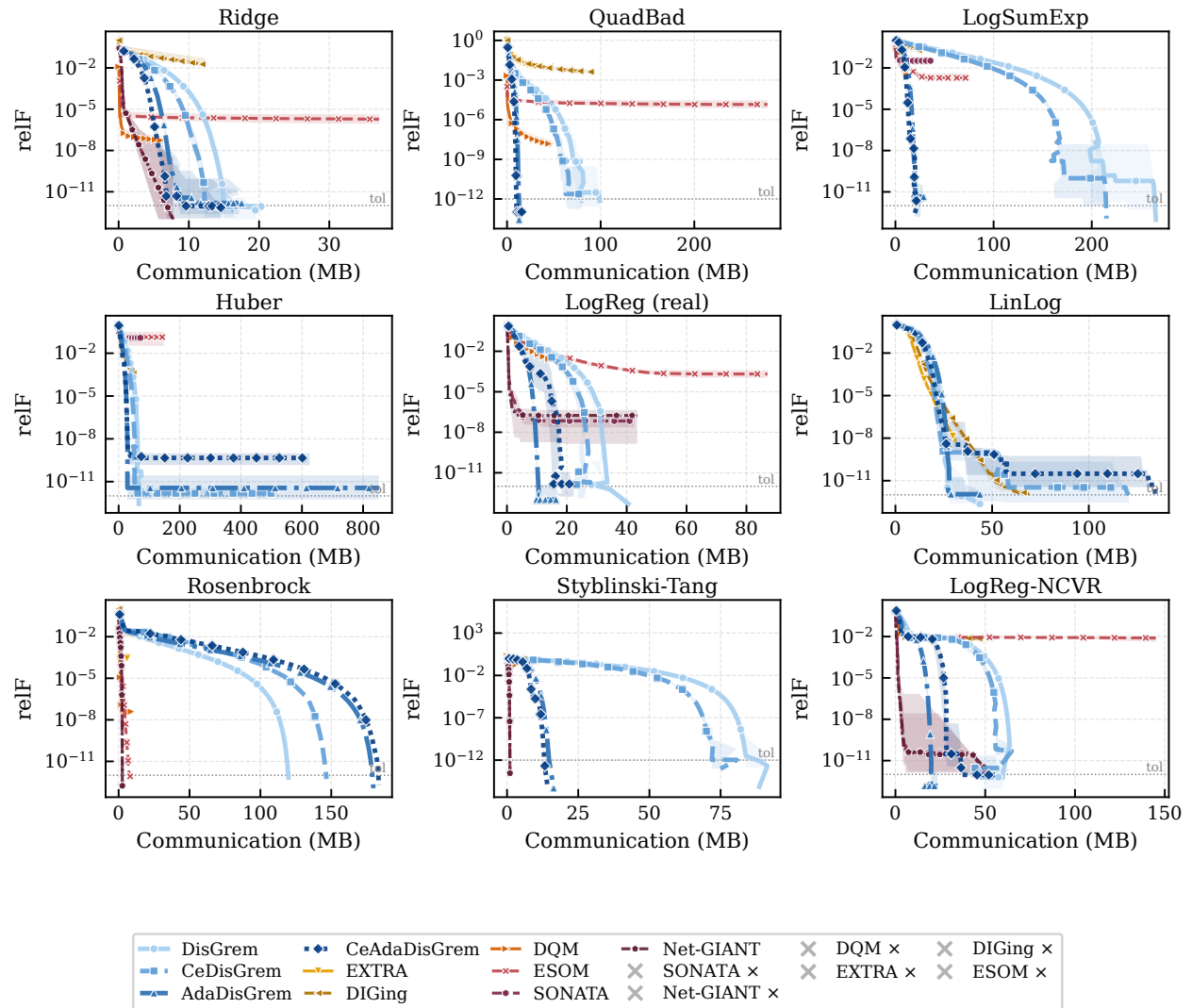


Figure 10: relF vs. cumulative communication cost (MB) for all nine functions.

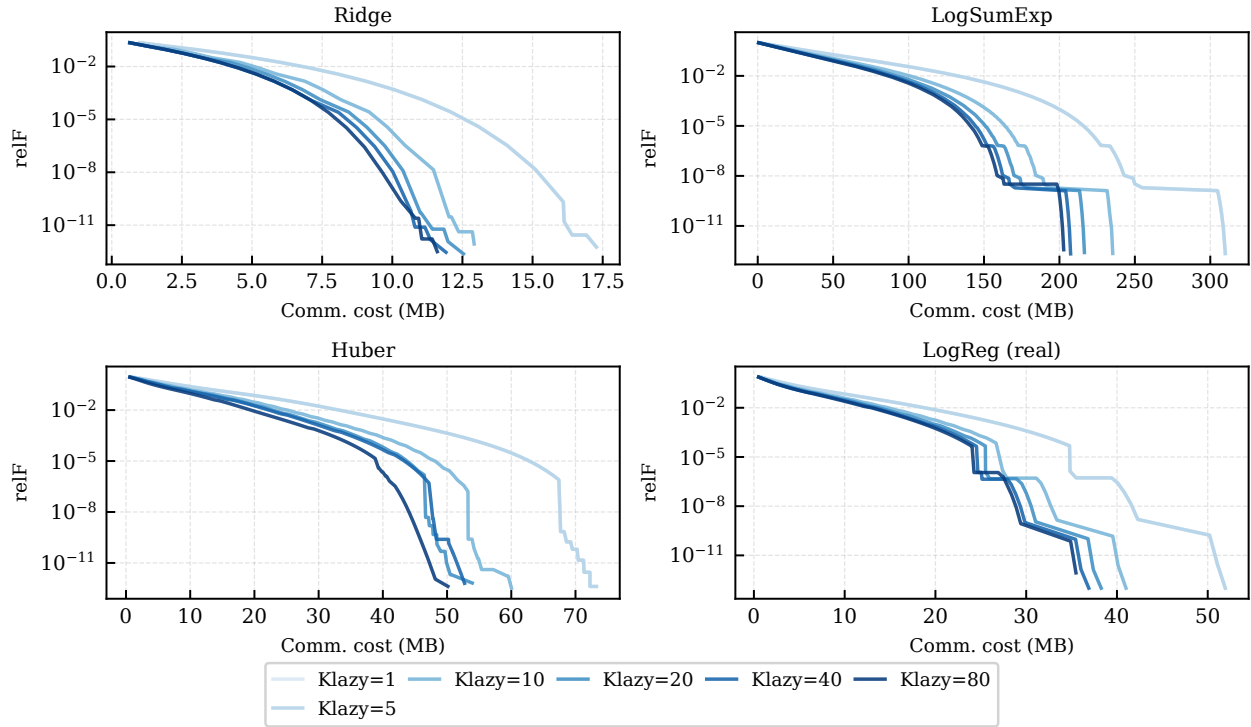


Figure 11: Effect of  $K_{\text{lazy}}$  on the communication–precision trade-off for CEDISGREM. Gradient-coloured curves from light to dark:  $K_{\text{lazy}} \in \{1, 5, 10, 20, 40, 80\}$ .

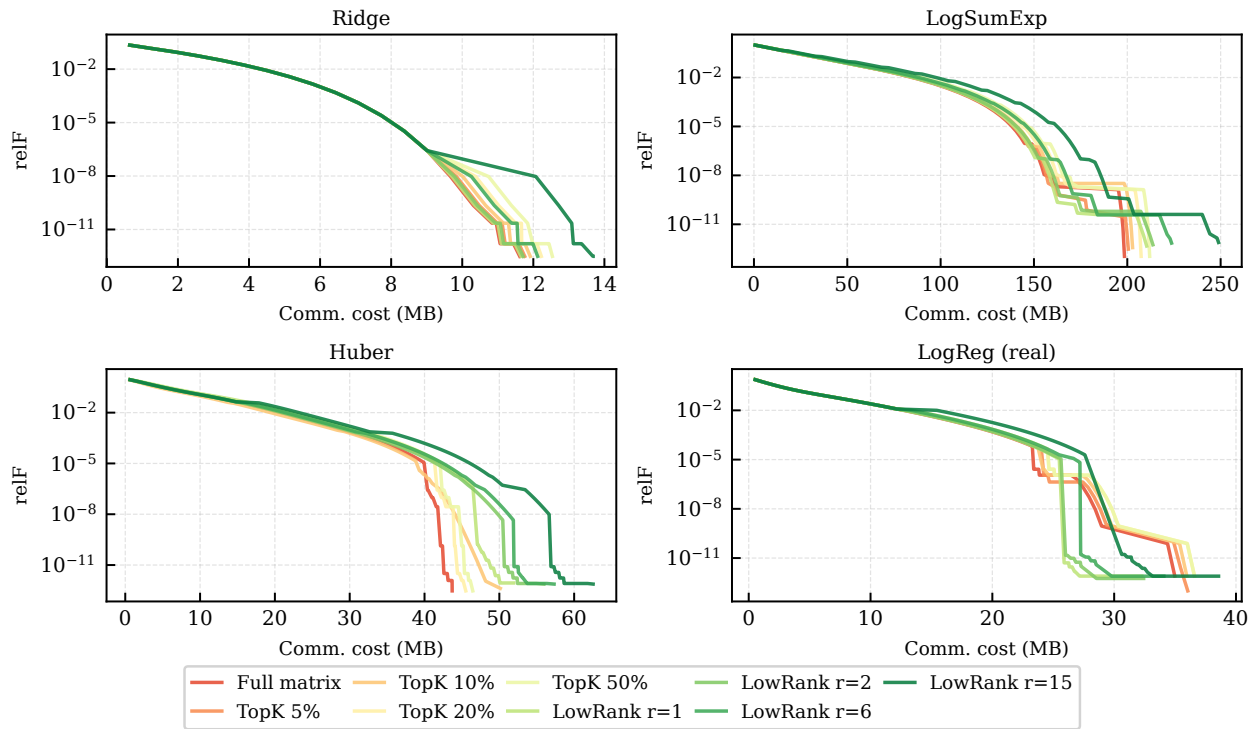


Figure 12: Effect of compression method and rank on the communication–precision trade-off for CEDISGREM. Configurations: full (no compression), Top- $k$  ( $k \in \{5\%, 10\%, 20\%, 50\%\}$ ), Low-Rank ( $r \in \{1, 2, d/5, d/2\}$ ).

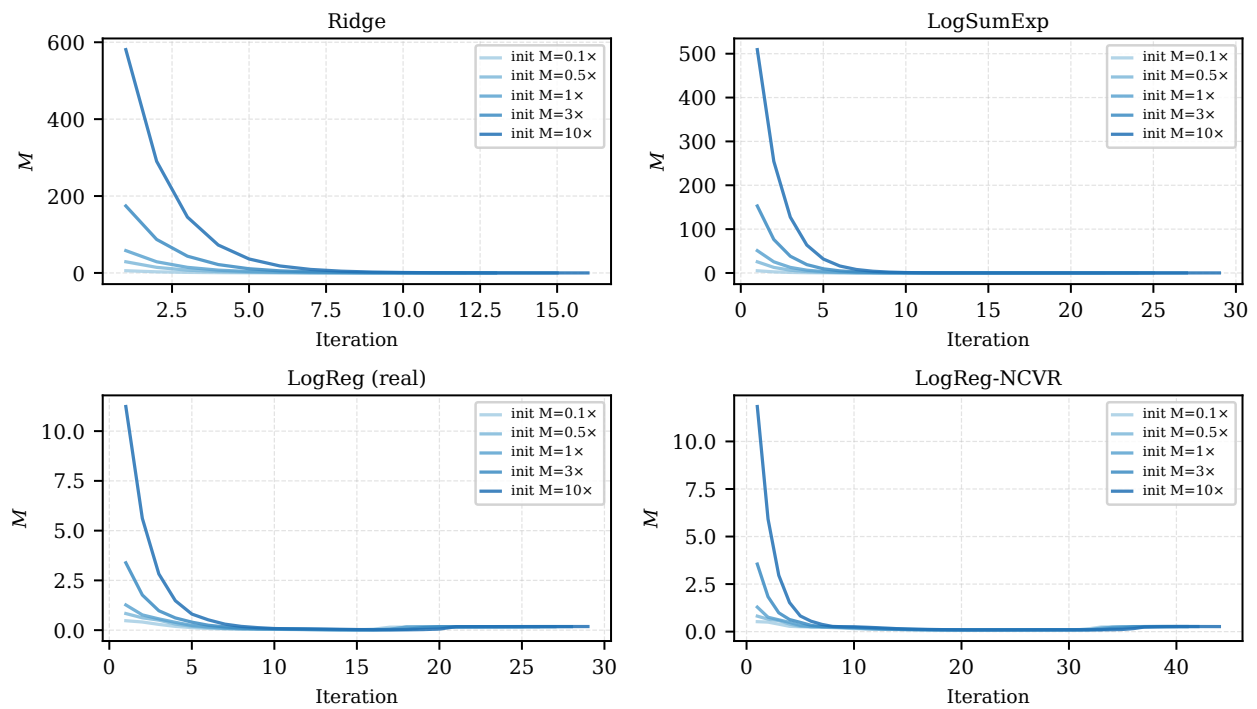


Figure 13: Robustness of ADADISGREM to initial  $M$ . Initial  $M_0 \in \{0.1M^*, 0.5M^*, M^*, 3M^*, 10M^*\}$ . All initializations converge to similar trajectories within 50–100 iterations.

DisGrem Family

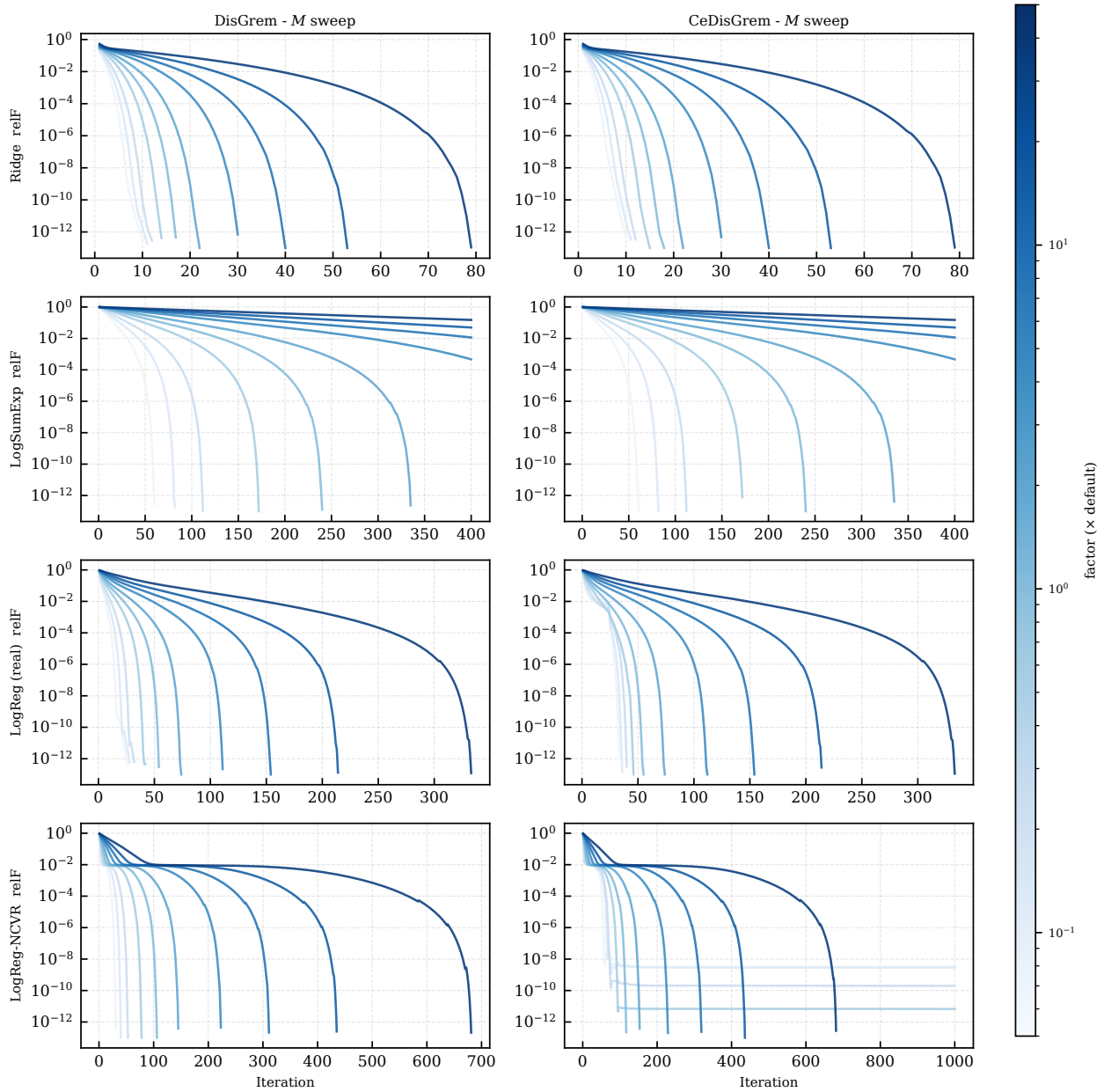


Figure 14: Parameter sweep for the DISGREM family on four functions. 10 values of  $M_{\text{fac}}$  (light-to-dark for increasing  $M_{\text{fac}}$ ). Rows: functions; columns: algorithms.

First-Order Methods

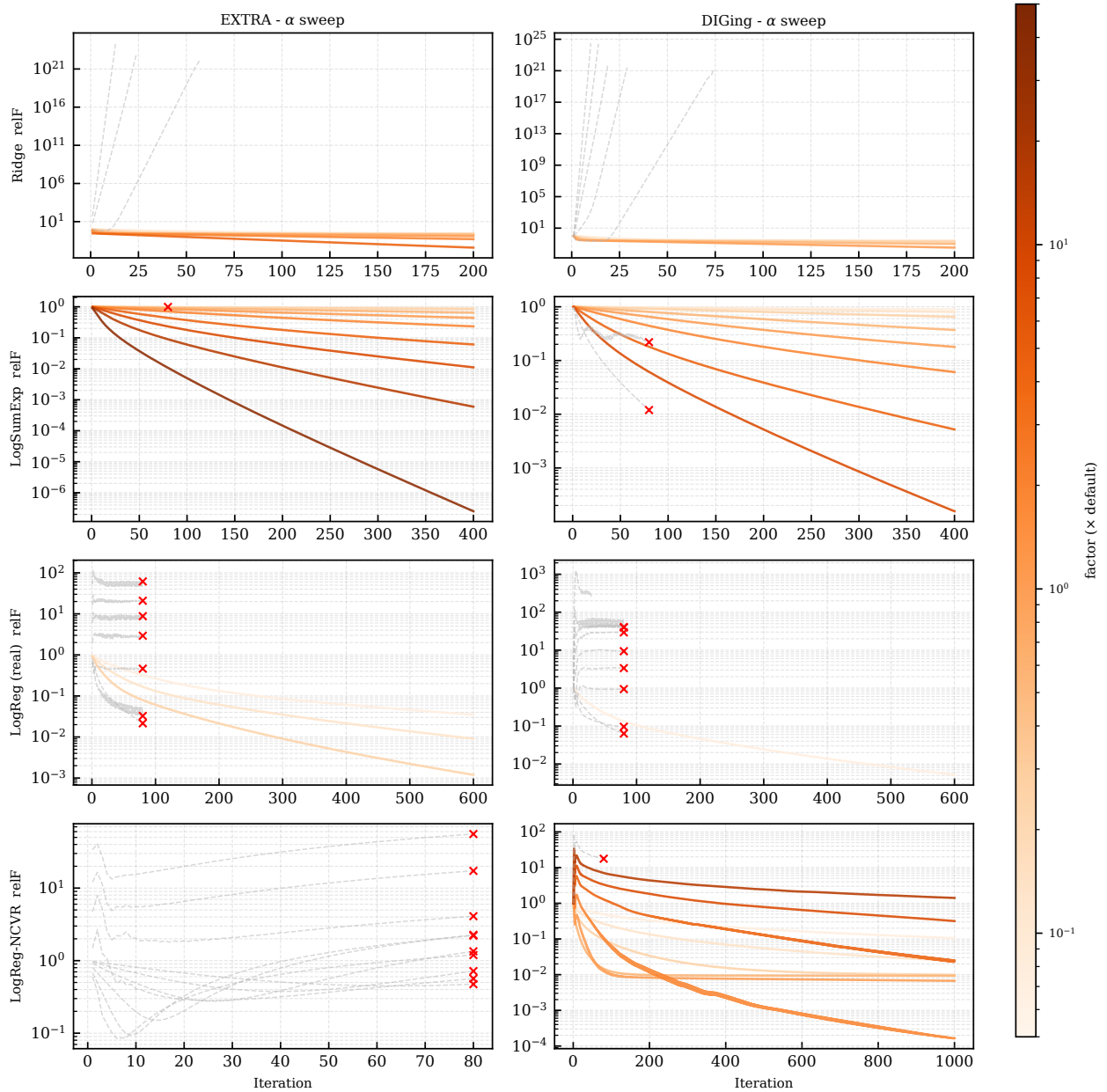


Figure 15: Stepsize sensitivity for first-order baselines (EXTRA and DIGing) on four functions. 10 values of  $\alpha$  (light-to-dark). Divergent runs are clipped at  $\text{relF} = 10^4$ .

## Second-Order Methods

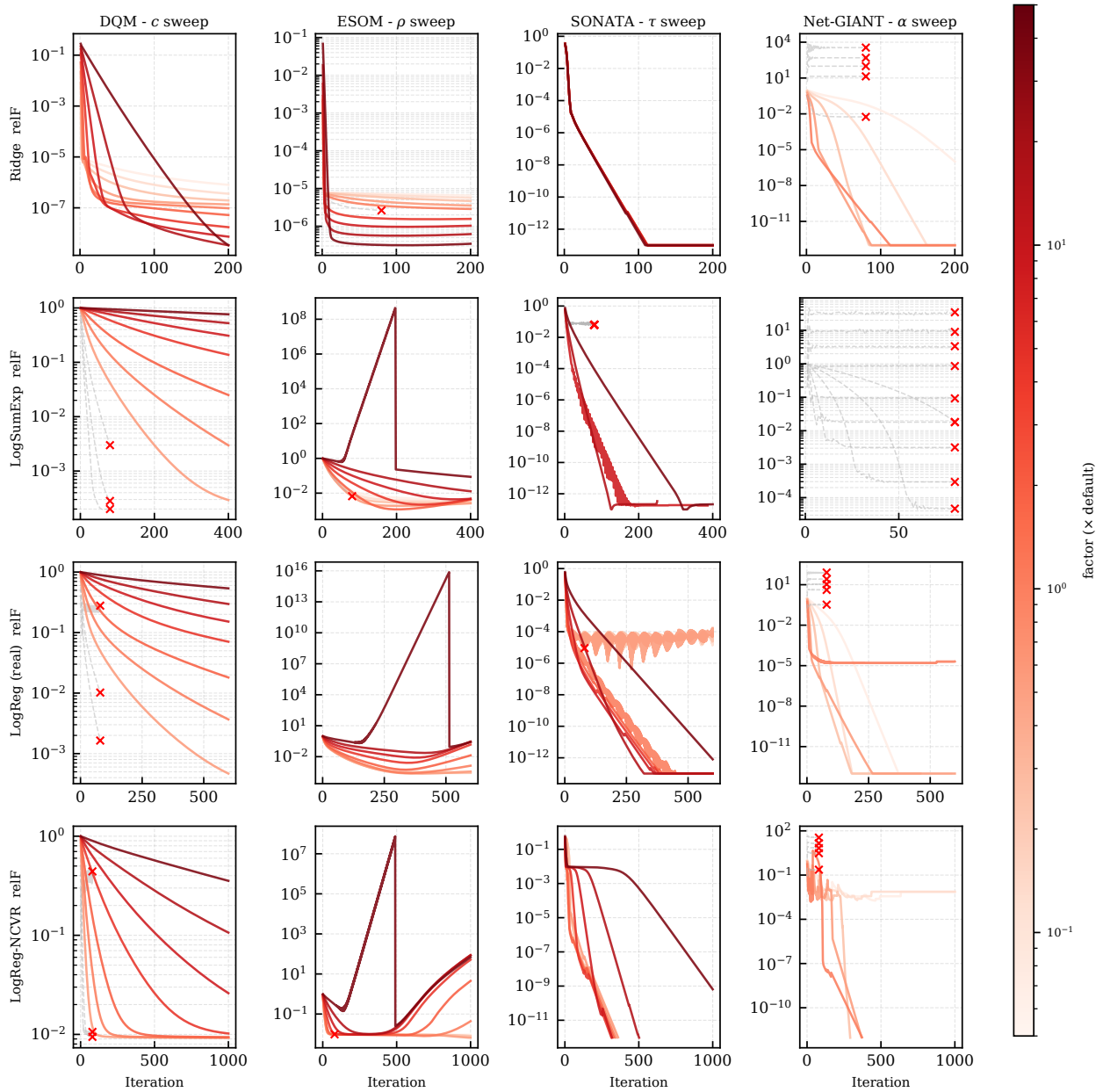


Figure 16: Key-parameter sensitivity for second-order baselines on four functions: penalty  $c$  (DQM), penalty  $\rho_E$  (ESOM), regularization  $\tau$  (SONATA), stepsize  $\alpha$  (Net-GIANT). Entries marked by  $\times$  indicate parameter settings with NaN, overflow, or divergence.